

FORMATION AND EVOLUTION CHARACTERISTICS OF NUCLEI MODE PARTICLES IN DENSE ATMOSPHERIC AND CONFINED AEROSOL ENVIRONMENTS

By

**MANISH JOSHI
PHYS01201104015**

Bhabha Atomic Research Centre, Mumbai

*A thesis submitted to the
Board of Studies in Physical Sciences
In partial fulfillment of requirements
for the Degree of*

DOCTOR OF PHILOSOPHY
of
HOMI BHABHA NATIONAL INSTITUTE

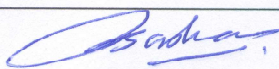
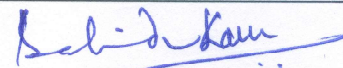
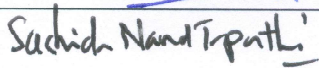
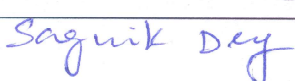
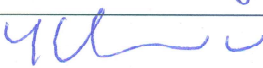
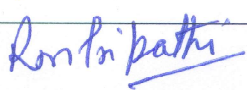


July, 2018

Homi Bhabha National Institute

Recommendations of the Viva Voce Committee

As members of the Viva Voce Committee, we certify that we have read the dissertation prepared by Manish Joshi entitled "Formation and evolution characteristics of nuclei mode particles in dense atmospheric and confined aerosol environments" and recommend that it may be accepted as fulfilling the thesis requirement for the award of Degree of Doctor of Philosophy.

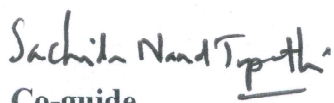
Chairman – Dr. R. Baskaran		Date: 4/7/18
Guide / Convener – Dr. B. K. Sapra		Date: 4/7/18
Co-guide - Dr. S. N. Tripathi		Date: 4/7
Examiner – Dr. Sagnik Dey		Date: 4/7/18
Member 1- Dr. Y. S. Mayya		Date: 4/7/18
Member 2- Dr. R. M. Tripathi		Date: 4/7/18

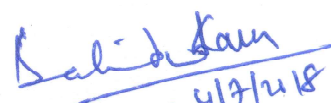
Final approval and acceptance of this thesis is contingent upon the candidate's submission of the final copies of the thesis to HBNI.

I/We hereby certify that I/we have read this thesis prepared under my/our direction and recommend that it may be accepted as fulfilling the thesis requirement.

Date: 04/07/2018

Place: Mumbai


Co-guide
4/7


Guide
4/7/2018

Khandare, Mariam and Armuta Nakhwa. Additional thanks to Mariam for her immense contribution towards data analysis.

I am grateful to my family and my friends for their selfless belief on my capabilities. I want to thank Mrs. Niyati Mukherjee for sharing her dream about my Ph.D.

I see heaven for blessings of my father at this crucial time of my life. I miss my friend Hansa Chauhan who supported me during my college days when I needed it most. No words will be enough to express my thanks to my wife Sudeshna who supported me in the most special way. And finally my daughter Ohanna, thank you for coming in life when I am submitting my Ph.D. I will wait for discussing this work with you.....

Manish Joshi

ACKNOWLEDGEMENTS

I would like to express my sincere thanks to my guide Dr. B. K. Sapra who supported me in all aspects during this journey. Her guidance, involvement and thoughtful inputs became key factors towards the completion of this work.

I am thankful to Dr Y. S. Mayya, adjunct professor, Indian Institute of Technology, Mumbai, who inspired me and helped me whenever I needed. I thank my co-guide Dr. S. N. Tripathi for many insightful discussions and providing me all the help while working at IIT Kanpur.

I thank Dr. S. Anand, Health Physics Division (HPD), Bhabha Atomic Research Centre (BARC), for sharing his expertise on theoretical extensions and data analysis. I acknowledge members of my doctoral committee, Dr. R. Baskaran, Head, Radiological Safety Division, Indira Gandhi Centre of Atomic Research (IGCAR) and Dr. R. M. Tripathi, Head, HPD, BARC, for their invaluable guidance related to reviews of this work.

I acknowledge the support of Dr. P. M. Shamjad during experiments at IIT Kanpur. I remember the efforts of Pampa Modak during her work on 'Hot wire nanoparticle generator'. I thank Dr. R. B. Oza, Head, Environmental Monitoring Section (EMS), BARC and Dr. R. S. Srivastava, EMS, BARC for helping me with data and guidance related to meteorological parameters. I remember discussions with Dr. Lothar Keck which cleared my doubts on SMPS measurements.

I will forever remain indebted for the help obtained from my laboratory colleagues. At all times during experiments and data analysis, I found them sharing pain of efforts and joy of satisfaction. A very special thanks to Arshad Khan, Pallavi

2. “Aerosol formation and evolution in continuously stirred chambers: A modelling study”, Y. S. Mayya, M. Joshi, B. Sreekanth, S. Anand and B.K. Sapra, Aerosol Technology conference, Karlsruhe, Germany June **2014**, T120A03
3. “On experimental observation of nucleation peaks in a stirred chamber: Aerosol Oscillations” Manish Joshi, Amruta Koli, Arshad Khan, S. Anand, B. K. Sapra and Y. S. Mayya, Aerosol Technology conference, Karlsruhe, Germany June **2014**, T120A10
4. “Enhancement in BC absorption under varying hygroscopic conditions”, P. M. Shamjad, S. N. Tripathi, S. G. Aggarwal, S. K. Mishra, Manish Joshi, Arshad Khan, B. K. Sapra, and Kirpa Ram, American Geophysical Union fall meeting, San Francisco, December **2012**, A51B-0025

Manish Joshi

List of Publications arising from the thesis

Journals

1. "Size evolution of ultrafine particles: Differential signatures of normal and episodic events", M. Joshi, A. Khan, S. Anand, B. K. Sapra , Environmental Pollution, **2016**, 208, 354-360
2. "Generation of high concentration nanoparticles using Glowing Wire Technique", Arshad Khan, Pampa Modak, Manish Joshi, Pallavi Khandare, Amruta Koli, Alka Gupta, S. Anand, B. K. Sapra, Journal of Nanoparticle Research, **2014**, 16, 2776
3. "Harmonisation of nanoparticle concentration measurements using GRIMM and TSI scanning mobility particle sizers", Manish Joshi, B. K. Sapra, Arshad Khan, S. N. Tripathi, P. M. Shamjad, Tarun Gupta, Y. S. Mayya, Journal of Nanoparticle Research, **2012**, 14, 1268
4. "Comparison of Experimental and Modeled Absorption Enhancement by Black Carbon (BC) Cored Polydisperse Aerosols under Hygroscopic Conditions" by P. M. Shamjad, S. N. Tripathi, S. G. Aggarwal, S. K. Mishra, Manish Joshi, Arshad Khan, B. K. Sapra, and Kirpa Ram, Environmental Science and Technology, **2012**, 46 (15), 8082–8089

Conferences

1. "Estimating number emission rates of nano-particle sources by "ÇConcentration Peaking" method", S. Anand, M. Joshi, B. K. Sapra, and Y. S. Mayya, Aerosol Technology conference, Karlsruhe, Germany, June **2014**, T220A02

DECLARATION

I, hereby declare that the investigation presented in the thesis has been carried out by me. The work is original and has not been submitted earlier as a whole or in part for a degree / diploma at this or any other Institution / University.

Manish Joshi

STATEMENT BY AUTHOR

This dissertation has been submitted in partial fulfillment of requirements for an advanced degree at Homi Bhabha National Institute (HBNI) and is deposited in the Library to be made available to borrowers under rules of the HBNI.

Brief quotations from this dissertation are allowable without special permission, provided that accurate acknowledgement of source is made. Requests for permission for extended quotation from or reproduction of this manuscript in whole or in part may be granted by the Competent Authority of HBNI when in his or her judgment the proposed use of the material is in the interests of scholarship. In all other instances, however, permission must be obtained from the author.

Manish Joshi

6.3	Long term behaviour of HWG aerosols in closed chamber conditions	147
6.3.1	Time series of number concentration and size distribution	148-149
6.3.2	Late time peaking of number concentration in decaying profile	149-150
6.3.2.1	Experimental validations	150-153
6.3.2.2	Secondary nucleation effects: aerosol oscillations	153-154
6.4	Summary	154
7.	Summary and conclusions	155-163
7.1	Future scope for this work	163-164
	References	165-191

4.4.1	Picking up events	107-109
4.4.2	Qualifying criterion and event statistics	109-110
4.4.3	Formation and evolution characteristics of events	110-111
4.4.4	Sinks	111-113
4.5	Summary	113-114
5.	Characteristics of Nuclei mode atmospheric particles:	115
	Case study 2- large scale fire event	
5.1	Deonar dump yard fire (March 2016)	115-116
5.2	Measurement of aerosol number characteristics: case and control days	116-117
5.2.1	Number concentration	117-120
5.2.2	Dynamics of size distribution	121-124
5.2.3	Diurnal variations	124-126
5.2.4	Statistical analysis	127-129
5.2.5	Comparison of parameters during case and control days	129-130
5.3	Evolution parameters for selected nucleation events	130
5.3.1	Picking up events	130-132
5.3.2	Qualifying criterion and event statistics	132-133
5.3.3	Formation and evolution characteristics of events	133-134
5.3.4	Sinks	134-136
5.4	Summary	136
6.	Characteristics of nuclei mode particles in confined environments: Case 3- Hot wire generated nanoaerosols	137
6.1	Role of experimental studies: validation of aerosol dynamics equation	137-138
6.2	Vapour to particle conversion: Role of hot wire generator	139
6.2	Experiments with high concentration nanoparticle aerosols	139-140
6.2.1	Continuous injection: Characteristic peaking effect	140-145
6.2.2	Size distribution evolution in different size ranges	145-147

3.3.1	Coagulation sink	63
3.3.2	Condensation sink	64
3.3.3	Growth rate	64
3.3.4	Nucleation rate	65
3.4	Various approaches to determine nucleation and evolution parameters	65-66
3.4.1	Conventional approach	66-69
3.4.2	Kerninen- Kulmala equation	69-73
3.4.3	PARticle Growth And Nucleation (PARGAN) model	73-74
3.4.4	Methodology adopted in this work	74-75
3.5	Summary	75-76
4.	Characteristics of Nuclei mode atmospheric particles:	77-78
	Case study 1- firecracker events	
4.1	Aerosol emission due to firecrackers	78
4.2	Nuclei mode particles during fireworks	78-79
4.3	Changes in atmospheric aerosol characteristics during Diwali festival	79
4.3.1	Measurements during Diwali 2012	79-80
4.3.1.1	Time series peaks	80-82
4.3.1.2	Size distributions	82-88
4.3.1.3	Size distribution evolution analysis	88-91
4.3.1.4	Differential signatures of normal and episodic events	92
4.3.2	Measurements during Diwali 2013	93
4.3.2.1	Comparison with inferences from 2012 campaign	93-97
4.3.2.2	Statistical analysis	97-101
4.3.2.3	Diurnal variations	101-104
4.3.2.4	PM and chemical composition	104-106
4.4	Evolution parameters for selected nucleation events	107

2.	Techniques and instrumentation	27-28
2.1	Measurement of aerosol mass characteristics	28-29
2.2	Measurement of chemical composition	29-30
2.3	Measurement of aerosol number characteristics	30-31
2.3.1	Number concentration	31-33
2.3.2	Number size distribution	33-34
2.3.3	Scanning mobility particle sizer	35-35
	2.3.3.1 Detection principle and theory	35
	2.3.3.1.1 Differential mobility analyser	35-38
	2.3.3.1.2 Condensation particle counter	38
	2.3.3.1.3 CPC and SMPSs used in this study	38-39
2.4	Aerosol generation	39-40
2.4.1	Electrical generation of nanoparticle aerosols	40
2.4.2	Hot wire generator	40-43
2.4.3	Operating parameters	43-44
2.4.4	Characteristics of generated aerosols	45-47
2.5	Harmonisation of ultrafine particle measurements with SMPS	47-48
2.5.1	Ambient conditions	48-50
2.5.2	Laboratory generated conditions	50-52
2.5.3	Harmonisation	52-54
2.5.4	Case study	54-55
2.6	Detection of nuclei mode particles	55-56
2.7	Summary	56
3.	Nucleation parameters and their theoretical formulations	57
3.1	Terminology	58-59
3.2	Criterion for defining a nucleation event	59-60
3.2.1	Identification of a NPF event	60-62
3.2.2	Behaviour of nuclei mode particles	62-63
3.3	Estimation of aerosol parameters	63

CONTENTS

Title	Page No.
SYNOPSIS	i-xii
LIST OF FIGURES	xiii-xvi
LIST OF TABLES	xvii
 Chapter	
1. Introduction	1-2
1.1 Aerosol properties and characteristics	2-3
1.2 Aerosol size distribution: modes	3-5
1.3 Atmospheric aerosol measurements	5
1.3.1 Literature survey	
1.3.1.1 Worldwide studies	5-6
1.3.1.2 Indian studies	7-8
1.3.2 Measurement of ultrafine and nuclei mode particles	8-9
1.4 Nucleation events in atmosphere	9
1.4.1 Literature survey	9-11
1.5.2 Characteristic Features	12-13
1.5.3 Importance and Scope for further studies	13
1.5 Aerosol emissions due to celebratory firecrackers	14
1.5.1 Mechanism and facts	14-15
1.5.2 Current state of knowledge	15-16
1.5.2.1 Worldwide picture	16-17
1.5.2.2 Indian context	18-19
1.5.4 Gaps in related studies	19-21
1.6 Aerosol emission due to large scale fires	21-22
1.7 Motivation	23-24
1.8 Objectives of this work	25-26

- 5) Kulmala, M., Maso, D. M., Makela, J. M., Pirjola, L., Vakeva, M., Aalto, P., Miikkulainen, P., Hameri, K., & O'Dowd, C. D. (2001), On the formation, growth and composition of nucleation mode particles, *Tellus* 53B, 479–490
- 6) M Joshi, A Khan, S Anand, BK Sapra (2016), Size evolution of ultrafine particles: Differential signatures of normal and episodic events, *Environmental Pollution* 208, 354-360
- 7) Anand S. (2012), Study of Coagulation of Dispersing Aerosol Systems. Ph. D. thesis, Homi Bhabha National Institute.

ultrafine and nuclei mode size ranges. Three campaigns were performed during atmospheric loading events and results of measurement of aerosol physical characteristics were interpreted. On the basis of analyses, episodic events (such as those induced by fireworks) could be differentiated from normal events weighing similar on integral aerosol number concentration scale. Atmospheric nucleation events were observed and nucleation/formation and growth rate of nuclei mode aerosols were estimated. Interaction of these freshly formed particles with background aerosols and their evolution was studied as well. On the other hand, controlled nucleation events using hot wire generator were studied to understand their evolution in chamber environment. The long term behaviour of these nuclei mode particles was also investigated and experimental verification of secondary aerosol oscillations was made.

References:

- 1) Ulrich Pöschl (2005), Atmospheric aerosols: composition, transformation, climate and health effects, *Atmospheric chemistry* 44, 7520-7540
- 2) Kulmala, M. et al. (2013), Direct observation of atmospheric aerosol nucleation, *Science*, 339, 943-946
- 3) Manish Joshi, B.K. Sapra, Arshad Khan, S.N. Tripathi, P.M. Shamjad, Tarun Gupta, Y.S. Mayya (2012), Harmonisation of nanoparticle concentration measurements using GRIMM and TSI scanning mobility particle sizers, *Journal of Nanoparticle Research*, 14:1268
- 4) Arshad Khan, Pampa Modak, Manish Joshi, Pallavi Khandare, Amruta Koli, Alka Gupta, S. Anand, B. K. Sapra (2014), Generation of high concentration nanoparticles using Glowing Wire Technique, *Journal of nanoparticles research* 16:2776

have been performed to validate codes based on general dynamic equation of aerosols. Experiments were performed with HWG aerosols in controlled chamber conditions under this work. In the first step, evolution of aerosol spectrum due to continuous injection of nuclei mode particles in a closed chamber was studied. Models predict a characteristic peaking effect due to coagulation at high concentration conditions⁷. In mixed chamber conditions, source injection is continuous while the background size distribution evolves simultaneously. Such condition involving aerosols of small as well as large sizes favours hetero-coagulation resulting in a characteristic peak.

The concentration was seen to be rising sharply due to the production of aerosols from the metal vapour to a peak value. Subsequently, the concentration decreases continuously without an indication of a steady-state, as being due to hetero-coagulation effect. The notable feature is the superimposition of sporadic concentration oscillations of decaying amplitude at multiple times. These small peaks in the decaying concentration may be attributed to build up of vapour pressure causing new particle formations. More than 90% of the increase in number concentration around these peaks was seen to be in particle sizes lesser than 10 nm resulting in a large decrease in geometric mean. The modification in the size distribution clearly indicated the role of nucleation induced generation captured by only lower size ranges.

Chapter 7, ‘Summary and Conclusions’ summarizes the key results and future scope for this work. This work started with conducting a case study with SMPS in order to harmonize and study issues related to measurement of ultrafine aerosol spectrum. It also focused on developing generator for production of nuclei mode aerosols and methodology to interpret measurement of aerosol size spectrum in

setup during the sampling. These measurements were carried out from 21st March to 28th March and then from 6th April to 7th April. Four days (for which 24 hour data was available): 23-26 March were selected as case days (when the fire was taking place intermittently) and two days i.e. 6-7 April were selected as control days for analysis. Integral number concentration was seen to be quite high during case days at many times. Subsequently, average size distributions (5-350 nm) for the whole day were compared. On control days, characteristic Aitken/accumulation peaks were noticed; however, number concentration was found to be highest at the lower size channels for 24-26 March. The next step i.e. studying size distribution evolution showed a clear formation of nuclei mode particles in the afternoon on these days. On the other hand, no such formation was noticed on 6th and 7th April. 3D contour plots were subsequently corroborated with time series of number concentration for identifying the peaks in number concentration profile due to increase in nuclei mode particles.

Subsequently, evolution parameters (coagulation sink, condensation sink, growth rate and formation rate) were estimated for all cases viz. Diwali 2012, Diwali 2013 and Deonar dump yard fire after identifying events (formation of particles) following standard criteria. These estimations were made based on the minimum detectable size (either 5 or 10 nm) for different cases. Growth rates of 0.17-0.73 nm/h⁻¹ were measured for events observed for Diwali while growth rates of 3.89-31.87 nm/h⁻¹ were seen for the case of fire. Only fire event was seen to be modifying the source rate to the atmosphere.

Chapter 6 of thesis ‘**Nuclei mode particles in confined Environments: case study 3- hot wire generated nanoparticle aerosols**’ discusses the results of the experiments performed in closed chamber conditions. Only few experimental studies

size ranges. Also, dynamics of nuclei mode particles in urban background conditions was studied. This study was performed during 26 October-13 November, 2013 (Diwali days: 3-5 Nov) where sampling was performed intermittently. Several instances of number concentration above 10^5 particles/cm³ were observed in which a few prolonged for sufficient time at high levels. Statistical analysis was performed on the measured data to interpret diurnal variations with respect to days as well as time periods within a day. Box-whisker plots for different modes distinctly showed highest 90th percentile of number concentration in accumulation mode. On comparing hourly averaged size distributions, midnight/late night nuclei mode formation for sufficiently longer times was noticed on several days.

Chapter 5 of thesis titled '**Characteristics of nuclei mode atmospheric particles: case study 2- large scale fire event**' focuses on results of another field campaign. This campaign was performed in March-April 2016 when large scale dump yard fire took place in Deonar region of Mumbai city. Although no gaseous measurements were performed directly on site, it was reported that trap gases such as methane got released to environment in sizable concentrations. Such atmospheric conditions may act as a precursor for atmospheric nucleation events particularly during noon times when the sun intensity is maximum (photochemical production). The aim in this campaign was 1) To measure atmospheric aerosol characteristics due to large scale fire event and 2) To identify nucleation events and estimate nucleation and growth characteristics of formed aerosols. The fire started on 20th March and continued with diminishing magnitude for a week. Sampling was performed from a high rise building situated approximately 5 km from the fire site. In contrast to previous two campaigns, M-DMA measuring down to 5 nm was also used in SMPS

fireworks bursting events were witnessed between 19:00-23:00 h on November 12-14, 2012. A marked increase in aerosol concentration (peak concentration 1.2×10^5 no/cm³) was observed at the time of firecracker bursting on Diwali night. Similar night peaks were also observed on pre and post Diwali nights as expected. It was noted that maxima in number concentration coincided with minima of geometric mean in time series of parameters, indicating the emission of aerosol particles in the ultrafine range. Increase in nucleation and small Aitken mode particles, formation of a distinct mode around 50 nm and shifting of coagulation peak was noticed while comparing night time average size distributions. Increase of particle concentration of size < 50 nm is in contradiction to most of the observations made worldwide for similar events. This is of relevance because short term air quality degradation due to fast evolution of ultrafine particle concentrations increases the deposition in alveolar interstitial region.

Size distribution evolution analysis was performed around each peak observed during sampling days. It was seen that characteristic Diwali size peak began around 60 minutes prior and became similar to background within 30 minutes after the peak time. In contrast, a similar peak observed at early morning time on a non-Diwali day followed a simple path where in number concentration for all size-ranges increased leading to peak-time size distribution which regained its pre-evolution shape in due course of time⁶. No distinct mode formation or signature was noticed for this case.

In the second campaign, measurements were performed at the same location but for more days around the festive period of Diwali 2013. Apart from confirming the new observations of previous campaign, target was set to interpret diurnal variations of atmospheric aerosol particles in nuclei, Aitken and accumulation mode

moderate and strong based on the growth of nuclei mode concentrations. Estimations of aerosol parameters, based on observations, were made using a model connecting growth rate (of observable size ranges), sink and nucleation rate. Connecting different dynamical processes, particle formation rates and growth rates (GR) have been calculated from the measured aerosol size distributions.

Chapter 4 of the thesis ‘**Characteristics of nuclei mode atmospheric particles: case study 1- firecracker events**’ is on results based on atmospheric measurements. Such measurements are routinely used to understand, validate and/or develop aerosol dynamics models which may also be coupled to global circulation models. Enormous growth in technology has enabled research based on measurements of aerosol particles having size down to almost nuclei size. Aerosol concentration in ultrafine range is of special concern due to possibility of higher deposition in deep lung airways. In the Indian context, atmospheric aerosol measurements, in terms of number distribution, have not been performed extensively. This study attempts to fill this gap by performing ambient aerosol measurements focusing on interpretations of ultrafine and nuclei mode particles. Two campaigns with different targets were carried out for this purpose.

In the first campaign, changes in atmospheric aerosol characteristics during episodic burst event (Diwali festival) were studied using SMPS measurements. Diwali is celebrated in India by burning firecrackers during the night for a few days. Measurements were made at approximately 50 m height in a high rise building. The focus was on measuring the changes in the ambient atmospheric aerosol concentration levels on and around the event days. Measurements were carried out for 6 days (November 10-15, 2012) with celebratory event on November 13, 2012. Most of the

was developed. A metal wire of low but sufficient resistance can be used as substrate for this generator. Flow rate of 1-1.5 Lmin⁻¹ and operative power of 30-35 Watts was found to be optimal for generating aerosol concentration more than 10⁷ per cm³ having geometric mean in the nuclei mode⁴. The high concentration nanoparticles generated can provide controlled and tunable source term to study coagulation effects. The developed generator was utilized for studying aerosol oscillatory effects as an effect of secondary vapour-aerosol (nucleation) dynamics. These experiments were performed in 3 chamber volumes viz. generator volume itself (0.45 L), small chamber (40 L) and large chamber (500 L).

Chapter 3 on ‘Nucleation parameters and their theoretical formulations’

focuses on theoretical foundations which were used for estimating required parameters from experimental observations. Coagulation sink for an event (evolving aerosol size distribution) determines how nm size aerosol particles are removed through coagulation while condensation sink determines how rapidly molecules will condense on pre-existing aerosols. Formation rate (cm⁻³s⁻¹) is generally used to determine rate of formation of minimum detectable size particles whereas growth rate (nmh⁻¹) is used to determine increase in the mean size of the aerosol spectrum. The minimum detectable size is usually larger than the critical cluster size. Hence, the nucleation rate which is formation of critical cluster size particles (cm⁻³s⁻¹), is best estimated by using models connecting these two sizes⁵. For defining a nucleation event in the atmosphere, different criteria have been developed. Such an event starts with the appearance of a distinct new mode of particles in the size distribution which must lie in the nucleation size range. Additionally, this mode must prevail over a time span of hours and must show the signs of growth. The events can also be classified as unidentified, weak,

Chapter 2 of the thesis discusses ‘**Techniques and Instrumentation**’ utilized during the course of the studies carried out. It discusses the principles and capabilities of instruments used to generate and measure ultrafine (and nanoparticle) aerosols. A study was carried out to understand the behaviour of nuclei mode particles in ambient atmospheric conditions. This can be used to interpret nucleation effects in presence of background aerosol particles. Another study focused on controlled chamber experiments where vapours/aerosols were generated and utilized for studying primary nucleation events as well as nucleation in presence of existing aerosols. SMPS with long (10 nm- 1 μ m) and/or medium (5 nm- 350 nm) Differential Mobility Analyzer (DMA) was used for studying atmospheric nucleation events (or nuclei mode evolution characteristics). Optical Particle Counter (OPC) was also coupled to size distribution measurement setup for covering aerosol particles up to 20 μ m for some cases.

As the ultrafine aerosol particles were measured using multiple SMPS units, a specific study was carried out for studying SMPS characteristics apriori. The main aim of this study was to harmonise the ultrafine particle measurements with different SMPS units. In these experiments, the performance SMPSs of two different makes viz. GRIMM and TSI were evaluated and compared. The concentration difference was also found to be size dependent becoming highest for nuclei mode particles³. An important outcome of this study was the development of standard protocols which were followed for all subsequent measurements involving multi-instruments.

To simulate freshly nucleated particles in laboratory conditions, it was felt necessary to generate aerosol particles via evaporation-condensation route. For this purpose, an electrical heating based aerosol generator (Hot Wire Generator, HWG)

studies have been carried out to study atmospheric aerosol loading events such as natural vapour to particle conversion process or anthropogenic injection of ultrafine particles into the atmosphere. Diwali (celebrated in India) is one such high aerosol concentration event where aerosols are generated/injected in atmosphere due to emission caused by burning of firecrackers. Very few studies (Indian and worldwide) have attempted to interpret the behaviour of ultrafine (and nuclei mode particles) during such events. A detailed analysis of size distribution (formation as well as evolution) can give better insights into prediction of inhalation hazard. Differences in number concentration peaks due to different sources (natural and anthropogenic) can be probed as well. Similarly, changes in atmospheric aerosol characteristics due to large scale fire is another domain where sufficient knowledge of formation of nuclei mode particles doesn't exist.

Natural atmospheric processes offer a way to study 'new particle formation events'². Instruments which are used to measure aerosol characteristics, as yet, are unable to visualise signals at critical formation stage, however, models exist to relate the growth and evolution of aerosol spectrum in observable range to the formation rate. Observing and interpreting nucleation events in the atmosphere is a recent highlighted domain in aerosol research. Atmospheric measurements performed during Diwali and large scale fire can be analysed in order to find formation rate of aerosols in such conditions. On the other hand, several studies are being performed in closed chamber conditions where aerosol effects under high concentration conditions are discussed. Controlled experiments in closed mixed chamber conditions can be performed for validating the predictions of aerosol dynamics models as well.

episodic events is difficult due to their weak signals and fast interaction with background aerosols. Nevertheless, they are an important source to study particle formations and subsequently estimating atmospheric loading. Number particle distribution evolution studies can be effectively used for probing dynamics of these freshly formed nuclei mode particles. Real scale atmospheric aerosol dynamics is highly complicated; hence, controlled chamber studies are often used to supplement the understanding on aerosol dynamic models aimed at estimation of nucleation rates and for validation of these models.

The contents of this thesis are focused towards studying the dynamics of nuclei mode particles formed in atmosphere and in controlled chamber conditions. As illustrations, aerosol emissions during fireworks (Diwali festival) and large scale fire episode were investigated and aerosol dynamic characteristics of these events were interpreted. Size distribution evolution of ultrafine particles was utilized to differentiate a normal and an episodic event. Coagulation sink, condensation sink, growth rate and formation rates of aerosols were estimated for different cases. A separate study was also carried out in closed chamber conditions with high (number) concentration of nuclei mode particles. Long term effects during evolution of these particles have been interpreted. This work carried out has been summarized in 7 chapters.

Chapter 1 titled “**Introduction**” focuses on literature survey discussing present state of understanding/knowledge related to number concentration characteristics of nuclei mode particles, in atmosphere as well as closed chamber (engineering) applications. Atmospheric aerosol measurements form an important database relevant for studies on inhalation toxicology and climatic effects¹. Several

SYNOPSIS

Aerosols are becoming increasingly relevant to society from air quality, public health, process engineering and climate change perspectives. Since, aerosol pollution is partly an inevitable by-product of meeting the energy, industrial and economic growth requirements of fast developing societies, multi-pronged approaches are required to address the adverse health effects, societal and environmental impacts and their mitigation strategies. An important step in this direction pertains to controlling emission at the source level. However, an unresolved issue pertains to the metric to be given priority, whether the emphasis should be on mass, surface area or number emission control. This understanding is crucial to predict their fate, be it their interactions or removal. In the recent years, there has been a shift of focus in aerosol characterisation from mass based measurements to number based parameters. Atmospheric aerosol size distribution can be broadly classified as consisting of nuclei mode (1-20 nm), Aitken mode (20-100 nm) and accumulation mode (>100 nm) with significant fraction of particles lying below 100 nm (called as ultrafine particles). The formation and evolution of aerosol particles in the ultrafine size range, down to about 3 nm, are studied by following their size distributions measured using Scanning Mobility Particle Sizer (SMPS).

Particles in the nuclei mode exhibit several interesting features which signal the formation of particles in the atmosphere. They act as cloud condensation nuclei and affect cloud microphysics. Episodic events such as celebratory fireworks, large scale fires, volcanic eruptions etc. can form particles in the nuclei mode. However, studies of nuclei mode particles are challenging due to difficulties in their measurements and interpretations. Identifying nucleation bursts resulting from

6.1 (b)	Experimental arrangement in 40 L chamber	140
6.2	Behaviour of continuously injected particles: coagulation peak	141
6.3	Experimental results for number concentration evolution in all chambers	143
6.4	Peaking for the case of smoke particles	145
6.5	Size spectrum evolution as a result of coagulation	146
6.6	Number concentration evolution: long term observations	148
6.7	Size distribution evolution for the case of Fig. 6.6	149
6.8 (a-c)	Selected secondary peaks in experiments	151
6.9 (a-c)	Abrupt change in size distribution near a minor peak	152

LIST OF TABLES

Table. No.	Description	Page No.
2.1	Measurement of aerosol characteristics	32
2.2	Parameters of the SMPSs used in the study	49
4.1	Size distribution characteristics (averaged over 4 hours)	88
4.2	Mass concentration of total suspended particles and elements	106
4.3	Event statistics (case study 1)	110
4.4	Formation and evolution characteristics of NPF events	111
5.1	Event statistics (case study 2)	133
5.2	Formation and evolution characteristics of NPF events	133
5.3	Formation and evolution characteristics of NPF events: Comparison of case study 1 and 2	134
6.1	Emission rate for nichrome wire used in HWG	144
6.2	Comparison of emission rate for incense stick and HWG (40 L chamber)	145
6.3	Size distribution parameters in different size ranges	147

4.22	Typical plot for coagulation and condensation sink: Time-series	112
4.23	Condensation sink and nuclei mode concentration	113
5.1	Time series of number concentration and geometric mean (all days of case study 2)	118
5.2	Case and control days: time profiles of number concentration and GMD	119
5.3	Time-series of temperature and relative humidity for case days	120
5.4	Wind-rose diagram for case days	120
5.5	Number size distribution for all days (averaged over 24 hours)	121
5.6 (a-f)	Size distribution evolution for case and control days: 4 hourly averages	122-123
5.7 (a-d)	Modification of size characteristics during day times for case days	124
5.8 (a-b)	Diurnal variation of number concentration (total and different modes) for case days 25 th and 26 th March	125
5.9 (a-b)	Diurnal variation of number concentration (total and different modes) for control days 6 th and 7 th April	126
5.10	Box-whisker plot for total number concentration: all days	127
5.11 (a-c)	Box-whisker plot for number concentration in different modes: all days	128-129
5.12	Corroborated number concentration and geometric mean for case days	131
5.13	Corroborated number concentration and size distribution for 24th March, a case day	132
5.14	Parameters during a qualified event	133
5.15	Typical plot for coagulation and condensation sink: time-series	135
5.16	Condensation sink and nuclei mode concentration	136
6.1 (a)	500 L chamber used in experiments	140

4.1 (a-b)	Time series of aerosol and meteorological parameters	80
4.2	Time series of number concentration (no/cm ³) as measured by OPC	82
4.3	3D plot of aerosol size distribution (all days)	83
4.4 (a-d)	Average number size distribution during the days of the study (averaged over 4 hours)	84
4.5 (a-h)	Hourly averaged size distribution for the time block 16:00-20:00 and 20:00-24:00 (all days)	85-86
4.6	OPC measured size distributions for time block 19:00-24:00 hrs: Comparison for all days	87
4.7 (a-d)	Evolution history of size distribution and wind-rose diagram for the days corresponding to peaks A and D of Fig. 4.1 (a)	90
4.8 (a-d)	Evolution history of size distribution at peaks B, C, E and F of Fig. 4.1	91
4.9	Time series of number concentration for all days	94
4.10	Time series of number concentration and mean size close to event days	94
4.11 (a-b)	4 hourly averaged size distributions for different days	95
4.12 (a-b)	Hourly averaged size distribution evolution on Diwali night	96
4.13	Size distribution evolution on a normal day	96
4.14	3D time series for size distribution for 2 nd November	97
4.15	Box-whisker plot for all days: Total concentration	98
4.16 (a-c)	Box-whisker plot for all days: Concentration in different modes	99-100
4.17	Diurnal variation of number concentration: Diwali day	102
4.18 (a-b)	Diurnal variation of number concentration: Pre and Post Diwali day	103
4.19 (a-b)	Diurnal variation of number concentration: Normal days	104
4.20	Corroborated number concentration and geometric mean	108
4.21	Illustrative example for a qualified event	109

LIST OF FIGURES

Fig. No.	Description	Page No.
2.1	Schematic diagram of cylindrical DMA	37
2.2	Photographs of GRIMM-SMPS (5.403) and TSI-SMPS (3775)	39
2.3	Hot Wire Generator in glowing condition	42
2.4 (a)	Effect of carrier gas flow rate on the output number concentration of the HWG for a fixed voltage of 7V applied to the metallic wire	44
2.4 (b)	Effect of applied voltage on number concentration	44
2.5 (a)	Short term output recorded at the exit of HWG	45
2.5 (b)	Long time stability of output from HWG	46
2.6 (a)	Size distribution of generated aerosol particles from HWG	46
2.6 (b)	Temporal stability of geometric mean size of the generated particles	47
2.7	Time series of particle concentrations recorded by all CPCs in ambient environment	49
2.8	Time series data of ambient number concentration for SMPS inter-comparison	50
2.9 (a)	Comparison of all CPSs by measuring number concentration of nebulised aerosol particles	51
2.9 (b)	Size distribution measured by GRIMM and TSI SMPS	51
2.10 (a)	Relating CPC differences with measured concentration	53
2.10 (b)	Effect of aerosol concentration on concentration ratio measured by GRIMM and TSI SMPS	54
3.1	Evolution of number size distribution at sampling site during a large scale fire event	60
3.2	Characteristics of nuclei mode particles at daytimes for same data as of fig. 3.1	61

properties of the aerosol particles. Operating parameters and characteristics of generated aerosols from hot wire generator developed under this work are discussed in detail. This chapter also presents results of a study performed to harmonise ultrafine particle concentration measurements with twin SMPS system. Terminologies related to nucleation parameters and their characteristics are presented in chapter 3. This chapter also discusses qualifying criterion for defining a new particle event and different models to estimate formation and evolution characteristics of freshly formed and/or observed nuclei mode particles. Chapter 4 of this thesis presents results from atmospheric aerosol measurements made during days of Diwali 2012 and Diwali 2013. Signature of Diwali emissions, distinction from background peaks and dynamics of nuclei mode particles for both the cases (Diwali and background) has been shown/interpreted in this chapter. Evolution parameters for selected new particle events from case studies are also presented. Characteristics of nuclei mode particles during a large scale fire event are discussed in chapter 5. Differences in number based statistical parameters for case (fire days) and control (background days) have been brought out. Identification of new particle events and estimation of their characteristics for this case have also been shown in this chapter. Chapter 6 of this thesis presents results from validation experiments conducted against theoretically predicted features for high aerosol number concentration conditions. Inferences from closed chamber experiments to study coagulation peaking effect and aerosol oscillatory effect are discussed in this chapter. Last chapter i.e. chapter 7 summarizes this work by providing summary of each chapter, conclusions drawn from this work and future scope of this work.

1.8 Objectives of this work

This study focuses on studying characteristics of nuclei mode particles in high concentration ambient and laboratory conditions. Following are the specific objectives of this work:

- 1) Harmonizing number concentration measurements with two SMPS units of different make for ambient low concentration and laboratory elevated concentration conditions.
- 2) Development of nanoparticle generator to be used as a source of nanoparticle/nuclei mode aerosols with controllable characteristics.
- 3) Number characteristic measurements of atmospheric aerosols at the time of fireworks during Diwali festival days for establishing signature features of Diwali induced aerosol emissions.
- 4) Differentiation of background and episodic events (similar on the scale of total number concentration) on the basis of size distribution evolution analysis.
- 5) Study of modifications in number concentration characteristics of atmospheric aerosol spectrum due to emissions from large scale fire.
- 6) Identification of new particle formation events during episodic and background events and estimation of formation and growth characteristics of generated nuclei mode particles.
- 7) Validation experiments for theoretical coagulation peaking effect and aerosol oscillatory effects in high number concentration conditions in closed chamber.

The work carried out to achieve these objectives has been presented in seven chapters of this thesis. The present chapter (chapter 1) introduces basic concepts, terminologies and facts in the context of the proposed work. Literature survey of studies conducted for atmospheric aerosol measurements, nucleation events and aerosol emissions due to celebratory firecrackers and large scale fires has been discussed in this chapter. Chapter 2 of this thesis discusses general techniques and instrumentation for generation and measurement of

concentration conditions expected in the case of aerosol pollution episodes can't be ruled out. A detailed study based on the dynamics of nuclei mode particles (involving formation and evolution characteristics) in background and elevated aerosol concentration environment is missing for Indian context.

Dynamics of high number concentration particles in controlled chamber conditions is utilized for studying their coagulation characteristics. Coagulation models predict a peaking in number concentration for continuous source scenario. Predicted behaviour of coagulating particles in closed chamber requires due experimental validations. For such controlled experiments, aerosol generator with tunable characteristics is desirable. Aerosol generation via glowing wire technique can be implemented as such a generator providing high concentration output in nuclei mode size ranges. Using such a generator, evolution of aerosol size distributions can be interpreted with focus on nuclei mode size ranges. Oscillations in number concentration have been studied theoretically and are an important phenomenon in the context of aerosol reactor applications. Utilizing controlled particle-vapour interactions in continuous source conditions, such aspects can also be validated experimentally.

Although SMPS (Scanning mobility particle sizer) is a commonly used instrument in aerosol laboratories worldwide, there are issues such as inter-instrumental harmonization which can be helpful for improving the precision of results of field campaigns employing multiple units. Differences in measured parameters for multiple unit tests/experiments have been reported. These differences depend on the concentration level being measured and are shown to be higher for laboratory generated high concentration conditions (in comparison to ambient aerosol concentration). An effort to harmonize number concentration measurements with SMPS can be made by performing experiments with twin SMPS units in different environmental conditions. Conclusions drawn from such study may strengthen protocols for SMPS based measurements.

1.7 Motivation

Significant amount of research has been performed to study the impact of aerosol emissions during celebratory fireworks on ambient aerosol characteristics. However, studies focused on aerosol number characteristics are relatively fewer, leading to contradictory conclusions as well. Increase of particles in accumulation mode size ranges is consistently observed but behaviour of ultrafine and nuclei mode particles is open domain to be investigated. Many of the measurement campaigns or experimental set-ups have been conducted/made near ground level or not at large heights. Changes in aerosol parameters for such a case don't represent the regional characteristics, appropriately. For a source term which is diversified (in comparison to that for local mass gatherings), measurements at sufficient height may provide better summary indices. In Indian context, few studies aimed at understanding aerosol number concentration evolutions during Diwali emission are conducted. Additionally, no effort has been made to delineate the dynamics of nuclei mode particles from the size distribution evolution data for such cases. For urban conditions where several background sources are present, total number concentrations at times are expected to be similar or even larger than that at the time of Diwali emissions. In such a scenario, size distribution evolution analysis around these number concentration peaks offer the novel way to distinguish an episodic and a background event. Similar study targets are applicable for the context of other episodic events e.g. large scale fire as well. Interpretation of complexities related to features of number concentration evolution for background aerosol spectrum has potential to offer new findings.

Background/normal as well as episodic events offers condition where number concentration in nuclei mode becomes quite high which can be studied in detail. Source rate of these small size range particles and their growth rate to higher sizes is an important input for atmospheric global circulation models developed for predicting climatic changes. Possibility of new particle formation during background aerosol conditions as well as high

differential mobility particle sizer and scanning electron microscope^{207, 208}. Differences in particle size parameters for aged and regional smoke has also been interpreted in some studies²⁰⁹⁻²¹¹. Fire emissions in Southeast Asia for years 1997-2006 were estimated combining satellite data and atmospheric modelling²¹². Up to 200 $\mu\text{g}/\text{m}^3$ of annual average PM_{2.5} was estimated for strong El Niño years in their work. Impact of fires on climatic changes has also been discussed²¹³⁻²¹⁵. Global estimates of fire emissions have been obtained in several studies^{199, 216, 217}. Contribution of different factors and global fire emissions for years 1997-2009 have been summarized²¹⁸.

Similar work has also been carried out for Indian regions with varied contexts. Intense crop residue burning is a regular activity during post-monsoon season mainly in northern India²¹⁹. Agricultural residue burning is the major cause of aerosol emissions in Indo-Gangetic region. Wintertime aerosol optical depth (AOD) increase coinciding with rice residue burning season was reported²²⁰ for their observations in this region. Changes in AOD values, Ångström exponent, PM_{2.5} concentration and aerosol index gradient due to paddy crop residue burning was measured using MODIS data²²¹. An increased AOD with peaking in the month of May for vegetation fires in the Himalayan region has been reported²²². Authors of this work also measured height of smoke plume using CALIOP retrievals. Emissions of aerosol chemical constituents from burning of biofuels and forest fires²²³ were estimated for the years 1996-1999. An integration of the inventory approach with high-resolution MODIS active-fire and land cover data for discussing emissions from open biomass burning in India has been discussed²²⁴. Higher concentration of black carbon during the forest fire season was measured in tropical urban region of Hyderabad²²⁵. Recent examples of severe air quality deterioration due to large scale fires include the example of New Delhi²²⁶ and Deonar dumpyard, Mumbai²²⁷.

For Indian context, although several studies have been conducted for measuring mass loadings and changes in chemical characteristics, an extensive campaign for studying effect of fireworks on number characteristics is missing. Short term or long term measurements are required to delink natural diurnal variations with the spikes expected during Diwali emissions.

1.6 Aerosol emission due to large scale fires

Atmospheric budget of trace gases and aerosols gets hugely influenced by fires¹⁹⁵. Wild fire, coal burning and burning of wood fuel are primary sources of organic carbon which is significant component of atmospheric carbonaceous aerosols^{196, 197}. One of the main global sources of natural aerosol load is biomass burning. It is also estimated to be an important atmospheric source of heavy metals and black carbon. Causes of other fires affecting the background aerosol characteristics include crop residue burning, vegetation burning and accidents. Chemical composition of directly emitted aerosol particles from vegetation fires in Amazon basin was measured¹⁹⁸. A similar effort for the case of aerosol emissions from Savanna fires in southern Africa was also made¹⁹⁹. Aerosols were measured to be mainly composed of organic and black carbon. Emission of aerosol particles due to vegetation burning in southern hemisphere Africa was discussed²⁰⁰. Satellite and ground-based observations were combined to develop a modelling framework to estimate emissions from fires in North America²⁰¹. An overview of vegetation fire emissions, their environmental and climatic impacts has been presented elsewhere²⁰².

Physical properties of biomass burning particles have been reviewed²⁰³. Smoke particles generated from biomass burning have 80-90 % of volume in the accumulation mode and are composed of 50-60 % organic carbon and 5-10 % black carbon²⁰³. These particles have been shown to possess various morphological forms for different studies²⁰⁴⁻²⁰⁶. Dry particle size distribution has been measured in several studies using optical particle counter,

Wen and Chen¹⁵⁸ observed a significant increase of ultrafine number concentration in their study on firework emissions during Chinese new-year celebration. An increase of number concentration in this size-range (apart from usual signature in accumulation mode) was obtained (sampling height during measurements~ 32 m) but was related with local activities¹⁶². Although reduction of nuclei mode particles has been related to the large values of sinks, evolution of particles in ultrafine and nuclei mode size ranges is a debatable issue. Barring a few studies, sampling arrangement for measuring number characteristics were set up at near ground level in these measurement campaigns. The possibility of missing changes in atmospheric characteristics occurring at slightly elevated heights (possible for aerial fireworks) can't be ruled out. Additionally short term modifications (if any) due to such events represent regional characteristics only for representative measurements at sufficient heights.

A comparison of mass concentrations due to aerosol emission from Saharan dust outbreak, a windy day and a firework display in Spain was presented¹⁹⁴. Although TSP was measured at 35-40 $\mu\text{g}/\text{m}^3$ for these events, mass size distributions were found to be distinctly different. Fireworks were related to the liberation of particles lesser than 0.5 μm . PM levels and chemical compositions during fireworks can also be similar to that due to other sources such as industrial emissions. The situation is tricky considering the large background pollution levels for an urban environment. Complexity further increases when modifications in number concentration and number size distribution profiles are aimed to be studied during the times of emissions from fireworks. It is quite possible to get high number concentration peaks (similar to that expected during fireworks) in background aerosol number profile for a megacity. In that case, evolution of number size distribution near the appearance of such peaks holds the key.

concentration of anions and cations during Diwali emissions was done from collected PM_{2.5} and PM₁₀ samples¹⁸⁶.

An important observation is related to the small build-up of ozone which could not be correlated with NO_x concentration on Diwali night¹⁴⁶. 1.2-3 times increase in ozone and black carbon concentration during the festival period is also reported¹⁸⁷. An elaborative chemical characterization including carbonaceous fractions of elemental and organic carbon and water soluble ionic species during Diwali has been done¹⁸⁸. A study to compare the characterization of major pollution events (dust storm, haze, Diwali and Holi) was conducted for Agra region¹⁸⁹. In this work, highest concentration of carbonaceous aerosols was detected during Holi while highest secondary organic carbon concentration was measured during haze (haze > Dust Events > Diwali > Holi). A short term marginal impact of Diwali fireworks on PM₁₀ characteristics was noted in rural Brahmaputra valley¹⁹⁰. Radiative impact of aerosols emitted by fireworks has also been discussed¹⁹¹ on the basis of their measurements in Indo-Gangetic plain. Particle's morphology plays an important role towards dynamic evolution and deposition. Particles sampled during and after Diwali were found to have non-spherical multi legged structure¹⁹².

In comparison, fewer studies have been conducted to investigate evolution of number characteristics during Diwali^{63, 156, 193, 194}. Mazumdar and Nema¹⁵⁶ discussed temporal variability of number concentration due to the wide source term in their study conducted in Nagpur. Aerosol number concentration values were compared for contrasting events: dust storm and Diwali¹⁹³.

1.5.3 Gaps in related studies

An increase in large Aitken and accumulation mode particles with simultaneous death of nucleation and small Aitken mode particles⁶³ has been observed and made part of conclusions in most of the studies discussed in the above section^{154, 159, 160, 162}. However, on the contrary,

1.5.2.2 Indian context

An equally significant amount of research has also been carried out in India in order to study the environmental perturbations due to aerosol emissions from fireworks. It is to be noted here that a striking difference of using fireworks (particularly during Diwali festival) in India is large scale utilization and multipoint source term conditions. It is different to the scenario where fireworks are displayed at a common place in mass gatherings. Most of the Indian work in this subject is focussed on measuring mass and chemical characteristic changes during burning of firecrackers and subsequently interpreting the effects.

Increase in PM₁₀ (Particulate matter: mass concentration of particles lesser than 10 μm diameter) concentrations by up to a factor of 5 during Diwali was observed in Kolkata¹⁸¹. Al, Zn, Pb and Cd were shown to be increasing 5-12 times; Cu, Fe and Mn 25-40 times and Co and V 70-80 times on Diwali night compared to a normal night in their work. PM₁₀ increased by a factor of 2-7 in day-time and night-time during a study conducted during Diwali in Lucknow¹⁸². In this study, trace metals (Ca, Fe, Zn, Cu, Pb, Mn, Co, Cr, Ni, Cd) associated with PM₁₀ were also measured. Metal concentrations in ambient air were observed much higher as compared to background values on previous days in a study performed in Hyderabad¹⁸³. Concentrations were measured to be higher than industrial sites for some of the metals with K at the highest concentration level during the event. Sarkar et al.¹⁸⁴ commented that pollutant cocktail generated by Diwali fireworks could be best represented with Ba, K and Sr as tracers on the basis of their campaign conducted in Delhi. They also quantified (2%) increase in non-carcinogenic hazard index associated with Al, Mn and Ba in the exposed population due to chronic exposure of Diwali pollution. In another study conducted in the same region, significant increase of elements (Sr, Ba, Ti, Mg, Cu, K, S, V, Cl, Bi, Ga) produced by firework combustion was observed¹⁸⁵. Characterization of ionic

was compared with that of firework and bonfire contaminated aerosol samples collected from Spain and London¹⁶⁴. Ba, K, Sr, SO₄²⁻, NO₃⁻ concentrations during bonfire nights was observed to be 5 times higher than background for Beijing lantern festival¹⁵². Presence of potassium, sulphate, total organics and chloride and increased trace gas mixing ratios of methanol, acetonitrile, acetone and acetaldehyde were observed in a study carried out during New Year celebration in Mainz, Germany¹⁴⁹. Significant increase of Mg and Al during holiday period arising from the discharge of fireworks in lower atmosphere was noticed¹⁶⁵. Octachlorinated dioxins, furans and hexachlorobenzene were measured by blowing blue-lighting rockets and fountains in a laboratory experiment¹⁶⁶.

The effect of firework prohibition on air quality has also been studied¹⁶⁷⁻¹⁶⁹. Real time monitoring of aerosol emissions during such episodes has been carried out¹⁷⁰. A detailed composition data and comprehensive analysis of the aging processes of particles emitted during Chinese spring festival has been presented¹⁷¹. PM oxidative burden and individual trace metals are shown to be correlated during celebratory events¹⁷². The impact of aerosol emissions resulting in health hazards, accidents, injuries and visibility reduction has been studied separately¹⁷³⁻¹⁷⁹. An overview on possible hazards arising from fireworks has been provided elsewhere¹⁸⁰.

Number characteristics of atmospheric aerosols during Diwali event in New Delhi were studied⁶³. In this study, authors tried to explain the non-existence of nuclei and Aitken mode particles and shifting in accumulation mode on the basis of coagulation and condensation sink values. These authors also studied diurnal variations of number size distribution (3-800 nm) and modal parameters for New Delhi in their measurement campaign conducted for 2 weeks⁶⁴. They estimated formation rate and growth rate of nuclei mode particles on the basis of inferences from the measured data.

emissions include mainly ozone, nitrogen oxides, sulphur dioxide and aerosol particles¹⁴⁶⁻¹⁴⁸. As this work is focused on the physical characterization of emitted particles, this section mainly focuses on the knowledge gathered on aerosol characteristics (including mass and chemical composition).

1.5.2.1 Worldwide picture

Changes in the particulate matter (PM) levels, chemical characterization and the emission of metals have been associated with Diwali festival. Studies have been performed worldwide linking the festival/celebration activities to the aerosol loading of atmosphere¹⁴⁹⁻¹⁵². These studies have well-established outcome in terms of increase in PM as well as metal concentrations and their deleterious effects on health¹⁵³. PM concentrations in different size cut-off ranges have been shown to be increasing as an effect of fireworks¹⁵⁴⁻¹⁵⁹. Relatively fewer studies have been performed to study the change in number concentration and size distribution evolution. Mainly emissions during fireworks have been seen to be modifying number concentrations and number size distributions in entire size range. Number concentration during such events has been shown to be increasing several times above the control level¹⁶⁰. Increase of number concentration in accumulation mode and shift of particles from nuclei and Aitken mode at the time of event has been noted¹⁵⁹. Accumulation mode particles have been shown to be most affected by firework activities by several researchers^{148, 154, 161, 162}.

Several studies have been performed in order to measure change in chemical compositions of aerosol particles during fireworks. SO₂, CO, Cl⁻, NO₂⁻, SO₄²⁻, Na⁺, K⁺ and Mg²⁺ were measured as primary emissions in PM 2.5 (Particulate matter: mass concentration of particles lesser than 2 µm diameter) generated due to the combustion of black powder¹⁵⁸. Increased levels of barium (Ba) in snow during snowfall after firework episode were reported¹⁶³. Chemical composition of aerosol particles collected during Las Fellas celebration

oxidizers (nitrates, chlorates or perchlorates) for providing oxygen, phosphorus for glow effects and zinc for creating smoke effects are used in making firecrackers.

Ejection of by-products containing above mentioned chemicals in gaseous and aerosol form is a hazard issue which has forced regulators to keep a close view on their levels and characteristics. Potential toxicity of burning firecrackers/fireworks depends on the composition of the device and the amount of black powder used as the primary component. People suffering from asthma, chemical sensitivity, skin allergies and heart diseases are most susceptible to the effects due to inhalation of smoke generated during fireworks. On the basis of research focused on estimating health risk due to usage of fireworks, several countries have made regulations to limit their quantities, control emissive characteristics and reduce exposure of humans.

Apart from using firecrackers for other purposes, Indian people use these at large scales during Diwali, the festival of lights. Variety of firecrackers in the form of fountains, ground spinner, sparklers, rockets, snakes, wheels, sound crackers, pencil and garlands etc. are used in plenty as essential part during weeklong celebrations. Due to such large utilization, turnover of Indian fireworks industry grows each passing year. In recent times, public perceptions about the involved hazards have also risen. In spite of this, it is a normal phenomenon to get a severely affected air quality during and after Diwali celebrations. All leading newspapers/websites highlight this aspect each year by publishing many articles¹⁴⁴,¹⁴⁵. Central agencies e.g. pollution control board and various judicial agencies debate this subject frequently and intensively in order to safeguard public and cultural interests both at once.

1.5.2 Current state of knowledge

Many measurement campaigns conducted worldwide and in India have enabled researchers to gather enough knowledge about the hazard due to emissions from fireworks. Overall,

1.5 Aerosol emissions due to celebratory firecrackers

Emission of aerosol particles during fireworks has been well studied due to their impact on the air quality. Smoke generated from the burning of firecrackers induces short term air quality degradation. Sometimes it leads to visibility reduction and severe air pollution for several days as well. Firecrackers are burned in large quantities during mass gatherings to celebrate events such as New Year day, marriage, sports etc. In India, Diwali festival is celebrated by using fireworks at much larger scale where whole city/town/village/locality participates. Air pollutants including suspended particulate matter emitted due to fireworks modify the atmospheric air characteristics. Conclusions gathered on the basis of measurement and interpretation of such modifications has become a crucial study database for researchers, public and policy makers at large.

1.5.1 Mechanism and facts

Fireworks or firecrackers (low explosive pyrotechnic devices) are used to produce noise and light for aesthetic and entertainment purposes. These are tuned to provide coloured flames and sparks for illustrative display purposes on ground or aerial route. Their origin can be traced to 7th century in China and are used worldwide to mark significant events, celebrations, rituals, competitions and festivals. Fuel, oxidizer, colour producing chemicals and binders are essentially used as components of these devices for producing visual and sound effects. However several gases, particles and fliers also get emitted to the environment as by-products, many times in hazardous levels. Strontium-lithium (red), calcium (orange), sodium (yellow), barium (green), potassium-rubidium (violet), cesium (indigo), copper (blue), titanium-aluminium-magnesium-beryllium (white) and charcoal-iron (gold) are used as compounds or powders for colour effects in firecrackers. Additionally black powder (mainly carbon, sulphur) as propellant providing fuel for burning, iron for producing sparks,

Nuclear Research). The present estimate of the size at which atmospheric nucleation occurs is 1.5 nm (± 0.4 nm)⁷⁰.

In a study performed in New Delhi⁶³ at the time of Diwali, high concentration of accumulation mode particles was recorded. Huge drop in nuclei and Aitken mode particles was also noted which was explained by authors on the basis of substantial coagulation sink values viz. $0.673\text{--}2.04 \times 10^{-4}$ per sec for particles of diameters 1 to 100 nm and high condensation sink values viz. $0.075\text{--}1.29 \text{ s}^{-1}$.

1.5.3 Importance and scope for further studies

15-55 % of global CCN population is contributed by NPF¹³⁹. It is an important source of aerosol particles on a global scale^{140, 141}. Although experimental measurements of atmospheric NPF events are constantly building an accurate database, understanding of nucleation mechanisms is still limited resulting in several discrepancies. The prediction of atmospheric nucleation events needs to be improved by advancing (or adopting better techniques) modelling of process/phenomenon. Kinetic treatment of nucleation process based on the measured thermochemical data for the cluster formation may lead to considerable improvement over the classical nucleation theory¹⁴². It is equally important to perform field measurements and laboratory experiments at different locations by targeting physical as well as chemical characteristic measurements below 2.5 nm. Improved parameterizations of aerosol nucleation and understanding of growth is required to be implemented in regional and global atmospheric aerosol models¹⁴³. Apart from the natural atmospheric processes, evidences of NPF are needed to be collected for anthropogenic activities. Experimental observation of NPF during fireworks and fires has not been investigated and measurements are required to probe this domain. Only few studies for observing NPF in atmospheric environment of Indian locations have been performed. Any future work carried out in this direction may contribute towards the local and global balance equation for aerosol dynamics.

1.4.2 Characteristic features

Formation rate of new particles has been shown to be correlated with the gas phase sulphuric acid¹²⁸⁻¹³¹ and surface area of background aerosol population¹³². Ions¹³³, ammonia¹³⁴ and organic compounds¹³⁵ have also been seen to affect the formation and growth dynamics. Meteorological conditions¹³⁶, traffic/power plant and long range transport can be related to observed NPF events⁷⁹. Nucleation bursts were seen to be mostly occurring on sunny days¹³⁷. Different chemical species may take part in nucleation and growth⁶⁶. In long term campaigns, many days are found where significant aerosol formation happens. In SMEAR (Station for measuring Ecosystem-atmosphere relations) II campaign, 24 % of days (out of 8 year data) resulted in events mostly during springs and autumn⁹⁶. Particles formed at nuclei mode grow to Aitken mode within a span of hours. Formation rate of 3 nm particle was estimated to be in the range $0.01\text{--}10\text{ cm}^{-3}\text{ s}^{-1}$ in the boundary layer, up to $100\text{ cm}^{-3}\text{ s}^{-1}$ in urban areas and $10^4\text{--}10^5\text{ cm}^{-3}\text{ s}^{-1}$ in coastal areas and industrial plumes, respectively⁸⁴. Growth rates for these cases were estimated to be in the range of $1\text{--}20\text{ nm h}^{-1}$ in mid-latitudes reducing to as low as $0\text{--}1\text{ nm h}^{-1}$ in polar areas. Growth of nuclei mode particles can be described by diffusion/kinetically limited condensational process⁷⁹. The growth of particles can be studied either by graphical method or by numerical simulation of aerosol evolution and fitting simulated distributions to the data. However for particles smaller than 5 nm, graphical method results in significant errors. Growth rates coupled with vapour measurements are required to reduce the uncertainty of estimated parameters. Concentration of acid vapours and number concentration was linked to estimate growth rates⁸⁵. Recent approaches to estimate nucleation parameters in atmosphere include gaseous and ion measurements apart from aerosol measurements. NPF is also found to be proportional to negative ion concentration¹³⁸. Particles of 1.7 nm diameter have been used to determine nucleation rate in recent CLOUD (Cosmics Leaving Outdoor Droplets) experiment at CERN (European Organization for

coupled to three mode integral aerosol dynamics model was used to simulate formation of $\text{H}_2\text{SO}_4\text{-H}_2\text{O}$ particles in rural, urban and marine conditions¹¹⁷. Some models have also been developed in which electrical processes are included^{113, 118}. Different simulation schemes have also been developed for solving aerosol dynamical equation for such contexts. Some of these offer simulation tool¹¹⁹ which can be used for understanding the role of complex atmospheric dynamics in studying nucleation bursts. As observance of NPF is at diameters which depend on the minimum size range of detection, theories also connect real nucleation rate (NPF at critical cluster size) and apparent nucleation rate (NPF at observable size). Formulations which can be used for connecting real and apparent nucleation rates are discussed in detail in chapter 3.

Very recent developments are related to observations down to 1 nm mobility diameter comprising of 3 size ranges below 2 nm⁷⁰. This study showed that organic compounds play important role in atmospheric aerosol formation. Parametric values and problems related to the formation and evolution parameters of around 100 studies conducted worldwide have been combined⁸⁴. Models for simulating atmospheric nucleation are also compared¹²⁰⁻¹²³. A review of particle formation events and growth in the atmosphere in various environments and mechanistic implications has been done¹²⁴.

As the nucleation and growth of new particles seem to occur almost everywhere in the atmosphere, better understanding of new particle production is crucial for global and regional climate models¹²⁵. An instrumental setup to measure atmospheric concentrations of both neutral and charged nanometer-sized clusters aimed at making direct measurement of atmospheric nucleation has been introduced¹²⁶. Discussion of instruments, reliability of methods, requirements for proper measurements, data analysis and protocols have been presented¹²⁷.

aerosol particles in different seasons. For instance in continental environment, particles grew by condensation of low pressure vapours formed by gas phase homogeneous chemical reactions during summers while due to the condensation of low pressure vapours and heterogeneous oxidation of aerosol precursor gases inside the liquid droplet during winters⁹⁷.

Gas to particle conversion in atmosphere occurs via various chemical mechanisms⁹⁸.⁹⁹. Understanding of these mechanisms is important as it is directly linked to the formation of sulphuric acid and sulphate particles from sulphur dioxide emitted from natural and anthropogenic sources. Due to the large values of sinks, identification of NPF is difficult in urban locations¹⁰⁰ and therefore relatively lesser experiments have been performed at these locations. Nevertheless, NPF has also been observed at urban locations such as New Delhi⁶⁴, Atlanta⁷⁶, Birmingham¹⁰⁰, St Louis¹⁸, Pittsburg¹⁰¹, Mexico¹⁰² and Beijing¹⁰³ etc. Formation of new particles can also occur on a larger regional scale¹⁰⁴⁻¹⁰⁷. Mostly these kind of observational studies rely on continuous size distribution measurements in the form of field campaigns. A campaign at Boreal forest measurement site at Hyytiälä Finland was carried out where size distribution was continuously measured for 8 years (1996-2003) in the size range 3 nm- 500 nm⁹⁶. Regional NPF in urban and background environments in North China plain has been studied¹⁰⁸. In their work, precursor gases and high condensational sinks were shown to be characterizing NPF.

Aerosol growth mechanisms and growth laws have also been developed^{109, 110}, simultaneously. In atmosphere, different nucleation mechanisms e.g. binary water–sulphuric acid nucleation¹¹¹, ternary water–sulphuric acid–ammonia nucleation¹¹² and ion-induced nucleation¹¹³ have been used to simulate NPF. Organics are also shown to be contributing towards growth of nucleated particles^{114, 115}. Kulmala et al. ¹¹⁶ developed a set of equations from the parameters of evolving size distribution, which are frequently used to estimate properties of newly formed particles. An atmospheric chemistry gas phase box model

not available for episodic events (e.g. burst releases due to fireworks, biomass burning, large scale fires etc.).

1.4 Nucleation events in atmosphere

In recent times, significant amount of progress has been made towards studying and understanding formation of aerosol particles in atmosphere. This domain of research is important with regards to several deliverables. A precise prediction and understanding of number and properties of cloud condensation nuclei is an important factor towards reducing the existing uncertainty in aerosol radiative forcing calculations. As ambient atmospheric aerosol formation acts as a global source of aerosol population, its observation is the first step for utilising this information for other purposes. Direct observation of atmospheric aerosol formation is made possible with advanced instrumentation and techniques in recent past. New particles formed in atmosphere grow as a result of aerosol dynamical processes to Aitken and accumulation size ranges where they interact with radiation in direct/semi-direct/indirect ways. Several field campaigns have been performed in order to pick new particle formation (NPF) events in atmosphere. Simultaneously, theoretical models have also been developed to simulate the formation and evolution characteristics of freshly formed particles.

1.4.1 Literature Survey

Appearance of ultrafine particles growing to sizes where they can have climatic impacts has been observed and studied in remote boreal forest⁷⁹, heavily populated urban site⁶⁴, Antarctic areas⁸⁰, coastal boundary layer⁸¹, industrialized agricultural region⁸², mountains⁸³⁻⁸⁵, stratosphere⁸⁶, remote polar area⁸⁷ and sub-Arctic Lapland⁸⁸. New secondary particle formation bursts occur frequently in the atmosphere⁸⁹. Role of biogenic aerosols in NPF has been interpreted^{90, 91}. In studies conducted in free troposphere, a large number of nuclei mode particles has been detected⁹²⁻⁹⁵. The effect of seasons on NPF has also been investigated in several studies^{66, 96, 97}. Atmospheric processes differ in affecting the formation and growth of

foggy and non-foggy periods were made in Kanpur region⁶⁵. At the same location, seasonal variation of size segregated number concentration of atmospheric aerosols was interpreted⁶⁶. Authors in this work discussed the role of new particle formation by studying the deviations in the ratio of Aitken to accumulation mode particles.

1.3.2 Measurement of ultrafine and nuclei mode particles

Measurement and characterization of ultrafine and nuclei mode particles of atmospheric aerosol spectrum holds crucial significance due to their higher lung deposition fractions. As surface of ultrafine particles can carry higher toxicity⁶⁷, exposure of ultrafine particles is a concern. Also since mass of particles in this size range is negligible, number concentration and chemical composition measurements become the necessary option. Counting of particles in this size range was made possible as early as 1930s⁶⁸ while size distribution measurements started after few decades with mobility and optical analysers. Low pressure impactors⁶⁹ have also been designed enabling determination of particle's chemical composition in ultrafine size domain. Technological advancement made in recent few decades have made it possible to detect particle dimensions just above the molecular size⁷⁰ as well as precisely resolved chemical compositional measurements⁷¹⁻⁷² in this size range. Several studies have been performed specifically to target aerosol properties in ultrafine and nuclei size ranges⁷³⁻⁷⁴. Combustion products from mobile source emissions (automobile exhaust) generate ultrafine particles in atmosphere which include metals, elemental carbon and organic compounds^{19, 75-76}. Traffic has also been linked with the source of nucleation mode formed in atmospheric aerosol size distribution^{16, 18}. It has also seen to be contributing towards the increases in ultrafine particles in urban conditions^{17, 77}. Exposure assessment for atmospheric ultrafine particles and implications in epidemiologic research has been discussed⁷⁸. Although a lot of studies focus on background atmospheric aerosol measurements, similar kind of database is

1.3.1.2 Indian studies

In India, aerosol characteristic measurements started three decades earlier in southern cities³⁶⁻³⁸ which later expanded to other regions³⁹⁻⁴⁸. In classic Indian Ocean experiment³⁷, regional aerosol loading for Indo-Asian haze was estimated by integration of satellite, aircraft, ship, ground and balloon observations. Focus of atmospheric measurements shifted to Indo-Gangetic region⁴⁹⁻⁵² where both population and pollution is higher compared to other Indian regions. Increase in pollution level and aerosol loading over the Ganga basin using POLDER (Polarization and Directionality of the Earth's Reflectance) data has been demonstrated⁵³. Sulphate aerosols formed due to anthropogenic activities are shown as major pollutant in this region⁴⁶. Chakraborty and Gupta⁴⁹ showed crustal elements (Ca, Mg and Fe) as main contributor to elemental concentrations in PM₁ (Particulate matter: mass concentration of particles lesser than 1 μm diameter) for Kanpur. Measurements of EC (Elemental carbon), OC (Organic carbon) and water soluble ionic species in ambient aerosols collected from Hisar and Manora peak was made⁵⁴. Higher OC/EC ratio reflected the contribution of biomass burning sources for urban sites in comparison to rural sites⁵¹. Above mentioned studies focused on mass characteristics, determination of chemical composition and radiative properties of atmospheric aerosols. Cloud condensation nuclei measurements for ambient atmospheric aerosols have been performed in a number of studies⁵⁵⁻⁵⁸.

Aerosol number characteristics were determined over Indian Ocean and Arabian Sea via field campaigns⁵⁹⁻⁶¹. As a part of Indian Ocean Experiment (INDOEX), number concentration and size distribution of aerosols representing northern Indian Ocean were measured⁶². Elevated concentration of nucleation mode particles in a layer between 8 and 12.5 km height was noted in the constructed vertical profile of number concentration. Measurements of aerosol number concentration were performed in New Delhi for the year 2002⁶³⁻⁶⁴. Real-time measurements of chemical characteristics of ambient aerosols during

interpreted on the basis of results obtained from measurement campaigns. Number concentration characteristics of airborne particulates for different locations e.g. Birmingham⁹, Taipei¹⁰, European cities¹¹ and Germany¹² etc. have been studied. An extensive database for background aerosol number characteristics for urban conditions is available in literature^{9, 13-18}. A comprehensive study focusing on the characterization of aerosols in a subtropical urban atmosphere was carried out¹⁹. Such studies have also been extended for other environmental conditions such as rural background²⁰⁻²¹, polar background²² etc. In the similar way, mass characteristics of atmospheric aerosols have been measured and interpreted for different background conditions. Measurements of chemical components of aerosols have been done by using gross collectors, impactors and aerosol mass analysers in contrasting environments. Dodd et al.²³ performed chemical analysis of size-segregated atmospheric aerosol samples in rural conditions. Parametric inferences for chemical characterization of atmospheric aerosols in Sapporo was done by Ohta and Okita²⁴. Noble and Prather²⁵ measured compositionally resolved particle size distributions of ambient aerosol particles. Few studies have also been carried out in order to measure simultaneous properties e.g. number distribution and chemical composition of atmospheric aerosol particles²⁶⁻²⁷. Hygroscopicity and cloud condensation potential of atmospheric aerosol particles have been studied in a number of studies²⁸⁻³⁰. Extreme events such as haze have also been characterized for various purposes by studying light scattering and extinction data³¹⁻³⁴. Aerosol size distribution in Arctic haze was measured in Polar Sunrise Experiment³⁵. Many programs, techniques and instruments such as AVHRR: Advanced Very High Resolution Radiometer , AERONET , CALIPSO (CALIOP- Cloud-Aerosol Lidar with Orthogonal Polarization), CERES- Clouds and Earth's Radiant Energy System, MODIS-Moderate-Resolution Imaging Spectroradiometer etc. are conducted/utilized for the characterization of atmospheric aerosols. This is done by coupling satellite observations with in-situ experimental data and algorithms.

nucleated particles and their growth rates are coupled to quantify the formation characteristics of atmospheric aerosols. Near source monitoring of aerosol particles is challenging for high concentration sources (such as forest fire) and models are developed for linking measured evolving size distributions at far sites with that at the source term.

1.3 Atmospheric aerosol measurements

Atmospheric aerosol particles contain water, non-volatile species (e.g. soot, metals, crustal oxides and salt) and semi-volatile compounds (nitrates and organics). The distribution of semi-volatile compounds between the gas and particle phase varies with the amount of available particulate matter on which they can accumulate, the thermodynamic properties of the semi-volatile compounds, and the gas and particle composition⁵. Discussions on the fixed-point sampling pertaining to the sampling inlets, media, methods, uncertainty etc. have been presented⁶. McMurry⁵ supplemented it with the measurements made via aircraft sampling in his review work focused on measurements of aerosol physical properties, chemical composition, calibration issues and reference methods. Deshler⁷ reviewed studies focused on characteristics of global stratospheric aerosols. Aerosol networks such as AERONET (Aerosol Robotic Network⁸) etc. provide valuable database from long-term observations of particle's property of interest.

1.3.1 Literature survey

1.3.1.1 Worldwide studies

Several studies for atmospheric aerosol measurements have been performed world over focusing on varying aspects. The complexity in terms of covering wide size range of atmospheric aerosol particles has been handled by utilizing instruments working on the basis of size dependent techniques. Both manual and automated methods are employed and integral as well as size segregated analysis has been sought for the determination of property of interest of aerosol spectrum. Site specific characteristics of atmospheric aerosols have been

and incorporation of different evolution processes; atmospheric aerosol distributions consist of number of modes. Nucleation mode (size range $\approx 1-20$ nm) represents the size spectrum of freshly formed particles via gas to particle conversions. These particles grow due to condensation of water-vapour and other process gases and self-coagulation to Aitken mode (10-100 nm). Accumulation mode (100-1000 nm) gets formed by coagulation and condensation processes of the particles in the sub size ranges and by primary emissions. Coarse mode (> 1000 nm) represents particles formed due to dynamical evolution of fine particles as well as primary particles (e.g. dust). Size distribution also gets modified by evaporation processes where mass gets transferred from higher to lower size ranges. Some other sub-division modes (small Aitken: 20- 50 nm and large Aitken: 50-100 nm) and process modes (e.g. droplet sub-mode) are also used, wherever applicable.

In general, atmospheric aerosol mass size distribution consists of two modes formed in accumulation ($\approx 0.1-2$ μm) and coarse ($\approx 2-50$ μm) size ranges. In contrast, number size distribution for atmosphere is mostly dominated by contribution in nucleation mode with almost negligible fraction of particles in the coarse mode size-ranges. Number size distribution for urban aerosols is dominated by particles in the nucleation and Aitken mode. For marine atmospheric aerosols, it is characterized by three modes in Aitken, accumulation and coarse size ranges³. Size spectrums (number, surface area and mass) are distinctly different for rural continental, remote continental, free tropospheric, polar and desert background conditions⁴. Apart from that, concentration values for these regions are diverse and could be highly variable spatially and temporally. Measurement of concentration in different modes and modification of size distribution is the key component for source identification and source-receptor modelling. A lot of studies in recent times have been focused on the measurement of aerosol characteristics in nucleation mode which is made possible due to the rapid advancement in instrumentation capabilities. Formation rate of

(μm) micrometre (rain drops). Governing laws for aerosol dynamics change with size-ranges resulting in complexities. Relative length scale (ratio of particle size to characteristic length of medium/air) affects the behaviour of particles in the medium modifying their evolution characteristics. Dynamic evolution of aerosol particles from source to receptor is an important component of methodology for determining their impacts. Aerosol concentration is the next important characteristic which quantifies intrinsic dynamic evolution of system as well as extrinsic features (e.g. deposition and exposure). Measurement of offline/online chemical composition of particles is needed for accurate understating of phase change processes. Mass concentration of chemical components of aerosol particles could also be a concern if release is more than the safe limits. It becomes crucial for some contexts in terms of hazard estimations, e.g. aerosol generation due to sources such as chemicals and binders (used in mosquito coil, incense sticks and fireworks etc.). Equivalent diameter (e.g. aerodynamic diameter) and shape factor are used while dealing with non-spherical aerosol particles. The agglomerate structure of aerosol particles can be characterized by fractal dimensions. Such agglomerates made up of primary particles possess quite different properties e.g. density, collision rate in comparison to an equivalent volume sized sphere. Although ignored in past, recent studies focused on charge on aerosol particles have highlighted the importance of charge for defining their dynamical behaviour.

1.2 Aerosol size distribution: modes

Particle size distribution is the most important physical characteristic for a polydisperse aerosol system. Size distribution function is utilized for mathematically defining aerosol mass/number size distribution. Surface area and volume distributions with respect to particle size are also used for specific contexts. Mode of the size distribution refers to the most frequent size and could be more than one for a multi-modal distribution. In general, mode of distribution reflects the signature of aerosol sources. Due to the presence of multiple sources

are also projected to be evolving from mass to number based indices. As transportation and biofuels are the main sources of aerosol particles in Indian mega cities, mass concentration is expected to be reduced in future by adopting cleaner technologies. However the effect on ultrafine number concentration remains doubtful as it has been observed to be increasing with decreasing mass concentration in western cities². Due to higher adsorption capacity and lung penetration fractions, measurement and characterization of ultrafine and nuclei mode atmospheric aerosol particles becomes significant. Characteristics of nuclei mode particles are studied via laboratory experiments, measurement campaigns and theoretical simulations. This domain is relatively new and offers insights to several interesting aspects.

The modification in background aerosol number characteristics (concentration and size distribution) during episodic events results in short term spikes leading to air quality deterioration and long term health complications. In mega cities where background aerosol concentration remains high, identification of episodic characteristic changes and source term analysis is challenging. For Indian context, aerosol emission during celebratory fireworks is one such domain where number characteristics of atmospheric aerosol spectrum (particularly in nuclei mode size ranges) are required to be studied attentively. Possibility of similar inferential potential is true for the case of large scale fires as well. Characteristics of freshly formed particles for both these events has potential to supplement the anthropogenic source terms.

1.1 Aerosol properties and characteristics

Aerosol properties not only define aerosol systems, but dictate their life, journey and fate. Particle size, concentration and chemical composition are mainly used to characterize aerosol systems although particle shape, charge and optical properties could be important as well. Size (refers to ‘diameter’ in this work) of aerosol particles is the most determining factor for aerosol dynamics. Generally, it can vary from 1 (nm) nanometre (molecular clusters) to 100

CHAPTER 1

INTRODUCTION

Aerosols being important component of atmosphere affect us through different processes and in different ways. Aerosols have potential to affect the quality of inhaled air at local level and impact climate changes globally. The direct, semi direct and indirect effect of aerosols on radiation budget of earth is crucial research domain focusing on accurate radiative forcing estimations. Dynamics of atmospheric aerosols can only be determined by measuring, modelling and interpreting their formation and evolution characteristics. Atmospheric aerosol characteristics are modified by natural and anthropogenic emissions. Rapid growth in industrial activities and technological advancement in recent years has led to an uncontrolled and drastic modification in background aerosol characteristics. These changes have been linked with detrimental health effects, visibility degradation and variations in earth's radiation budget. Epidemiological studies have established a relationship of mortality and morbidity rates with the rise in aerosol concentrations. Impact of aerosol particles on the earth-atmosphere system has been recognised as an important topic of atmospheric environmental research at present¹.

It is difficult but significant to understand the initial steps/processes involved in atmospheric aerosol formation. Nucleation and growth of atmospheric aerosol particles is a vital source term to cloud condensation nuclei (CCN) concentration. Understanding of characteristics (i.e. concentration, size distribution, composition and source-sink rates etc.) of atmospheric aerosols is pre-step towards managing/controlling their effects. Several field campaigns are conducted to measure aerosol characteristics in urban, rural and remote sites. As the health effects are shown to be relatively larger for smaller sizes, focus has been shifted to atmospheric aerosol characterization in fine and ultrafine size ranges. Recent years has seen a coordinated effort towards measuring the number concentration characteristics of atmospheric aerosols ahead of mass, chemical and radiative characteristics. Regulatory limits

generation and control of engineered nanoparticles. In recent times, studies on the formation of molecular clusters and their growth to larger sizes^{89, 276} and direct observation of atmospheric aerosol nucleation⁷⁰ highlight the importance of research in this field. This work was focused on measuring number characteristics of nuclei mode particles using SMPS. Results from measurements were interpreted in a way to gain new insights about dynamics (formation and growth) of these particles.

2.7 Summary

This chapter discusses instrumentation and techniques employed for the measurement of aerosol mass/number characteristics and chemical composition. SMPS was used in all experiments for studying number characteristics of aerosol systems as per the main objective of this work. A detailed inter-comparison study of GRIMM-SMPS (model no 5.403C) and TSI-SMPS (classifier 3080 with CPC 3775) was performed for harmonising inter-instrumental differences towards measuring number concentrations. In the first level of comparison, CPCs of these units were compared with another standalone CPC in ambient and laboratory generated aerosol environment. CPC differences were found to be reasonable for the tested conditions. For the case of SMPS, number concentration measured by GRIMM-SMPS was found to be approximately 20 % higher than TSI-SMPS in ambient conditions. This difference increased to ≈ 80 % when these units were challenged with high concentration aerosol particles. Ratio of the concentrations measured by GRIMM SMPS and TSI SMPS was seen to be increasing with aerosol concentration (average of both). This chapter also discusses the development of HWG which was used for the generation of high concentration nanoparticle aerosols as a part of closed chamber experiments performed under this work. Optimization experiments were conducted in order to fix the operating parameters for this generator. This generator was tuned to generate particles of mean size (calculated from SMPS data) in the range of 15-20 nm and of number concentration $> 10^6$ per cm^3 .

was measured using T-SMPS. However, prior to these measurements, inter-comparison of mode diameters was also made. The focal parameters (i.e. mode and GSD) were seen to be quite close to each other (within 3 and 1 % respectively). Subsequently, growth factors were determined on the basis of hourly average mode diameters of size distributions (dry and ambient conditions). These were found to range from 1.02 to 1.18 for RH varying between 59.3 and 76.5 %.

These factors were used in a study on quantification of the radiative impacts of light absorbing black carbon²⁷⁵. In their work, Zdanovskii– Stokes–Robinson (ZSR) approach was used to develop a model to predict chemical composition of particles based on the measurements. Then, core-shell assumption and Mie theory induced light extinction estimates were utilized to calculate absorption and scattering coefficients. Several studies are based on the number concentration and GM calculated from multiple-SMPS units and these generally rely on sizing calibration only. Conclusions from inter-comparison study performed under this work highlight the importance of harmonising these measurements beforehand.

2.6 Detection of nuclei mode particles

As discussed above, progress in the development of aerosol instrumentation has enabled researchers to generate observational data of high quality. Although number characteristics of aerosol systems have often been studied, focus on the ultrafine and nanosize ranges yield several interesting and unexplored features/results. At the same time; issues such as sensitivities, diffusional losses, too low signal strength etc. affect the detection capabilities of instruments for nuclei mode particles. Size segregated studies in sub 2 nm region are extremely rare due to the requirement of highly sophisticated instruments. The results of atmospheric measurements in ultrafine and nuclei size range domain yield contradictory deductions as well for some of the cases. At the same time, the role of ultrafine particles towards climatic effects is crucial. Similar conceptual knowledge is instrumental for the

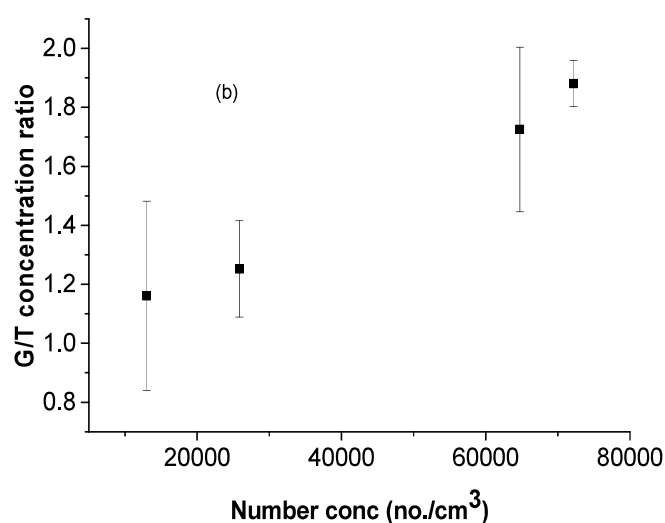


Fig. 2.10 (b): Effect of aerosol concentration on concentration ration
measured by GRIMM and TSI SMPS

Multiple units (Medium and long DMA units of GRIMM SMPS) were used only for one atmospheric field campaign and these insights were adopted in practice as protocol for measurement and data interpretation. However, conclusions drawn from this ‘Harmonisation study’ are applicable for wider cases where SMPSs are used for characteristic measurements. To demonstrate this, a separate case study is also discussed here where these same units (for which inter-comparison study was targeted) were utilized for specific purpose.

2.5.4 Case study

Hygroscopicity describes the interaction of atmospheric/engineered aerosol particles with water vapour and can be measured by using Hygroscopic tandem differential mobility analyzer (HTDMA)³⁰. Alternatively it can also be measured by comparing ambient (wet) and dry particle size distributions obtained using two SMPSs operating in parallel. In the latter approach, growth factor is estimated as the ratio of mode diameters of wet and dry size distribution. In this study, dry distribution was measured using G-SMPS attached with a silica bead dryer at its inlet (reducing inlet RH to below 5 %). Ambient (as such or wet) distribution

the standalone CPC were plotted as a function of the concentration (measured by standalone CPC). It was observed that, in concentration range of 10,000–40,000 cm^{-3} , concentration ratio for both CPC increased with concentration. However, CPC of G-SMPS (to standalone CPC) ratio was seen to be saturating, while that of CPC of T-SMPS was observed to be increasing, in the above-stated concentration range. Similarly, Fig. 2.10(b) shows the ratio of the concentrations measured by G-SMPS and T-SMPS as a function of the aerosol concentration (average of both). This ratio increased with increase in aerosol concentration.

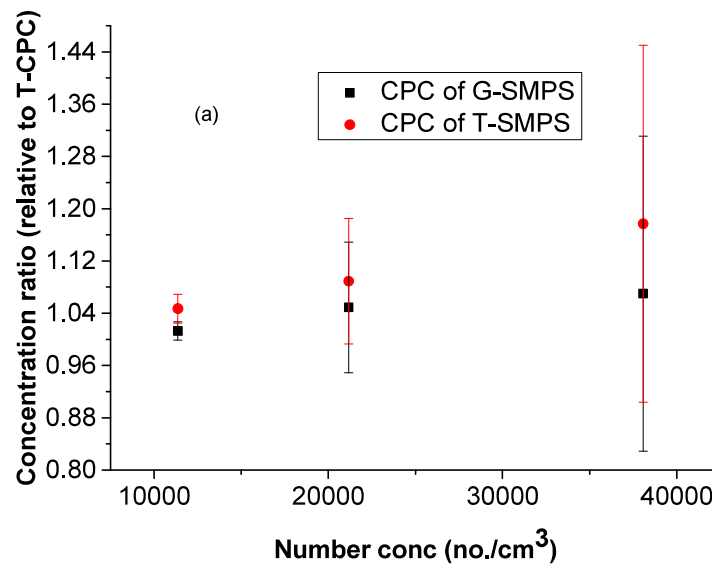


Fig. 2.10 (a): Relating CPC differences with measured concentration

This observation is in agreement with the work of Schlatter²⁷³ wherein a 5 % variation (factor of 1.05) was seen up to 1,000 particles cm⁻³ which increased to 10 % (factor of 1.1) for 10,000 particles cm⁻³. A larger variation in the present study is seen owing to higher observed concentrations. The second step was the comparison of G-SMPS and T-SMPS in controlled chamber conditions using two different types of test particles generated from sodium chloride (0.01 % v/v) and ammonium sulphate (0.03 % v/v) solutions. After conditioning through the diffusion dryer, these were passed into the chamber. Fig. 2.9 (b) shows the steady state average size distribution for NaCl aerosol particles as measured by these units. For this case, the geometric means recorded by the G-SMPS and the T-SMPS were 53 and 64 nm (G- SMPS 15.6 % lesser than T-SMPS), respectively. The geometric standard deviations obtained from the size distributions were similar at 1.88 and 1.87, respectively. The total number concentrations were compared in the common size ranges of the two SMPSs. It was found that the G-SMPS showed a higher concentration by a factor of about 1.881(± 0.078). Similar results were obtained for the case of (NH₄)₂SO₄ aerosol particles as well. Relative concentration factors (difference relative to the lower concentration) were calculated for different size ranges and a size dependency was observed where these factors reached even 4 for nano size ranges.

The sources of uncertainty which might be causing these differences could be CPC responses, DMA transfer functions, efficiency corrections, instability of the flows and the differences in neutralized charge distributions. Further, aerosol flow changes and insufficient neutralisation may also lead to the difference between CPC and SMPS²⁷⁴.

2.5.3 Harmonisation

Based on the results of the measurements, an attempt to achieve harmonisation when measuring particle concentrations using systems from different manufacturers was made. As shown in Fig. 2.10(a), the ratios of the concentrations recorded by CPCs of the two SMPSs to

particle concentration showed higher concentration by a factor of $1.089(\pm 0.096)$ and $1.049(\pm 0.100)$ compared to CPCs of TSI SMPS and GRIMM SMPS. On injection of the test aerosols (concentration measured by standalone CPC was $40752(\pm 6452) \text{ cm}^{-3}$), this factor changed to $1.177(\pm 0.273)$ and $1.070(\pm 0.241)$ for CPCs of T-SMPS and G-SMPS, respectively (Fig. 2.9 (a)).

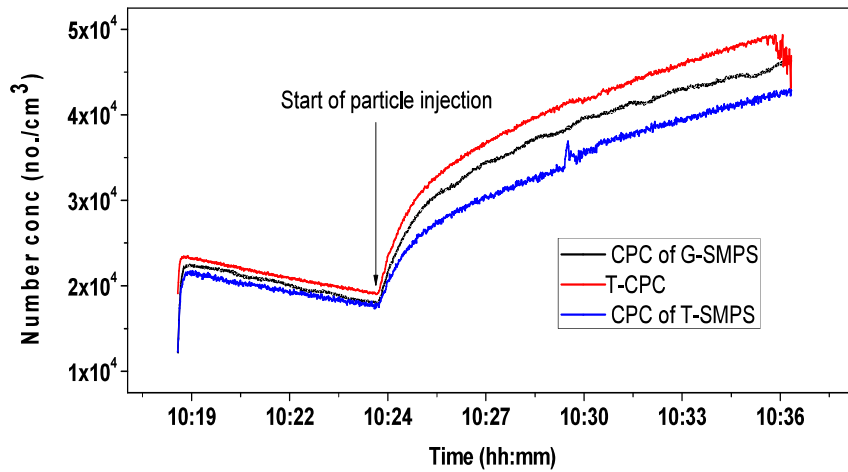


Fig. 2.9 (a): Comparison of all CPSs by measuring number concentration of nebulised aerosol particles

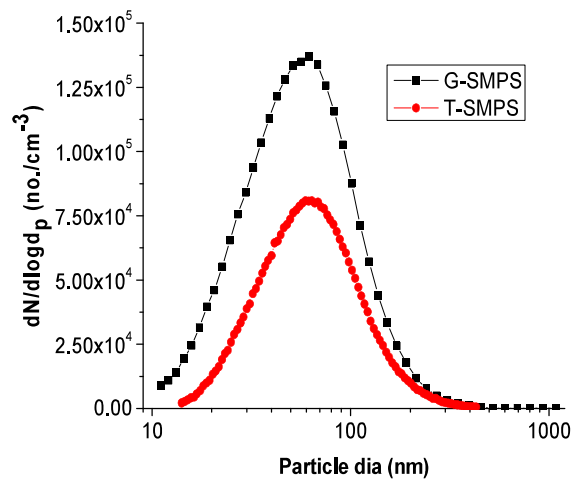


Fig. 2.9 (b): Size distribution measured by GRIMM and TSI SMPS

were performed by following set protocols. Figure 2.8 shows the time series of number concentration measured by all units (for one overnight ambient sampling).

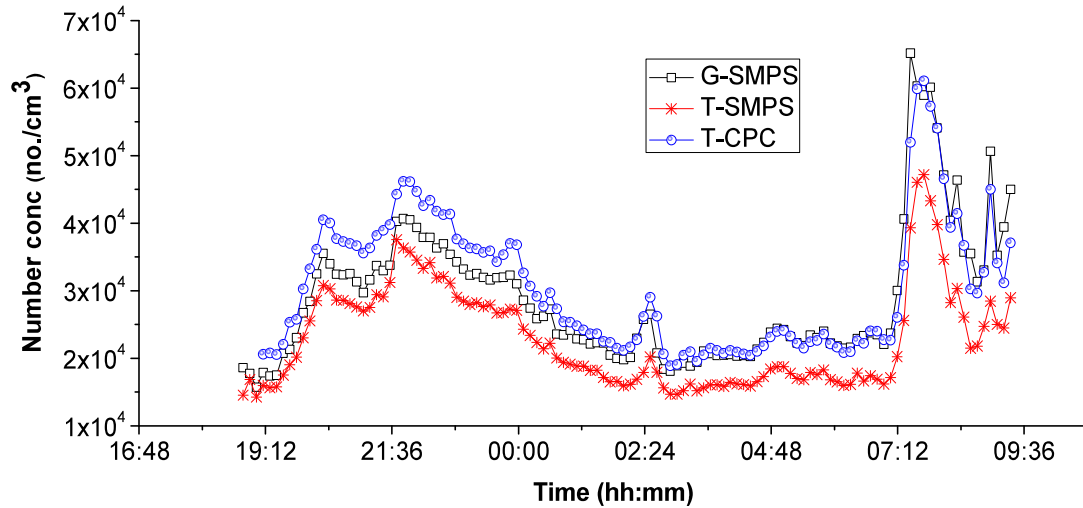


Fig. 2.8: Time series data of ambient number concentration for SMPS inter-comparison

Gross parameters (total number concentration, mean size and geometric standard deviation) measured by both SMPSs followed each other. In the comparison of representative mean size distribution measured by these units, a difference of about 10% in measuring geometric mean was noted. All environmental changes e.g. bimodality were captured by both the instruments. No convincing size segregated effect was observed. As observed for low concentration (ambient) conditions, the G-SMPS number concentration results were approximately 20 % higher than T-SMPS. A small part of this difference can be linked to the CPC differences ($\approx 5\%$). Similar experiments were consequently repeated for laboratory conditions where these instruments were exposed to higher number concentrations generated via atomization of solutions.

2.5.2 Laboratory generated conditions

CPCs of both the SMPSs were compared with the stand-alone CPC in the test chamber, using particles generated from atomized sodium chloride solution (0.01 % v/v). Prior to the injection of atomized aerosols, stand-alone CPC which recorded $21172(\pm 1290) \text{ cm}^{-3}$ average

Table 2.2: Parameters of the SMPSs used in the study

Parameter	G-SMPS	T-SMPS	Stand-alone T-CPC
Model	5.403C	3696	-
DMA	Vienna type	TSI- 3081	-
Aerosol sampling rate (lmin ⁻¹)	0.3	0.3	-
Sheath air flow rate (lmin ⁻¹)	3	3	-
Neutralizer	Am ²⁴¹ (alpha emitter)	Kr ⁸⁵ (beta emitter)	-
Diameter range (nm)	11.1 nm – 1083.3 nm	14 - 800 nm	-
Impactor	1185 nm	1282 nm	-
CPC type	Butanol based	3775: Butanol based	3776: Butanol based
CPC maximum concentration	10 ⁷ cm ⁻³	10 ⁷ cm ⁻³	10 ⁶ cm ⁻³
CPC lower limit	4.5 nm	4 nm	2.5 nm
Single particle counting threshold	1.4 x 10 ⁴ cm ⁻³	5 x 10 ⁴ cm ⁻³	3 x 10 ⁵ cm ⁻³

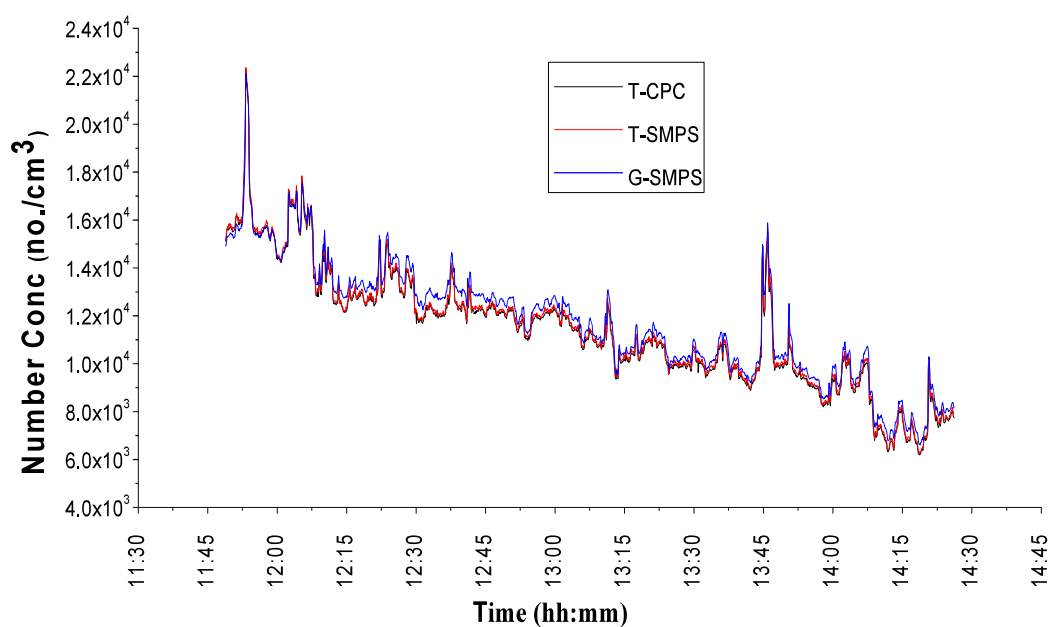


Fig. 2.7: Time series of particle concentrations recorded by all CPCs in ambient environment

The CPCs were then coupled with their respective DMAs (to form SMPSs). The two SMPSs along with standalone T-CPC were connected to a flow divider, and measurements

conducting a separate series of pre-experiments. These experiments were performed with 2 different make SMPS units in ambient as well as laboratory conditions in order to develop protocols for relevant part of the experimental work. A detailed inter-comparison study with GRIMM-SMPS (model no 5.403C) and TSI-SMPS (classifier 3080 with CPC 3775) was undertaken for this purpose (to be called as G-SMPS and T-SMPS respectively in the following description). Apart from studying the inter-instrumental differences towards measuring number concentrations, inferences about capabilities of these instruments in measuring the nanoparticles were also drawn. As a first level of comparison, only the CPCs of both the SMPSs were compared to a stand-alone TSI-CPC (model no CPC 3776) which was taken as a reference. Subsequently, the second level of comparison was made between the two SMPSs. Parameters of the SMPSs used in these experiments are represented in Table 2.2. The units used in this study are shown in Fig. 2.2.

2.5.1 Ambient conditions

For ambient aerosol experiments, sampling was performed by comparing CPCs (2 of SMPSs and standalone unit) and then comparing SMPSs (2 units). First, all the three CPCs (T-CPC, CPC of G-SMPS and the CPC of T-SMPS) were compared to check the differences in the total number concentrations recorded by these instruments. Fig. 2.7 shows the results in the form of time series recorded for a period of about 2.5 h. As can be seen, CPC variations were low as expected for ambient conditions for calibrated instruments. The average aerosol concentration as measured by T-CPC during this period was $11,363 (\pm 2555) \text{ cm}^{-3}$. As the concentration was low (below the threshold of single counting mode), close matching of CPCs indicates that coincidence corrected single particle counting for all these CPCs is reasonable.

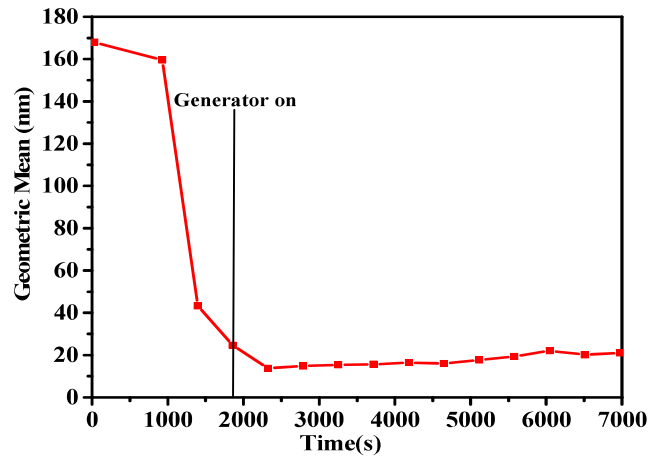


Fig. 2.6 (b): Temporal stability of geometric mean size of the generated particles

Primary size of the generated nanoparticles as well as precise size distribution parameters cannot be obtained by SMPS due to its limitation at the lower cut off size (10 nm for the present case). Hence Tandem electron microscopy (TEM) analysis was sought to obtain the true information about the primary size of the generated nanoparticles. It was seen that primary particles generated in the chamber had sizes as low as 3 nm.

2.5 Harmonisation of ultrafine particle measurements with SMPS

The accuracy of SMPS measured size distribution is governed by several parameters such as the DMA construction, sampling and sheath air flow rates, voltage accuracy, particle charge distribution, CPC counting efficiency, particle transport time and particle transmission efficiency²⁶⁸. The SMPS is generally calibrated using spherical particles²⁶⁹. In most cases, calibration is only with respect to size and not particle concentrations due to the absence of reference particle number concentrations. In the absence of an absolute standard, intercomparisons become imperative and only means of checking the accuracy and reasonableness of measurements. Some inter-comparison studies on size-classifying particle concentration measurement systems have been reported in the literature^{268, 270-272}.

As this work employed various SMPS units (different DMAs) for experimental measurements; accurate data collection and proper interpretations were made possible by

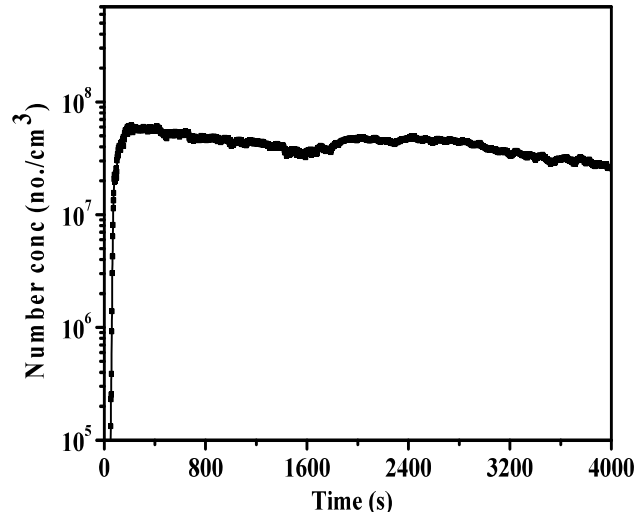


Fig. 2.5 (b) Long time stability of output from HWG

The follow-up trend and the transient concentration are the functions of flow rate, operating conditions, and the inter-play between generation due to nucleation and removal due to coagulation and other processes in the generator volume. In order to measure the size distribution of the generated aerosols, SMPS was connected at the aerosol exit of the generator, and similar operating conditions (as for CPC measurements) were maintained for aerosol production. The short-term and long term inferences from size distribution of generated aerosols are shown in Fig. 2.6 (a) and Fig. 2.6 (b), respectively. For nichrome wire, the geometric mean size obtained was $\approx 15\text{-}20\text{ nm}$ with a geometric standard deviation (GSD) of ≈ 1.4 . As can be seen, this mean size was preserved for considerably long times as well.

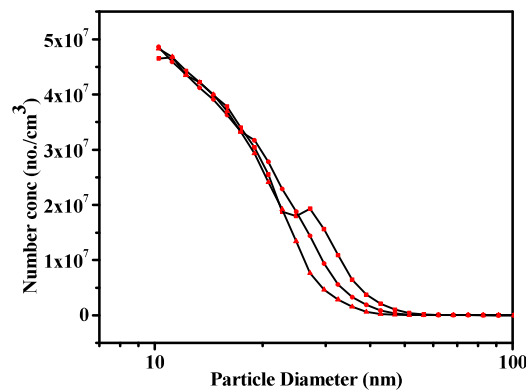


Fig. 2.6 (a): Size distribution of generated aerosol particles from HWG

2.4.4 Characteristics of generated aerosols

Before using HWG as aerosol generator for chamber experiments, the output of the generator was characterized in terms of aerosol properties. For short-term response of number concentration of generated particles, various experiments were conducted with nichrome wire at similar operating conditions i.e. 1 Lmin^{-1} carrier flow and applied voltage of 7 Volts. Fig. 2.5 (a) represents temporal response of number concentration at the outlet of the generator. As can be seen, the wire took about 50 seconds to warm up for vapour production and further 50–100 seconds for achieving a saturation aerosol concentration. It can also be seen that the saturation number concentration was of the order of 10^7 per cm^3 . Fig. 2.5 (b) shows the long-term behavioural response of the same wire under similar operating conditions. It can be seen that the number concentration remained in the order of 10^7 per cm^3 or more when the output was measured at the generator exit. For continuous source condition, the number concentration after reaching a peak decreases as an effect of onset of coagulation.

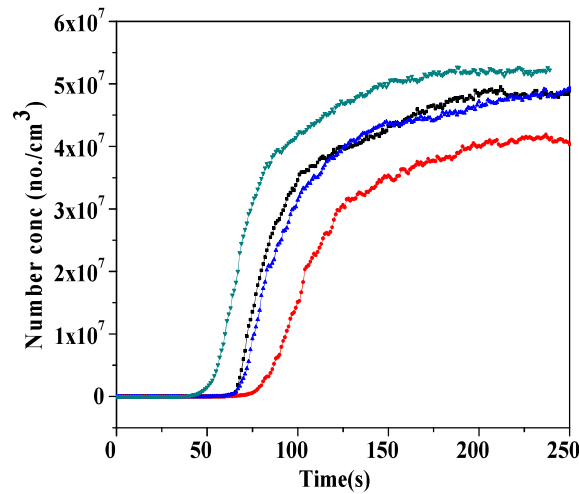


Fig. 2.5 (a): Short term output recorded at the exit of HWG

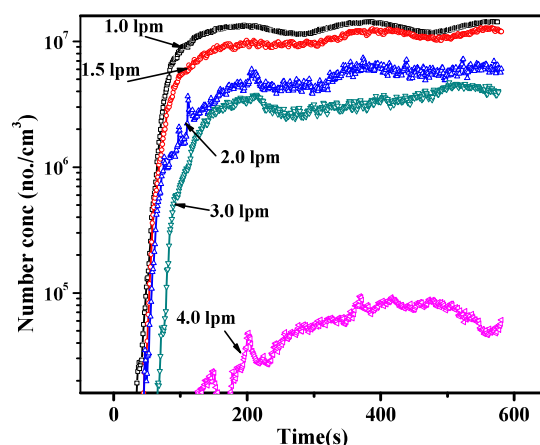


Fig. 2.4 (a): Effect of carrier gas flow rate on the output number concentration of the HWG for a fixed voltage of 7V applied to the metallic wire

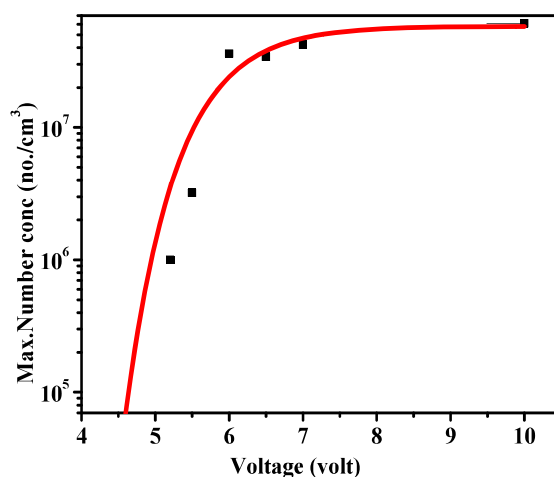


Fig. 2.4 (b): Effect of applied voltage on number concentration

Similarly, experiments were performed by varying applied voltage by keeping the carrier gas flow rate fixed at 1 Lmin⁻¹. For these conditions, variation of maximum number concentration at outlet was plotted with respect to the applied voltage (Fig. 2.4 (b)). As observed, the maximum number concentration reached to a saturation level after about 6 V. Based on these optimization experiments, operating parameters (applied voltage 6-9 V: equivalent power 30-50 Watts, carrier gas flow rate: 1-1.5 Lmin⁻¹) were fixed for experiments aimed to generate nanoparticles for controlled experiments in confined chamber conditions.

weighting can be used to estimate effective evaporation rate of the wire. The source emission rate can then be calculated using the information on Evaporation rate, surface area of the coil and reaction chamber volume as follows:

$$SE = \frac{(r * S)}{V}$$

where S is the total surface area of the evaporating material and V is the generator volume. The value of SE for a typical experimental case was estimated to be around $\approx 10^{25}$ molecules per $\text{m}^3\text{-s}$ when nichrome wire was used.

2.4.3 Operating parameters

A series of experiments were carried out for obtaining optimum operating conditions for the generation of stable high number concentration nanoaerosols. Results indicated that carrier gas flow rate and applied voltage are two main factors affecting the generator output. Carrier gas flow rate plays an important role in the generation and transport of the aerosols. During the generation process, hot vapours carried by a cooler carrier gas become supersaturated and then nucleate and form critical size nuclei. Residence time of vapours in hot region changes due to the flow variations affecting stability of the generator output. Fig. 2.4 (a) shows the temporal variation in aerosol number concentration of nichrome wire recorded by CPC at the generator exit. These measurements were performed by changing the flow rate of the carrier gas (1-4 Lmin^{-1}) when the applied voltage was fixed at 7 Volts. As could be seen from the figure, optimum carrier flow rate was seen to be between 1 and 1.5 Lmin^{-1} , resulting in maximum and stable number concentration. As the flow rate was increased above 4 L min^{-1} , aerosol number concentration was reduced appreciably. At higher carrier gas flow rates, wire cools more efficiently, reducing its temperature and, hence lowering the evaporation rate. Also these vapours no longer remain supersaturated due to lesser temperature gradient between vapour and carrier gas affecting the number concentration.

hot emitting vapours which nucleate under suitable conditions to generate nanoparticles. These particles formed via gas to particle conversion coagulate to form an evolving size spectrum whose parameters can be controlled by suitably optimising the operating parameters.

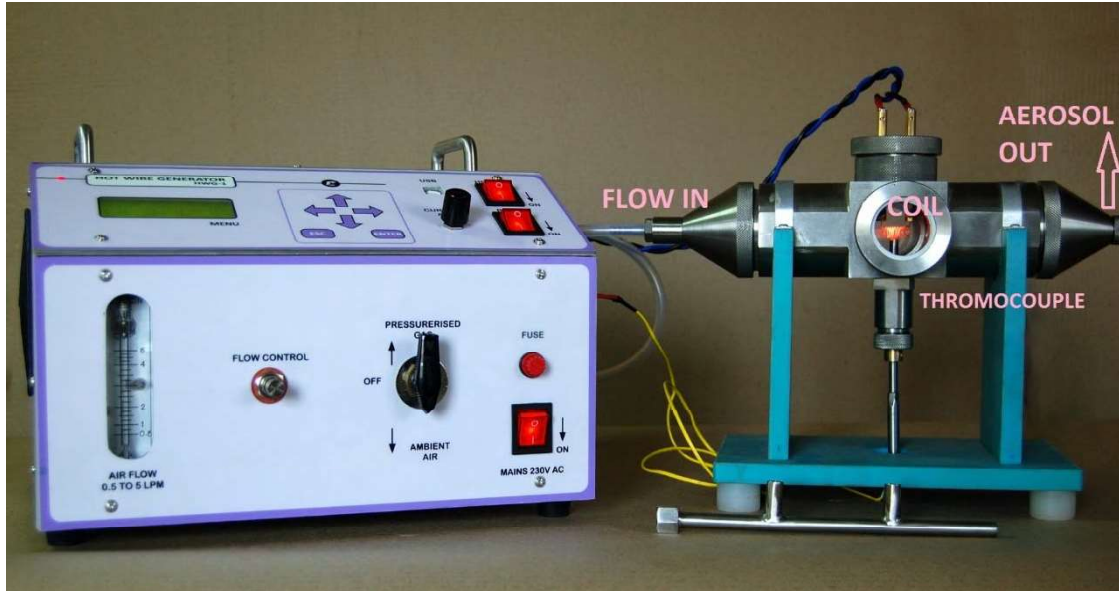


Fig. 2.3: Hot Wire Generator in glowing condition

Evaporation rate of the heated wire forms the basis of the vapour source term which subsequently leads to nucleation. The saturation vapour pressure of constituents of wire is one important input for calculating its vapour emission rate. Evaporation rate can be calculated using Hertz–Knudsen equation

$$r = \lambda \sqrt{\frac{1}{2\pi MN_a k_b T}} (p_s(T) - p_0)$$

where λ = accommodation coefficient, M = molar mass, T = temperature, $p_s(T)$ = saturation vapour pressure, p_0 = vapour pressure, N_a = Avogadro number, and k_b = Boltzmann constant. Accommodation coefficient accounts for vapour scattering back to the wire surface and should be < 1 . For the case of HWG, it can be assumed as 1 along with $p_0=0$ when device is operated under flow. In the case where the material of wire is an alloy or mixture of elements, evaporation rate can be calculated for the individual components and then proportional

also be obtained from these methods appropriate for the validation of coagulation-based aerosol evolution models. The challenges involved in using of electrically heated wire for generation of nanoparticles are the control of the operating parameters and characteristics of the generated aerosols. Several factors e.g. chemical composition of wire, electronic stability, change of wire's electrical resistance with increasing temperature and carrier gas flow affect the generation and stability of particle concentration. In past, various hot-wire generators have been designed for different purposes²⁶⁵⁻²⁶⁷. Different generators using this technique were employed mostly for two purposes, i.e. to demonstrate and utilize the capability of nanoparticle aerosol production and to study specific aspects (such as charge fraction of aerosols, implications toward evolution models, etc.). One of the objectives of the present work was studying the characteristics of nanoparticles/nuclei mode particles in controlled laboratory conditions and HWG was developed for this purpose.

The HWG (Fig. 2.3) consists of a metallic coil enveloped by a small volume reaction chamber. The coil is electrically connected to a constant current power supply (0-5 Amp) providing heating energy to glow the material of the wire. The horizontal sampling ports have been provided to guide the generated particles to the measuring instruments. Alternatively, the output can also be directed towards an experimental chamber for other purposes. A thermocouple is also connected in HWG enabling the measurement of temperature of the wire surface or the chamber environment. Wire of specific chemical composition (single or composite) can be used for the generation of nanoparticle aerosols of the material of interest. Usually, one port of this generator is connected to aerosol measuring instruments while the other can be used for providing carrier gas flow for purging and thermal quenching. The carrier gas can be chosen depending on the type of aerosols required for the study. For example, the particle-free air will generate oxidized metal particles while inert gas like argon will generate metallic particles. Under the action of electrical heating, the wire becomes red

becomes an important factor. These are generated by wet chemistry methods or via gas synthesis based aerosol route. Electrical heating of low resistivity metallic wires is also used leading to the generation of metallic nanoparticles in the aerosol form. In this work, wet atomization was used for instrument calibration tests and glowing wire technique was utilized for the generation of nuclei mode particles.

2.4.1 Electrical generation of nanoparticle aerosols

There are various wet chemistry methods²⁵⁹⁻²⁶² available for the generation of airborne nanoparticles. Contamination within the particles and unwanted surface chemistry due to the use (and impurities) of the solvents make these methods undesirable for controlled/high purity applications. Nanoparticle generation via aerosol route provides a powerful way of manufacturing nanostructured materials of well-defined morphology and chemical composition. Advantages such as purity, absence of liquid wastes and feasibility of continuous operation make gas phase induced nanoparticle production an attractive technique. Various gas-phase synthesis processes for particle formation include plasma reactors, infrared laser analysis, laser ablation and spark discharge. Hot-wire synthesis i.e. electrical generation of aerosols is analogous to inert gas condensation and spark generation, except that the metallic wire is directly heated and quenching is achieved by a purging gas flow. This method is able to generate particles in the nano size range via gas to particle conversion and offers a controlled way to study the formation and evolution characteristics of nuclei mode particles.

2.4.2 Hot wire generator

The Glowing/Hot wire generator (GWG/HWG) where material is evaporated from resistively heated wire and subsequently quenched by gas stream was introduced by Schmidt-Ott et al.²⁶³. The main advantage of this method is that it offers a precise control over contamination and generated particles have sizes in nanometer range²⁶⁴. High number emission rates can

different units of SMPSs were obtained. These units are shown in Fig. 2.2. CPC units of these assemblies were also compared with a third CPC (TSI make) in ambient and laboratory generated conditions. Subsequently, GRIMM SMPS 5.403 C with long DMA was used for aerosol measurements during atmospheric campaigns and controlled chamber experiments. In one of the campaigns, long DMA SMPS and medium DMA SMPS were also simultaneously used. The specifications and operating characteristics of all above mentioned instruments/units are mentioned in the forthcoming sections. All SMPS measured plots shown in this work refer to particle diameter as ‘mobility equivalent diameter’ on x-axis.



Fig. 2.2: Photographs of GRIMM-SMPS (5.403) and TSI-SMPS (3775)

2.4 Aerosol generation

Aerosols can be generated by several ways; the generation process depends on the context and the application. The methods for generating monodisperse aerosols with spherical particles include the atomization of a suspension of monodisperse particles, formation of uniform droplets by dispersion of liquid jets with vibrating or spinning disk and the growth of uniform particles or droplets by controlled condensation²⁵⁸. Some of these techniques can also be used for the generation of non-spherical particles as well. For the generation of polydisperse aerosols; dispersion and plasma synthesis techniques are used. Generation of nanoparticle or nuclei mode particles is a challenging domain where control of the process

‘Hygroscopic tandem differential mobility analyser (HTDMA)’ etc. which have been fine tuned for diverse applications.

2.3.3.1.2 Condensation Particle counter

Condensation Particle Counters measure the total aerosol number concentrations larger than a stated minimum detectable size. It samples the aerosols at a constant flow rate through a saturator, a condenser and an optical detection assembly. CPCs are often used as counters for size classifiers such as DMPS and SMPS. In CPC, small aerosol particles are grown by condensational techniques to a size which is conveniently detected by optical techniques. Due to strong condensational abilities, CPCs can detect ultrafine particles easily. Based on the technique to achieve supersaturation; expansion type, conductive cooling based, differential diffusion type and mixing type CPCs are used in laboratories. A working fluid (having enough vapour pressure) capable to grow particles in a small time scale is necessary for controlled condensation. Due to sufficiently high supersaturation of condensing vapour, CPC response becomes insensitive to composition of the measured particles. The counting efficiency and the effective flow rate are required to be known precisely for correct measurements. Also, the uncertainties in these parameters and knowledge of coincidence error and shifting of counting logic from single particle mode to photometric mode (at high concentrations) should be known, while employing a CPC. Recent years have seen the development of CPCs based on water instead of butanol (for attaining supersaturation), and these have been compared and evaluated²⁵⁵⁻²⁵⁷.

2.3.3.1.3 CPC and SMPSs used in this study

As the main objective of this work pertains to the study of number characteristics of aerosol systems, SMPS was used in all experiments (atmospheric and chamber measurements). Additionally, a separate study was carried out in order to understand issues related to ultrafine measurements with SMPS. In this study, comparative response characteristics of 2

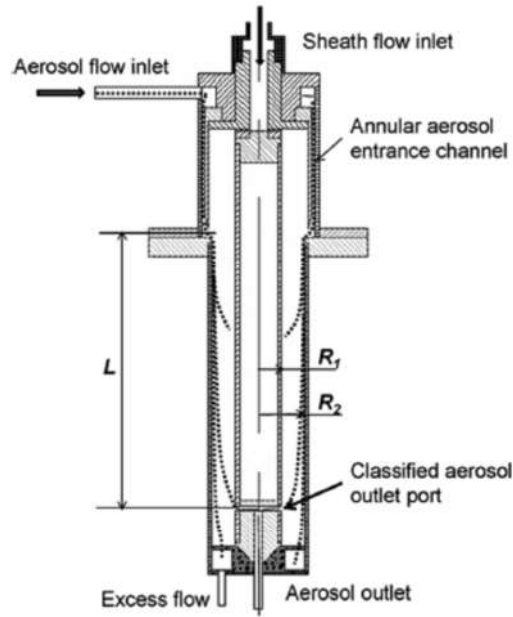


Fig. 2.1: Schematic diagram of cylindrical DMA²⁴⁵

The DMA designed by Knutson and Whitby was utilized in the first commercial version manufactured by TSI incorporation, USA which was used effectively for several experimental measurements of particles between 10 nm-1 μm . A number of modifications were subsequently made to DMA designs mainly to improve the efficiency, response time, diffusional losses and to extend lower limit^{251, 252}. Advanced DMA designs are focussed on measuring freshly formed particles at the size limit even close to 1 nm. The usage of DMA type, however depends on the context/application where change in design characteristics and operating parameters are utilized for specific size ranges and concentrations.

The working principle of DMA has been adopted towards size classification in two ways. In Differential mobility particle sizer (DMPS), particle concentration is measured in steps where voltage is stepped up at instants after a delay for achieving steady state aerosol signal²⁵³. This technique offered good resolution but compromises on the detection time for entire size distribution. Later, the applicability of the same transfer function for the case of continuous change in voltage²⁵⁴ led to the development of SMPS. There are other devices based on similar classification principle as well, e.g., 'Fast mobility particle sizer (FMPS),

sheath at exit or deposit on the central electrode, respectively. At given flow rates and applied voltage, classified characteristic mobility can be written as

$$Z^* = \frac{(Q_{sh} + Q_e) \ln \frac{R_2}{R_1}}{4\pi V L}$$

where V is the applied voltage, L is DMA length, R_1 is radii of the inner electrode and R_2 is that of the outer electrode. Q_{sh} and Q_e represent sheath air and excess air flow rates, respectively. When diffusion is negligible, uncertainty in classified mobility Z^* is related to the flows as

$$\Delta Z = Z^* \beta \text{ with } \beta = \frac{(Q_a + Q_c)}{(Q_{sh} + Q_e)}$$

(Q_a : aerosol flow rate entering DMA, Q_c : flow rate of classified aerosol leaving DMA).

The next important factor for DMA analysis is the ‘transfer function’. It accounts for the probability of inclusion of a specific mobility in the classified aerosol flow under selective conditions of characteristic mobility. It is usually denoted as $\Omega (Z, Z^*)$ where Z is mobility of the charged particle. For smaller particles, diffusion is expected to affect the transfer function of the classifier. A diffusional transfer function for a cylindrical DMA was given by Stolzenburg²⁴⁹ which can be used for cylindrical as well as radial geometries. As per this formulation, DMA resolution is expressed as the ratio of characteristic mobility and transmitted mobility size ranges. The Stolzenburg model has been validated by experimental and modelling studies²⁵⁰.

limits/resolution and developing standardized protocols for measurement of particle size distribution^{243, 244}.

2.3.3.1 Detection principle and theory

Knutson and Whitby²⁴⁵ presented the basic theory of operation of ‘Differential mobility analyser (DMA)’ designed to classify particles on the basis of their electrical mobility. For such a classification, charge size distribution on particles (over different sizes) should be known. As electrical mobility of a charged particle is a function of particle size and acquired charge, knowing the latter reduces unknowns of distribution to only particle size. Hence the aerosol sample to be measured in SMPS is first charge-conditioned by passing it through a bipolar charger. Particles of different sizes acquire respective equilibrium charge distribution before exiting the charger. Aerosol flow along with sheath flow is then directed to DMA (cylindrical or radial electrode assembly) where positive or negative voltage is applied to the central electrode. Particles of different mobility (with a known charge distribution) are attracted towards the central electrode in different trajectories, and those corresponding to a particular mobility range (at pre-fixed voltage) pass through the exit provided in the central electrode. They are then carried to the CPC where they are counted. Particles corresponding to different mobility groups are counted sequentially by changing electrode voltage resulting in the measurement of number size distribution. The accuracy of the theory of Knutson and Whitby was verified through a series of experiments conducted thereafter²⁴⁵⁻²⁴⁷. The effect of diffusional broadening of mobility class was also discussed simultaneously^{247, 248}.

2.3.3.1.1 Differential Mobility Analyser

A typical cylindrical DMA is shown in Fig. 2.1 (Knutson and Whitby design) where both aerosol and sheath flows are shown. Only mobility classified particles are extracted through the slit near the bottom of the DMA while lower/higher mobility groups pass to the annular

between two laser beams for accelerated particles is used for this purpose. Another technique to measure the same is by electrical detection of inertially classified particles in '*Electrical low pressure impactor (ELPI)*'. Inlet aerosol stream in this instrument is charge-conditioned using a unipolar charger and subsequently directed to a low pressure impactor. The charged particles get segregated as per their size and deposit on different impactor stages, which act as the charge collectors connected to sensitive electrometers. The current on each stage is subsequently converted to number concentrations. The measurement size range of ELPI is \approx 5 nm-10 μ m.

Classification and principle of these size classifiers and counters has been summarised in Table 2.1.

2.3.3 Scanning mobility particle sizer

Electrical techniques are employed to measure ultrafine particles where it is not possible/too difficult to use optical or inertial classification and detection techniques. Although complex and sophisticated, these techniques are attractive due to their fast responses and higher resolutions. SMPS is one such system which employs electrical mobility based size classification and subsequent counting in a particle counter. Such is the importance of SMPS or similar mobility classifiers that, these have become a necessary member of instrumentation family for any aerosol measurement exercise probing characteristics of ultrafine particles. Mobility classification based particle measurement started with the classic experiment of Langevin in 1902²³⁷. In this work, a coaxial cylinder was used to select charged particles having a mobility above a threshold value. Later this technique was employed for gas ions and particle measurements by several researchers²³⁸⁻²⁴⁰. Research in this domain also got extended as fabrication of working designs^{241, 242} which were utilized for commercial applications. Since then, a lot of progress has been made in this domain utilizing better designs, precise inversion algorithms, correction factors, improving detection

Number Concentrations are usually measured by an instrument named as '*Condensation Particle Counter (CPC)*' working mostly at a frequency of about 1 s. A detailed discussion on CPC has been presented in section 2.3.3.1.2. Number concentration can also be obtained as the cumulative sum of numbers representing size range histograms (i.e. area under the frequency distribution curve) obtained from any instrument measuring number size distribution. Another way of its measurement (indirect) is via '*Aerosol electrometer (AE)*' for restrictive cases. AE measures aerosol current of all aerosol particles (diameters larger than about 2 nm) sampled to a Faraday cup. This current can be converted to number concentration by knowing charge per particle of the aerosol particles. In an uncontrolled or real environment, charge per particle is difficult to determine; hence this technique is mostly used in controlled laboratory environments, sometimes for calibration purposes.

2.3.2 Number size distribution

Size of aerosol particles greatly influences their interactions, dynamics and fate. As already discussed, aerosol number size spectrum has different modes covering a wide size range. Hence different instruments are used for measuring number size distribution in different size ranges. '*Scanning mobility particle sizer*' measures number size distribution in sub- μm range (2 nm - 1 μm) and is discussed in detail in the next section. '*Optical particle counter (OPC)*' based on the principle of optical scattering of light by particles, measures number concentration in the size range of $\approx 200\text{ nm}$ - 20 μm . In this instrument, the aerosol sample is carried to an optical cavity where the sample stream passes between the laser light source and photo diode detector kept at an angle to the incident light. Number of pulses at the diode and pulse height is used to invert the electronic signal to number size spectrum using Mie scattering theory. '*Aerodynamic particle sizer (APS)*' measures the number distribution in the size range 500 nm-20 μm utilizing 'time of flight' principle. Measurement of transit time

Table 2.1: Measurement of aerosol characteristics

Aerosol characteristics		Technique/ Principle of operation
<i>a) Mass characteristics</i>		
Mass concentration	TSP sampler	Filtration based collection (gross filter sampler operated at 10-20 Lmin ⁻¹ during experiments)
	PM sampler	Size classification at inlet followed by filtration based collection
	Beta attenuation sampler	Intensity reduction of beta particles by mass loading, <u>real-time</u>
Mass size distribution	Impactor	Size classification by inertial impaction
	Quartz crystal microbalance	Change in natural frequency of quartz crystal, <u>real-time</u>
<i>b) Chemical composition</i>		
Atomic Absorption Spectrometer		Element specific wavelength light absorption (Model used in this work- Avanta M, GBC)
Atomic emission spectrometer		Element classification based on the intensity of emitted light at particular wavelength
Chromatographer		Separation of the constituents for their determination
Aerosol mass spectrometer		Speciation of converted ions formed from atoms for finding chemical composition, <u>real time</u>
<i>c) Number characteristics</i>		
Number concentration	Condensation particle counter	Growth of particles in supersaturated environment, counting by optical methods (Models used in this work- GRIMM CPC 5.403, TSI CPC 3776)
	Aerosol Electrometer	Collection of charged aerosol particles in a Faraday cup
Number size distribution	Scanning mobility particle sizer	Electrical mobility based size classification, counting by CPC (Models used in this work- GRIMM SMPS 5.403 L/M-DMA, TSI SMPS 3696)
	Optical particle counter	Optical scattering patterns for size classification and counting (Model used in this work- GRIMM 1.108 OPC)
	Aerodynamic particle sizer	Difference in time of flights of accelerated particles for size separation
	Electrical low pressure impactor	Inertial collection of charged aerosol particles for number determination
<i>d) Other characteristics- Shape, Charge, Activity, Density, Optical density</i>		
(Bold font- Techniques and models used in this work)		

concentrations as a better summary index²³¹, superior linkage with health effects²³² and direct impact on the visibility and climatic inferences^{233, 234} has already led policy makers to re-look at the concept of regulatory limits based on mass indices^{235, 236}. Simultaneously, technological growth has enabled probing of aerosol spectrum in terms of its number characteristics with cutting edge capabilities such as the detection of near 1 nm particles. This kind of understanding has also opened possibilities to fine tune models based on number concentration parameters. The parameters which are used for defining number characteristics are ‘Number concentration’ and ‘Number size distribution’.

2.3.1 Number concentration

The number of aerosol particles (of all sizes) per unit volume of air, as a simple summary index, is often used to classify different atmospheric aerosol types. Typical reference values of number concentrations for marine, remote (continental), rural and urban (polluted) region are 100-400, 50-10000, 2000-10000 and 10^5 - 4×10^6 per cm^3 , respectively⁴. It affects aerosol dynamics by modifying the deposition and coagulation processes. For example, order of number concentration changes the coagulation time scale affecting the evolution dynamics. It also serves as the first and foremost index to study diurnal and long term aerosol variations at any location. Factors such as number concentration peaking in the time series, comparison of number concentration at different locations etc. are used as the initial insights for source-receptor modelling.

anions etc. are present. Hence different techniques viz. absorption/emission spectrometry, ion/gas/liquid chromatography, speciation techniques, light attenuation etc. are used in order to assess the composition, appropriately. Most of these techniques involve offline conditioning of the substrates (filters in many cases) and follow-up analysis for the estimation of the chemical composition. Classification, principle and operating parameters of commonly used devices based on above techniques have been listed in Table 2.1. This work utilized ‘Atomic Absorption Spectrometry’ (AAS) for the measurement of mass concentration of specific trace metallic elements as a sub-part of one of the experimental campaigns. This technique relies on the element specific wavelength light absorption by ground state atoms in the flame. Concentration of different elements (up to ppb levels) can be obtained from the same sample by using different wavelengths. AvantAA (GBC Scientific Equipment Pvt. Ltd) make AAS has been used in this work for the determination of elemental concentration of particle’s chemical components. The flame in the instrument converts mist from sample solution to atomic vapour. Atoms in the ground state absorb radiation supplied by a hollow cathode lamp consisting of targeted element as its cathode. Specific amount of fixed wavelength light absorbed by atoms of the element gives its concentration.

In recent years, online chemical composition based mass measurements are being made possible by ‘Atomic Mass Spectrometry’. Here, speciation leading to the determination of chemical composition is done by converting atoms to ions and further separating these ions on the basis of their mass to charge ratio. Development of online *aerosol mass spectrometers* has enabled researchers to get real-time quantitative information on the size and chemical mass loading for non-refractory sub-micron aerosol particles²²⁸⁻²³⁰.

2.3 Measurement of aerosol number characteristics

Aerosol number characteristics are used in several applications such as cloud activation, clean room specifications, lung deposition calculations etc. Representation of number

used. In this device, intensity attenuation of beta particles is calibrated with respect to the mass load on the filter to obtain mass concentration.

Mass size distribution of an aerosol sample is measured mostly by using different versions of inertial impactors. Impaction is defined as the deposition process of aerosol particles during their curvilinear motion due to the difference in their inertia with respect to the flow streamlines. For an impactor plate with a particular cut-off, inlet size distribution can be segregated into two parts (one impacting on collection plate and other following the streamlines) in a *single stage impactor*. Analysis of the mass collected on the filter papers placed in successive stages of decreasing cut-off diameters provides mass size distribution (mass concentration in different histograms) in a *cascade impactor*. Resolution of the size spectrum in the lower size ranges can be increased by operating the downstream stages at low pressure (than atmospheric pressure) in *low pressure impactors*. As in the case of integral samplers, these impactors are generally used for offline analysis only. An approximate but quick estimate of mass (concentration) size spectrum can be made using an instrument named as *Quartz Crystal Microbalance (QCM)* where the change in natural oscillating frequency of the quartz crystal in different stages is coupled to the deposited mass.

Classification, principle and operating parameters of above mentioned devices have been summarised in table 2.1. As this work was mostly focused on number characteristics, only TSP samplers were utilized as a part of one of the field campaigns.

2.2 Measurement of chemical composition

Chemical composition of aerosol particles is an equally important parameter along with size, density, refractive index etc. in the context of particle-vapour interactions, radiative effects and phase transitions. It is of toxicological concern as well since particles may contain hazardous components such as heavy metals etc. Atmospheric aerosol particles have complex chemical composition where several inorganics, organics, refractory materials, cations and

data. Understanding of the issues related to aerosol instrumentation helps to obtain precise data and accurate insights of the measured parameters.

2.1 Measurement of aerosol mass characteristics

Mass characteristics of aerosol systems are most commonly measured ahead of other parameters. It is quite simple and insightful to estimate features of mass characteristics. As of now, regulatory limits for clean environments and air quality indices are based on the mass concentrations of airborne particles (*National Ambient Air Quality Standards, India; National Standards for criteria air pollutants in Australia; Air Quality Standards, European Commission; National Ambient Air Quality Standards, United States Environmental Protection Agency*). Mass concentration and mass size distribution are two parameters which are used for aerosol mass characterisation. Aerosol mass concentration is measured by adopting filtration based sampling system. In its simplest form i.e. a *Total Suspended Particulate (TSP) sampler*, it consists of a filtration assembly and a sampling pump. The aerosol laden air is passed in a leak-tight arrangement through the sampler which collects particles on the filter paper. Mass concentration of aerosol particles in the sample can then be calculated from the weight of deposited particles and the volume of sampled air. By providing a size cut-off at the inlet of the Particulate Matter (*PM*) sampler, mass concentration corresponding to different size ranges (*PM_x*: Mass concentration of aerosol particles having diameters lesser than x units, *PM_{x-y}*: Mass of aerosol particles having diameters between x and y units) can be estimated. Based on the same principle, larger filtration surface areas and higher flow rates are utilized in *High Volume Samplers (HVS)*. Although this technique is quite simple, robust and accurate; it can't provide real time results due to the requirement of offline analysis (generally, gravimetric) of filter papers. For the cases where it is desirable to get real time mass concentration, *beta attenuation samplers* are

CHAPTER 2

TECHNIQUES AND INSTRUMENTATION

Any typical aerosol size spectrum, whether pertaining to environmental or laboratory conditions, contains particles of varying diameters from few nm to tens of μm . The parameters of the spectrum could be quite diverse e.g. presence of single or multi modes, too small or large concentrations etc. Also, the spectrum may have a temporally evolving nature, thus modifying the covered size range and the modal values. It is challenging and often impossible to arrest the changes in aerosol parameters by adopting a single technique or one type of measurement system. Hence relying on a multitude of techniques for measurements is a customary practice in aerosol experiments. For example, for number size distribution, electrical mobility classification is used for measuring sub- μm particle sizes; while classification based on scattering intensity patterns is adopted for measuring size ranges from 0.1 to 30 μm . The challenge increases while probing multiple parameters (e.g. number concentration, mass concentration, size distributions, shape, charge etc.) for the aerosol system, simultaneously. Instruments based on different techniques have been constantly developed so as to measure these parameters. Different types of counters, size separators, collectors, spectrometers etc. are used for such purposes. With the advancement of technology, it is now possible to make such measurements at better sensitivities and finer resolutions. Real time measurement of aerosol mass, chemical composition and charge has become the prime focus of recent sophisticated aerosol campaigns. Study of formation and evolution characteristics of aerosols, whether in atmosphere or laboratory conditions mainly focuses on measurement of number and mass characteristics, chemical compositions and/or radiative properties. Other aspects such as charge, shape, density, activity etc. could also be important. Although several available instruments are routinely used, simple but crucial issues such as calibration, inversions, coupling of different equivalent diameters, inter-instrumental differences etc. play a great role towards the interpretation and analysis of the

basis of these approaches are also discussed. The chapter ends with discussing the key differences of this work with respect to the previously conducted studies. This was necessary so as to evolve a proper methodology which could be applied for characterisation of NPF events during episodic release scenarios.

understanding atmospheric formation processes. In contrast, this work targets NPF events due to episodic source terms mostly resulting in high (total) number concentration conditions.

Although it is suggested to use detected size as minimum as possible to improve the accuracy of the results of the models discussed in Sections (3.4.1-3.4.3), classification criterion (Section 3.2) was applied to the entire data. Classified NPF (based on observable nuclei mode particles) events were selected from this data. Corroborative evolution of total number concentration, nuclei mode number concentration and size distribution was studied for identified events. Subsequently, parameters (coagulation sink, condensation sink) which could be calculated from the size distribution evolution were estimated. Formation rate of nucleated particles (nucleation rate), formation rate of minimum detectable size and growth rate was estimated for these cases using applicable methods discussed in this section.

3.5 Summary

This chapter discusses the theoretical developments related to the estimation of formation and growth parameters of nucleation events. Methodology to identify such events has also been presented. It was seen that simultaneous increase of number concentration of nuclei mode particles and signs of growth of diameter in this size range is required to qualify any perturbation as an NPF event. Intensity of such an event is then decided on the basis of rate of increase of nuclei mode concentrations during the growth time. A case study was presented where steps for qualifying a signal as an NPF event have been shown. Theoretical framework used in atmospheric nucleation research is somewhat different from conventional nucleation theories. Therefore, terminologies and definitions used in describing such models have also been presented. Definitions, concepts and applications of coagulation sink, condensation sink, growth rate and nucleation rate were also discussed in detail.

Various mathematical approaches used for estimating nucleation and growth characteristics of an NPF event are presented. Some large scale models developed on the

of the calculated rates. Also, air mass homogeneity to determine spatial scale of nucleation is a requirement while applying it to atmospheric measurements. This was used for ambient measurements for studying characteristics of NPF events¹²⁸.

PARGAN code was further improved by an efficient data analysis of the ambient aerosol spectrum⁶⁶. Particle size distribution data was smoothened so as to improve the sensitivity to include noisy NPF events as well. Lognormal distribution was fitted to the smoothened data before deriving particle nucleation and growth rates. Growth rates, in parallel, were also estimated by fitting a first order polynomial line on the evolving geometric mean diameter data. For this modified PARGAN model, over and under-estimation of growth rate due to too large or too small fitting parameters was avoided, so as to increase the sensitivity of the parameter derivable frequency of the NPF events.

3.4.4 Methodology adopted in this work

This work deals with experimental observations/insights related to the characteristics of nuclei mode particles. Data from size distribution evolution measurements was obtained for three different campaigns. In two of these, size distribution parameters of particles emitted due to the bursting of firecrackers (during the Indian Diwali festival) were interpreted. The third case investigated the changes in atmospheric aerosol parameters due to a large scale fire event. In Diwali measurements, the minimum detectable particle size was ≈ 10 nm while sensitivity increased to ≈ 5 nm (due to M-DMA) in third campaign (i.e. fire event). Objectives of this work are mostly related to providing enhanced knowledge in behavioural response of nuclei mode particles. Ahead of that, attempts were also made to calculate the formation, growth and evaluation parameters for some cases. On the basis of growth/changes of number concentration in nuclei mode, extraction of NPF events and their parametric evaluation was carried out. It should be noted here that nearly all studies in this domain investigate NPF events in atmospheric conditions avoiding local nucleation sources and

$$J_{1.5}(t) = J_x(t + \Delta t) \exp[coagS(d_{1.5}) d_{1.5}^2 (\frac{d_x - d_{1.5}}{a d_{1.5} d_x} + \frac{b}{a^2} \ln(\frac{GR(d_x)}{GR(d_{1.5})} \frac{d_{1.5}}{d_x}))] \quad (3.24)$$

with t as growth time of clusters from 1.5 nm to observable size.

and for power-law case:

$$J_{1.5}(t) = J_x(t + \Delta t) \exp[\gamma d_{1.5} \frac{CoagS(d_{1.5})}{GR(d_{1.5})}] \quad (3.25)$$

$$; \gamma = \frac{1}{m-n+1} [(\frac{d_x}{d_{1.5}})^{m-n+1} - 1]$$

Growth time Δt used in above equations can also be related to model parameters as

$$\begin{aligned} \Delta t &= \frac{1}{b} \ln(\frac{a+bd_x}{a+bd_{1.5}}) \text{ (linear case)} \\ &= \frac{d_{1.5}^n}{GR_{1.5}(1-n)} (d_x^{1-n} - d_{1.5}^{1-n}) \text{ (power law case)} \end{aligned}$$

3.4.3 PARTicle Growth And Nucleation (PARGAN) model

PARGAN (PARTicle Growth And Nucleation) model²⁸⁰ uses inverse modelling procedure to determine the empirical nucleation and growth rates of particles based on the measurements of aerosol size distribution. The methodology used in this model consists of fitting the time evolution changes of aerosol size distribution by non-linear regression analysis of GDE. In this case, growth rate can be estimated using size intervals instead of total or parametric numbers. Formation time of measured particles can be determined using the evolution of growth rates. Subsequently, number concentration of nucleated particles can be calculated after accounting for the losses between formation and measurement. This concentration along with the time of formation can be used to derive the nucleation rate. As this approach directly uses GDE (in place of fitting the nucleation rate or connecting appearance rate) for nucleation rate, it is different from methods discussed in Sections 3.4.1 and 3.4.2. While using GDE backwards for size segregated number concentrations to estimate nucleation rates, within-mode coagulation is also accounted. This model includes deposition and dilution in GDE for describing aerosol dynamics. Accuracy of the measured size distribution affects the accuracy

Further, the effect of nuclei self-coagulation was incorporated by modifying coagulation sink and growth rate used in eq. 3.23 as

$$coagS_{tot}(d_1) = coagS(d_1) + coagS_{scg}(d_1)$$

$$GR_{tot} = GR_{cond} + GR_{scg}$$

Where $coagS_{scg}$ and GR_{scg} are for scavenging due to self-interactions which depend linearly on N_1 (number concentration of 1 nm particles) as

$$coagS_{scg}(d_1) = K_{eff} * N_1$$

$$GR_{scg} = 1.57 * 10^{-6} * \lambda * d_1^3 * \hat{c}_1 * N_1 * N_A$$

(K_{eff} : effective coagulation kernel, λ : dimensionless parameter, \hat{c}_1 : molecular speed of critical cluster, N_A : Avogadro's number)

In recent atmospheric measurements detecting particles close to 1 nm, particles growth rates below 3 nm were seen to be size dependent (such as linear¹²⁹). Korhonen et al.²⁸⁷, took two cases to take size dependency of GR accounted by

1) Assuming linear dependency (i.e. $GR(d_p) = a + bd_p$;

$$a = GR(d_c) - bd_c ; b = \frac{GR(d_x) - GR(d_c)}{d_x - d_c}$$

2) Or alternatively $GR(d_p) = GR(d_c) * (\frac{d_p}{d_c})^n$

$$(i.e. \text{ power law dependence with } n = \frac{\ln(GR(d_x)/GR(d_c))}{\ln(d_x/d_c)})$$

In their work, they selected $d_c = 1.5$ nm due to the indication of formation of critical clusters in diameter range 1-2 nm^{70, 288}. For the case of linear dependency, non-integer m values could not yield analytical solutions, therefore m was taken as -2 again.

Size dependent growth rates can be coupled to fundamental Kerninen-Kulmala approach estimating nucleation rate as

For linear case:

The above formulation can also be used to compute number concentration in any size range ($d_{j,1}$ - $d_{j,2}$) or alternatively for sizes $<d_j$ as well.

Using a revised formulation²⁸³, the power law dependence of coagulation sink and extrapolation of condensational sinks to calculate coagulation sink was replaced and a better computationally efficient particle formation model was presented. In this, GDE for nucleation mode size distribution can be written as

$$\frac{\partial n(d_p)}{\partial t} + \frac{\partial (GR(d_p)*n)}{\partial d_p} + coagS(d_p) * n = J_1 \delta(d_p - d_1) \quad (3.21)$$

where respective terms are for number distribution function evolution, condensational growth, coagulation scavenging and nucleation, respectively. Here, d_1 is same as d_c for 1 nm critical size.

Particle flux (J for large diameters) is related to $n(d_p)$ as

$J(d_p) = GR(d_p) * n(d_p)$ which leads to

$$\frac{dJ}{dd_p} = - \frac{CoagS(d_p)}{GR} * J \quad (3.22)$$

Again a power law dependence of the coagulation sink on diameter was assumed as

$$coagS(d_p) = coagS(d_1) * \left(\frac{d_p}{d_1}\right)^m \text{ or equivalently}$$

$$m = \frac{\log[CoagS(d_x)/coagS(d_1)]}{\log[d_x/d_1]} \text{ where } d_x \text{ is any observational diameter. Power exponent}$$

however can be estimated from experimental data. The values of m were observed to be between -1.5 to -1.75 for Finnish Boreal forest: Hyytiälä site^{96, 116}.

Eq. 3.22 can be integrated (using underlying assumptions, however avoiding condensational flux matching) to get

$$J_x = J_1 * \exp(-\gamma * d_1 * \frac{coagS(d_1)}{GR}) \text{ with } \gamma = \frac{1}{m+1} \left[\left(\frac{d_x}{d_1}\right)^{m+1} - 1\right] \quad (3.23)$$

This equation relates formation rate of x size particles (x can be minimum size detected by observational set-up) and nucleation rate corresponding to 1 nm critical size.

$$\sum_j K(d_0, d_{p,j})N_j = \gamma'' * 4\pi D_i CS'_{\alpha=1} = \gamma' * CS'_{\alpha=1} \quad (3.16)$$

(i. e. Coagulation sink for 1 nm particles is proportional to the rate of condensation of large vapour molecules on same particle spectrum, $CS'_{\alpha=1}$ is constant as there is no change in the background population)

Further, N_c and N_j are connected as

$$\frac{dN_j}{dt} = \frac{dN_j}{dd_j} * \frac{dd_j}{dt}, \quad \text{which on using above equations can be converted to}$$

$$\frac{dN_j}{N_j} = -\eta \frac{dd_j}{d_j^2} \quad (3.17)$$

$$\text{where pre-factor } \eta = \frac{d_0^2 \gamma' CS'_{\alpha=1}}{GR} = \frac{\gamma CS'_{\alpha=1}}{GR}$$

Eq. 3.17 can be integrated from $d_{c,ini}$ to d_j to obtain

$$N_j(d_j) = N(d_{c,ini}) * \exp\left[\frac{\eta}{d_j} - \frac{\eta}{d_{c,ini}}\right] \quad (3.18)$$

which can also provide the connection between real and apparent nucleation rate as

$$J_{app}(d_j, t') = J_{real}(t) * \exp\left[\frac{\eta}{d_j} - \frac{\eta}{d_{c,ini}}\right] \quad (3.19)$$

$$t' - t = (d_j - d_{c,ini})/GR : \text{time of growth of particles from } d_c \text{ to } d_j$$

Eq. 3.19 can be used in the case when some alternative nucleation theory provides $J_{real}(t)$ and $d_{c,ini}$ and η is obtainable from model variables. In the similar way, real nucleation rate can be estimated by measuring time evolution of particle number size distribution in the observable size range (d_j - $d_{j,max}$) from which CS' , GR and η can be calculated. In this case, $J_{app}(d_j)$ represents rate of change of number concentration in (d_j - $d_{j,max}$) range and $J_{real}(t)$ then can be estimated from

$$J_{real}(t) = J_{app}(d_j, t') * \exp\left[\frac{\eta}{d_{c,ini}} - \frac{\eta}{d_j}\right] \quad (3.20)$$

($d_{c,ini}$ in this expression can be obtained from nucleation theory or experiments. It is often taken close to 1 nm for atmospheric NPF cases)

Following the similar framework, number concentrations of particles in different modes can also be tracked using coagulation coefficients defined with mean size of these modes. Deposition velocity can also be introduced in these formulations which could be important for particles in coarse size ranges. Coupling of atmospheric gas phase chemistry model and three mode integral aerosol dynamics model to model the formation of H₂SO₄-H₂O particles in rural, urban and marine conditions has been discussed¹¹⁷.

3.4.2 Kerninen- Kulmala equation

Kerninen and Kulmala²⁸² derived analytical expressions connecting real and apparent nucleation rate and the nuclei number concentration for atmospheric nucleation events. Following three assumptions were made in this procedure:

- a) Sinks other than coagulation of nuclei to pre-existing aerosol particles can be neglected.
- b) Condensational growth of these nuclei happens at a constant rate.
- c) There is no change in the population of background particles during nuclei growth; which can be written in mathematical form as

$$\frac{dN_c}{dt} = -N_c \sum_j K(d_c, d_{p,j}) N_j \quad (3.12)$$

$$\frac{dd_j}{dt} = \text{constant} \quad (3.13)$$

$$\sum_j \frac{1}{2} d_j \beta_m(kn_j, \alpha) N_j = \text{constant} \quad (3.14)$$

Eq. 3.14 states the constancy of the vapour flux to background particles during nuclei growth. Apart from these assumptions, two approximations were also deduced related to coagulation between nanometer sized nuclei and larger particle sizes and rate of condensation, respectively. These can be written as:

$$K(d_c, d_{p,j}) d_j^2 = K(d_0, d_{p,j}) d_0^2 \quad (3.15)$$

(i. e. Brownian coagulation coefficient between cluster size and other particles is proportional to $d_c^{-\kappa}$, κ lies between 1.5-2, authors took $\kappa=2$ and $d_c=d_0=1\text{nm}$ for their context)

$$\omega_{ij} = \frac{(R_{ij} + \gamma_i)^3 - (R_{ij}^2 + \gamma_i^2)^{3/2}}{3R_{ij}\gamma_i} - R_{ij} \text{ with } \gamma_i = \frac{8D_i}{\pi \check{c}_i}$$

Coagulation sink used in eq. 3.2 can then be obtained using coagulation coefficients as

$$coagS = \sum_j K_{ij} N_j \quad (3.7)$$

The main outline of these equations is the possibility of determinations of parameters (eq. 3.3, 3.5 and 3.7) directly from the measured size spectrum evolution. Using these basis parameters, different approaches have been used for defining rate equations for number and mass concentrations for different modes (three/two). Time evolution of number concentration of nucleated particles (at critical cluster size: N_c) can be expressed as

$$\frac{dN_c}{dt} = J_R - coagS_c * N_c - J_{app} \quad (3.8)$$

Where $coagS_c$ represents coagulation sink for N_c 's. J_R and J_{app} here denotes real and apparent nucleation rate depending on the size of the critical cluster and detection limit of the observation. For steady state condition, $J_R = coagS_c * N_c + J_{app}$

Coagulation of N_c during their growth from real cluster size to apparent cluster size can be obtained from

$$\frac{dN_{c,app}}{dt} = -coagS_{c,app} N_{c,app} \quad (3.9)$$

where $N_{c,app}$ represents particle concentration growing from real to apparent size class and $coagS_{c,app}$ represents respective coagulation sink. The fraction of N_c 's coagulated and contributing to J_{app} can be estimated from this equation. Following this methodology, the equation for N_{app} can be written as

$$\frac{dN_{app}}{dt} = J_{app} - coagS_{c,app} * N_{app} \quad (3.10)$$

Equations (3.8-3.10) can be connected to provide nucleation rate of real cluster sizes as

$$J_R = \left(\frac{dN_{app}}{dt} + coagS_{c,app} N_{app} \right) e^{coagS_{c,app} t} \quad (3.11)$$

In eq. 3.11, t represents growth time from real to apparent particle size.

$$\lambda_V = 3 \sqrt{\frac{\pi * M}{8k_B T}} D \text{ (M: molecular mass, } k_B \text{: Boltzmann constant; T: temperature)}$$

Diffusion coefficient in the above relation can be found experimentally or from empirical relations (such as for air-gas system²⁸⁵).

Condensation sink used in eq. 3.1 can be estimated from the following expression using number distribution function $n(r)$

$$CS = 4\pi D \sum_i \beta_{m_i} * r_i * N_i = 4\pi D \int_0^\infty r * \beta_m(r) * n(r) dr \quad (3.5)$$

α used in eq. 3.4 stands for sticking probability, typically taken 1 most of the times.

CS varies as r^2 in free molecular regime (where $\beta_m \approx 3r/4\lambda_V$) and as r in continuum regime (where $\beta_m = 1$). Power exponent varies between 1 and 2 for aerosol particles having sizes in transition regime.

Coagulation is caused by Brownian motion of particles for which Brownian coagulation coefficient for size class i and j can be written as²⁸⁶

$$K_{ij} = \frac{K_C^B}{\frac{R_{ij}}{R_{ij} + \sigma_{ij}} + \check{c}_{ij} R_{ij}} \quad (3.6)$$

K_C^B , Brownian coagulation coefficient in the continuum regime is

$K_C^B = 4\pi(R_i + R_j) * (D_i + D_j)$; $R_i + R_j = R_{ij}$ is the contact radius of coagulating particles and $D_i + D_j = D_{ij}$ is the effective/binary diffusion coefficient.

Particle diffusion coefficient used in above formulation is given by Stokes-Einstein relation

as $D_i = \frac{kTC_c}{6\pi\mu R_i}$ with μ as dynamic viscosity and C_c as Cunningham slip correction factor.

Mean thermal velocity of m_i mass particle i.e. $\check{c}_i = \sqrt{\frac{8k_B T}{\pi m_i}}$ can be used to calculate relative thermal velocity between the coagulating particles \check{c}_{ij} used in eq. 3.6 i.e.

$$\check{c}_{ij} = \sqrt{\check{c}_i^2 + \check{c}_j^2}$$

The flux matching distance in eq. 3.6 is $\sigma_{ij} = \sqrt{\omega_{ij}^2 + \omega_{ji}^2}$, where

these theories built on and around aerosol dynamic equation. In the present context, mathematical procedures discussed in this section focus on nucleation rate and time evolution characteristics of clusters formed during the nucleation processes.

3.4.1 Conventional approach

This kind of phenomenological approach based on a set of basis equations^{79, 116} has been implemented in lot of studies carried out in ambient atmospheric conditions discussed above. In this method, growth characteristics of aerosol particles can be analysed in two or three modes (Nuclei/Aitken/Accumulation).

In a given environment of vapour and pre-existing aerosols, the rate of change of vapour concentration (C) can be expressed as

$$\frac{dC}{dt} = Q - CS * C \quad (3.1)$$

where Q is the source rate of vapour and CS is its condensation sink to existing aerosols.

The change of number concentration (N) in a size class is

$$\frac{dN_i}{dt} = J_i - coagS * N_i \quad (3.2)$$

In this equation J_i and N_i represents formation rate and number concentration for i^{th} size class particles. Coagulation sink for this size class particles is denoted by $coagS$.

The growth rate for a particle size r (or r_i) can be expressed as

$$\frac{dr}{dt} = \frac{m_v * \beta_m * D * C}{r * \rho} \quad (3.3)$$

where (m_v , D) are used for molecular mass and diffusion coefficient of vapour molecules, ρ is used for particle density. β_m is transition correction factor for mass flux given by Fuchs and Sutugin²⁷⁹ as

$$\beta_m = \frac{Kn+1}{0.377Kn+1 + \left(\frac{4}{3}\right) * \alpha^{-1} * Kn^2 + \left(\frac{4}{3}\right) * \alpha^{-1} * Kn}; \quad kn \text{ (Kundson number)} = \lambda_v / r \quad (3.4)$$

Mean free path of vapour molecules (λ_v) is connected with molecular diffusion coefficient D as

3.3.4 Nucleation rate

The focal quantity of interest i.e. nucleation rate can be calculated by relating the above discussed sinks, growth rates and rate of change in the number concentrations. In most of the modelling studies, it is the formation rate of 1 nm particles where 1 nm is assumed to be size of freshly formed particles. At the level of present detection limit of mobility sizers, nucleation rate is generally calculated for 3 nm particles from measurements. From the fraction of particles escaping from sinks, real nucleation rate can be estimated. In recent times, concentrations of nanoparticles and ions have been determined for size classes between 0.9 and 2.1 nm⁷⁰. Due to the presence of large amount of water vapour, hydrate formation competes with nucleation. The presence of hydrates tends to decrease the nucleation rate by affecting the number of monomers of the source term^{281, 117}. The potential of large concentration aerosol releases towards short term spikes in nuclei mode particles is another domain where need for estimating nucleation rate exists. As already discussed, expressions have been developed^{278, 282, 283} relating the formation rate of critical clusters (real nucleation rate) and the rate at which they appear at larger sizes (apparent nucleation rate). Nucleation rate can also be determined from growth rates for size-ranges using non-linear regression analysis of general dynamic equation (GDE) to fit the measured change of aerosol size distribution in time²⁸⁰. This kind of approach (PARGAN model) and further improvements by assisted statistical analysis⁶⁶ have been successfully implemented for improving the estimations of nucleation rates. Apart from the parameterization based models, nucleation rates have also been provided for large scale models¹³⁹. The formulation of nucleation rates for different contexts has been discussed in section 3.4.

3.4 Various approaches to determine nucleation and evolution parameters

Several mathematical models and solution techniques have been developed and adopted in order to predict the characteristics of nanoparticles in production industry and of nucleated particles for atmospheric research applications. Particle size distribution functions are used in

3.3.2 Condensation sink

The flux of vapour molecules towards condensing surfaces and the rate of condensation can be parameterized by condensation sink. It describes the ability of aerosol size distribution to remove vapour due to the condensation and is shown to be strongly depending on the shape of the size distribution of existing aerosols¹¹⁷. Diffusion coefficient of vapour molecules and transition regime correction factor²⁷⁹ are parameters other than the size distribution function which are used in the estimation of the Condensation sink from the measurement data. Due to significantly higher concentration of water vapour molecules in comparison to other source terms (such as acid molecules for the case of ternary water-sulphuric acid-particle system), condensed droplet remain in quasi state equilibrium with the water vapour. This condition has been used to calculate molar fraction of source terms by equating activities of water in the gas phase and liquid phase. The formulation of condensation sink has been discussed in section 3.4.

3.3.3 Growth rate

Growth rate (GR) together with coagulation rate constants serves as the input parameter for quantifying the evolution of particle size distribution in general dynamic equation. It can be related to vapour concentration utilising vapour molecular parameters and transitional regime correction factor. It can also be estimated by performing non-linear regression analysis on measured changes in cumulative size distribution over a finite time interval²⁸⁰ or by performing polynomial fitting to GMD evolution^{128, 131}. If specifically calculated for nuclei mode, it represents the growth of nuclei mode particles to Aitken and accumulation mode size ranges and hence can be connected to the growth of nucleated particles to this observable size range as well. The formulation framework of growth rates for different conditions has been discussed in Sections 3.4.

measurements conducted during ‘large scale episodic aerosol releases’ and ‘hot wire experiments’ led to new information for knowledge database in this domain.

3.3 Estimation of aerosol parameters

As discussed above, models discussing atmospheric NPF events are parametric and semi-empirical in nature. Generally, the growth-decay equations for condensable species/vapour and aerosol number concentration are coupled with the growth rate and sinks participating in the system for estimating aerosol parameters. These parameters are then connected to other process factors so as to arrive at apparent and real nucleation rate. In its simplest form, this approach calculates coagulation and condensation sinks from the size distribution evolution measured onsite. Characteristic parameters (such as GMD) associated with different modes (especially nuclei mode) are also used in some contexts as well (section 3.2). For comparing nucleation peaks due to ambient and episodic releases, size distribution evolution analysis around these peaks can be done for inferences.

3.3.1 Coagulation sink

Coagulation sink determines the loss of nucleated particles as an effect of their coagulation with existing aerosol particles. It can be estimated from size segregated number concentration data and coagulation coefficients for different size ranges. In the atmosphere, Fuchs Brownian coagulation kernel is the most appropriate one due to its applicability for varying Knudsen number regime. As the number concentration of a threshold/critical size (generally 1-1.5 nm for atmospheric NPF events) is not known, it is difficult to account for self-coagulation of these small clusters. Effect of self-coagulation of nuclei on the parameterization of formation rate of new particles has been discussed elsewhere²⁷⁸. In this work, ratio of nucleation rate to the source rate of condensable vapour has been used to provide ranges where the correction due to self-coagulation needs to be taken care of. The formulation framework for coagulation sink has been discussed in section 3.4.

requirements. Only when it satisfied one/both of the above two tests, it was accounted as an NPF event for further calculations.

3.2.2 Behaviour of nuclei mode particles

Once formed, critical cluster sizes grow to nuclei mode size ranges and evolve continuously by self-coagulation, coagulation with other sizes and by condensation. This evolution of freshly generated particles is often captured by particle sizers and subsequently, parameters associated with aerosol dynamics are estimated. It was also shown in section 2.4.2 that such interactive dynamics can be utilized to generate nanoparticle aerosols of controlled characteristics. For such cases, evolution of these small sized particles in closed chamber conditions leads to several interesting features such as evolution of bimodal size distribution from continuously injected nuclei mode particles²⁷⁷.

For atmospheric conditions, the flux of particles into an observable size range has been related to the number concentration changes in nuclei mode range, loss of particles due to coagulation and outward flux from this range. Although nucleation rate for the case of natural atmospheric processes has been well studied, behaviour of nuclei mode particles during high concentration conditions (episodic events) has not been discussed in detail. With underlying assumptions, similar kind of methodology can be adopted to substantiate nucleation and growth parameters for such episodic releases. The residence time of generated nuclei mode particles and their characteristics can help policy makers to develop guidelines to be followed in the case of such releases. On the other hand, models developed for simulating aerosol dynamics (particularly focusing on free molecular regime) rely on validation experiments conducted with the aid of nuclei mode particles.

This work attempts to fill the gap in understanding the formation and evolution dynamics of nuclei mode particles as per the defined objectives. As will be seen,

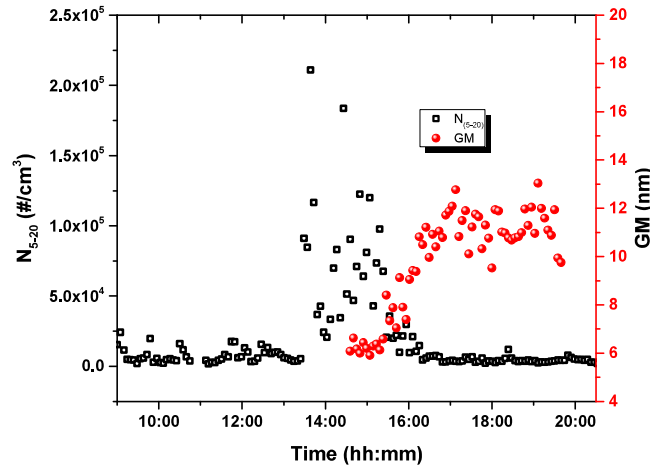


Fig. 3.2: Characteristics of nuclei mode particles at daytimes for same data as of fig. 3.1

A hot spot around afternoon hours (14:00-16:00 hrs.) can be noticed in fig. 3.1 indicating the formation of new particles. Observations showed that the total number concentration also increased significantly around this time period. On further analysis (Fig. 3.2), this increase could be linked to an increase of number concentration in the nuclei mode. As can be seen, the perturbation of number concentration continued for approximately two hours ultimately diluting to background concentration. It can also be seen that GMD corresponding to the nuclei mode increased, subsequently. Such an event with the above mentioned characteristics qualified to be called as an NPF event.

A detailed analysis of the parameters of the measured spectra (presented in Chapters 4 and 5) gave an insight into the methodology of identification of NPF events during the times of episodic emissions. Formation and growth characteristics were estimated for all such identified events during the study period. There were instances of sporadic increase of nuclei mode particles as well for which, the characteristics could not qualify the criterion set for classification as a NPF event. In all field campaigns conducted under this work, time series data (coupled number concentration of total and nuclei mode particles) was checked for getting primary nucleation signature which was subsequently tested as per the above

such a context, nucleation parameters during episodic releases can be obtained by modifying above mentioned methodologies accordingly.

3.2.1 Identification of NPF Event

Size distribution evolution analysis can be used to relate temporal changes in number concentration to NPF event. Interpretation of measured size distribution data for entire day (March 25, 2016) during a large scale fire event and its linkage with NPF characteristics is discussed in this section. Details of this event and measurements are discussed in section 5.2. These measurements were made in a high rise building situated approximately 5 km from the site of fire. Fig. 3.1 depicts evolution of number size distribution of aerosol particles measured by SMPS on March 25, 2016 during this fire event. Time series of number concentration and geometric mean diameter (GMD) of the nuclei mode in day times (calculated from same data set) has been plotted in Fig. 3.2.

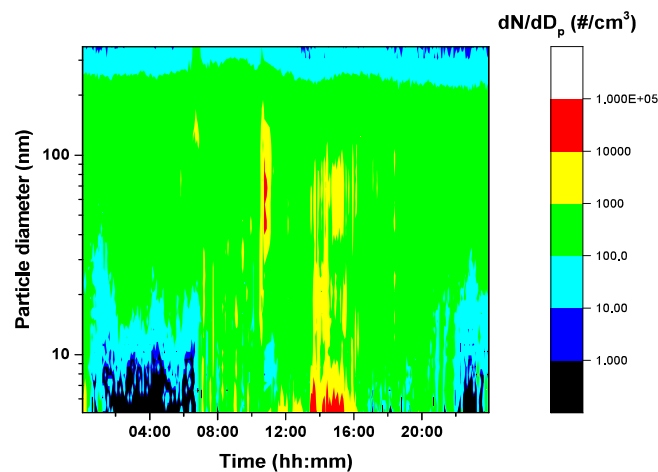


Fig 3.1: Evolution of number size distribution at sampling site during a large scale fire event

for studying the evolution of size spectrum in the measured size ranges (above minimum detectable size) which is then connected to the formation at the critical cluster size.

3.2 Criterion for defining a nucleation event

There are different ways to define a nucleation/NPF event. Typically, a day will be called as an NPF day when there is an appearance of a distinctly new mode of particles in nuclei mode, with prevalence of this mode over a time span of hours, showing signs of growth⁹⁶. As the growth characteristics are measured above a stated size, growth of nucleated particles is a priori and necessary condition. NPF events can be further divided into sub-classes on the basis of accuracy level of estimated formation and growth rates⁹⁶. If the data is large, these events can be classified on a daily basis. Event statistics may lead to annual trends peaking in particular months. If the focus is towards capturing atmospheric NPF events, segregation of events of formation via localised sources is a must. If the focus is on localized sources/episodic events, NPF signals may not be obtained for considerable amount of time in a day (as obtained for atmospheric formation cases). For such cases, a methodology of identifying formation of particles can be developed. The growth of nuclei mode particles is quantified by the slope of increase of geometric mean diameter of the nuclei mode particles. Lower limit of nuclei mode size range is dictated by the measuring instrument while its upper limit can be selected on the basis of growth rate. Another way suggests segregation of events on the basis of growth of the measured nuclei mode concentrations⁶⁶. In their work, events were classified as non-NPF or unidentified, weak, moderate and strong when $dN_{3-20}/dt \leq 2000$, $2000-4000$, $4000-15000$ and $\geq 15000 \text{ cm}^{-3} \text{ h}^{-1}$, respectively; where N_{3-20} is the number concentration of particles having diameters between 3 to 20 nm. A first order polynomial was fitted to the temporal evolution of geometric mean diameter to derive the growth rates.

The work carried out in this study is different from studies performed for atmospheric conditions as the focus here is on studying particle formation during episodic releases. For

3.1 Terminology

Homogeneous and heterogeneous nucleation occurs in the absence or presence of foreign or pre-existing seed particles, respectively. This process can occur for single species termed as homomolecular or for two or more species (heteromolecular). Atmospheric aerosol nucleation is generally heterogeneous and can be identified by observations. Binary and ternary nucleation, where two and three vapour species take part in the process respectively, are used to describe important atmospheric condensate system components e.g. sulphuric acid-water, sulphuric acid-ammonia-water etc. Nucleation events refer to the scenario where evidence exists for survival of particles having diameters above the critical cluster size. These events are also termed as New particle formation (NPF) events. Nucleation rate (in units of $\text{cm}^{-3} \text{h}^{-1}$) corresponding to the formation of particles past critical cluster size is termed as initial or real nucleation rate. Apparent nucleation rate is used for the detectable size based on the sensitivity of the measuring device. In addition to several other parameters, the major ones controlling nucleation rate are temperature and supersaturation of the vapour. Supersaturation, the driving force for nucleation refers to the condition when the vapour pressure is more than the saturated/equilibrium vapour pressure. Sinks in the context of calculation of nucleation parameters refer to the loss of molecules (condensable species)/particles in other processes such as coagulation and condensation. Classical nucleation theory uses forward rate constant and reverse rate constant to estimate critical cluster size, number of molecules in the critical cluster and nucleation rate. The source rate of condensable vapour affects growth of nucleated particles in clean and polluted environments. Based on the formation and evolution characteristics of nucleated particles, measurement campaigns generally categorize the observational day as NPF event day, non-event day and undefined day. In these campaigns, scanning mobility particle sizer, differential mobility particle sizer and hygroscopic tandem differential mobility analyzer are generally employed

CHAPTER 3

NUCLEATION PARAMETERS AND THEIR THEORETICAL FORMULATIONS

Thermodynamics of nucleation process is well understood but the efforts to understand the process dynamics are still continuing. The growth of tiny clusters past the critical cluster size occurs as a result of statistical fluctuation around the unstable sizes. Once clusters cross the critical size, growth becomes dominant leading to stable particle phase. Formation and growth processes of atmospheric aerosols are required to be well characterized due to their role in climatic effects. A sudden burst in concentration of nuclei mode particles can not only cause visibility degradation but also induce health hazards. For the case of engineered nanoparticles, similar kind of understanding is important for better control of the process parameters and characteristics. Statistical mechanics often has been used as a theoretical framework to describe nucleation. However, difficulties in the construction of statistical models, associated uncertainties and rigorous mathematics led to the development of simpler models. In classical nucleation theory, clusters are treated as droplets having some properties similar to the bulk phase. Constrained equilibrium cluster approach has also been used to study phase change transitions. Theoretical estimations of these models have shown wide differences or limited similarities from experimental observations, even in controlled conditions. For simulation of atmospheric aerosol formation events, an alternative approach based on coupling of model parameters with experimental observations has been used. As atmosphere is a complex system associated with several parameters/processes/components, semi-empirical approach remains the preferred choice at present. Measurement and prediction of nucleation rate (formation rate of new particles past the critical size) and growth rate (characterizing contribution of nucleated population to condensation nuclei size ranges) is the main focus of several recent developments in the field of atmospheric aerosol research.

particles was $0.06\text{-}0.73\text{ nmh}^{-1}$. Coagulation sink of minimum detectable size and condensation sink for aerosol spectrum was also estimated.

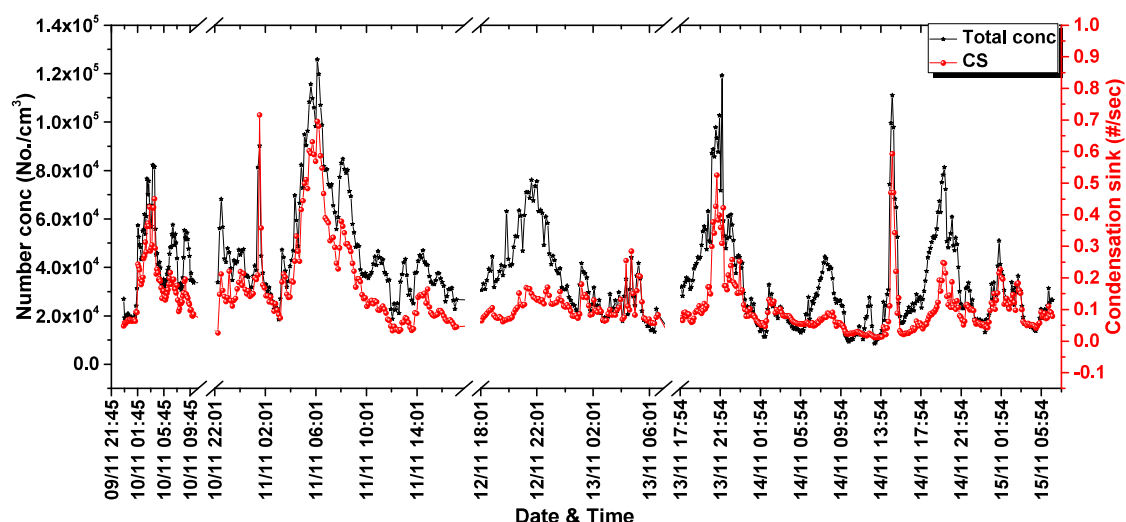


Fig. 4.23: Condensation sink and nuclei mode concentration

4.5: Summary

This chapter presents results of case study 1 performed under this work. Two measurement campaigns were conducted during the days near Diwali festival in 2012 and 2013. Number characteristics of aerosol particles sampled at a height of about 50 m were measured with SMPS. Several sharp number concentration peaks were observed during both these campaigns. The peaks observed at the times of Diwali were found to be similar to other background peaks on the scale of total number concentration. Increase of particle concentration in ultrafine size ranges and shifting of accumulation mode was noted at the time of Diwali emissions. Size distribution evolution analysis around the peak was utilized to differentiate a normal and an episodic peak. Changes in PM concentration and aerosol chemical composition was also measured during Diwali 2013. As the measurements were made for 17 days in 2013 campaign, it became possible to analyse diurnal variations and statistical variations. An analysis was performed to estimate formation and evolution parameters of NPF events picked from excursions of both these campaigns. Few NPF events could be identified during this analysis. For these events, formation rate of minimum detectable size was found to be 15-240 no./cm³/sec while growth rate of these freshly formed

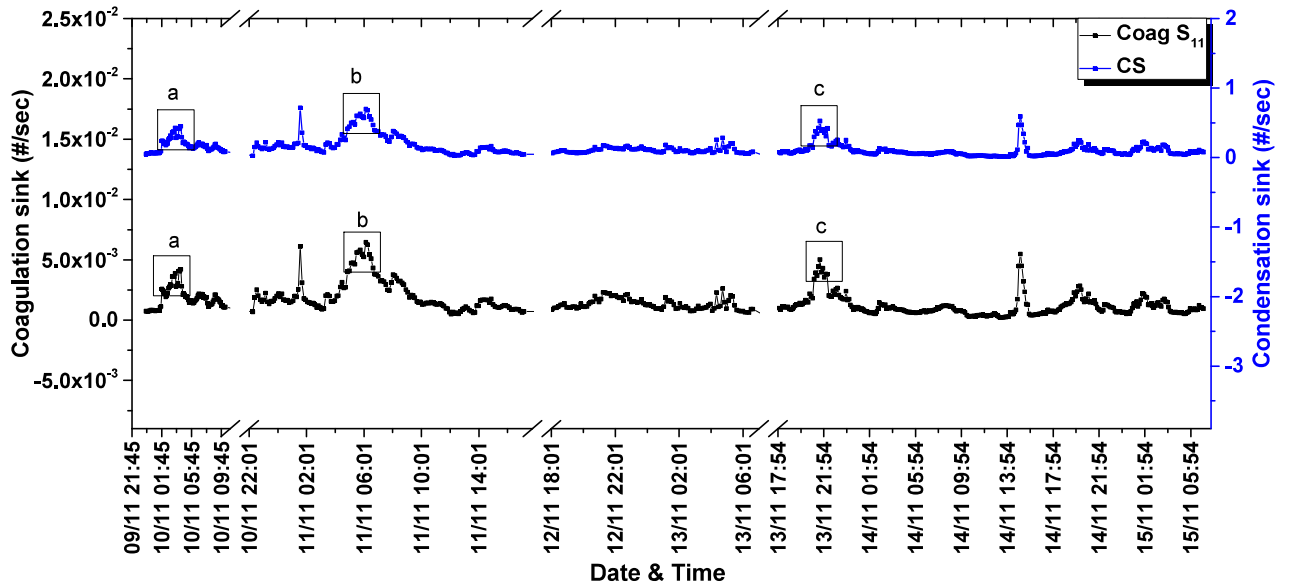


Fig. 4.22: Typical plot for coagulation and condensation sink: Time-series

Ranges for these values ($\text{CoagS}_{11} = 1.78 \times 10^{-4} - 6.45 \times 10^{-3} \text{ sec}^{-1}$, $\text{CS} = 3.27 \times 10^{-3} - 7.15 \times 10^{-1} \text{ sec}^{-1}$) are comparable for other measurements performed in regions of large aerosol population. Fig. 4.23 represents the time evolution of condensation sink and number concentration in nuclei mode size ranges, simultaneously. At some occasions (such as peaks a, b, c), a momentarily drop in condensation sink can be related to a follow-up increase in number concentration. With formation of fresh particles, condensation sink again increases afterwards. However at other times, CS follows changes in nuclei mode concentration reflecting the role of coagulation sink in the formation and depletion processes.

Calculated values of these parameters for both field campaigns of case study 1 are tabulated in table 4.4.

Table 4.4: Formation and evolution characteristics of NPF events

Events	Parameters			
	dN_{11-20}/dt (no./cm ³ /sec)	GR ₁₁₋₂₀ (nm/h)	J ₁₁ (no./cm ³ /sec)	CoagS ₁₁ (#/sec)
Diwali 2012	1.35	0.17	80.55	0.0043
Diwali 2013	1.54-8.67	0.28-0.73	57.31-225.44	0.0032-0.0044
Non-Diwali 2012	1.97-11.51	0.06-0.51	15.06-241.28	0.0011-0.0065
Non-Diwali 2013	1.45-12.28	0.13-0.54	22.26-146.76	0.0014-0.0039

As can be seen, estimated formation rate and rate of increase of nuclei mode particles was comparable for events observed on Diwali and non-Diwali times. It can also be seen from the above table that estimated parameters for Diwali events were comparable with those for non-Diwali (background) events.

4.4.4: Sinks

Time evolution of coagulation and condensation sink depends on the background aerosol population and hence varies as the population changes. An increase in ultrafine concentration at the time of emission due to celebratory fireworks¹⁶¹ was observed which was explained on the relatively lesser values of sinks present at the time of formation⁶⁴. Aerosol dynamics and source term modifies parameters of aerosol spectrum which then gets coupled to the sinks to yield ultimate surviving fraction. There are frequent variations in sink values which can be related to the increases/decreases in number concentration values. Fig. 4.22 depicts time series of coagulation sink of 11 nm particles and condensation sink (11-1083 nm) for entire sampling duration of Diwali 2012.

instances was analysed for estimating the formation and evolution characteristics. Table 4.3 presents event statistics for all sampling days of campaign 1 and 2 (Diwali 2012 and Diwali 2013) conducted as a part of this work (case study 1).

Table 4.3: Event statistics (case study 1)

	Diwali 2012		Diwali 2013	
Sampling days	6		3	
Peak classification	Instances			
	14		11	
	Events			
	At the time of Diwali emissions	Non-Diwali times	At the time of Diwali emissions	Non-Diwali times
Weak NPF	-	-	-	-
Moderate NPF	1	3	1	3
Strong NPF	-	1	1	1

In the above table, instances refer to any observed increase in total number concentration while events are times when these instances are qualified as a certain NPF case. Apart from observing NPF events at the times of Diwali emissions, these were captured at background times as well. For all these events, formation and evolution characteristics were estimated subsequently.

4.4.3: Formation and evolution characteristics of events

The rate of increase of nuclei mode particles (in detectable size range) which serves as the primary index for estimating other parameters related to NPF events, can be represented by $\frac{dN_{11-20}}{dt}$. GR_{11-20} represents the growth rate of nuclei mode particles and acts as an index which affects dynamics of these particles. J_{11} denotes the formation rate of minimum detectable size i.e. apparent nucleation rate. $CoagS_{11}$ represents the coagulation sink for 11 nm particles which is for minimum observable size. CS is used for the condensation sink which is the parameter estimating condensational flux of vapour molecules towards entire (measured) aerosol population. Physical significance, mathematical formulations and inter-relationships of these parameters have been discussed in detail in Section 1.5 and Section 3.3.

evolution of number concentration cannot be corroborated with increase in GM. Similar kind of first level analysis was also performed for second campaign performed during Diwali 2013. For second level detailed analysis, each of the above or similar peaks (including suspected non-NPF peaks) were re-checked studying the size distribution evolutions close to these peaks.

4.4.2: Qualifying criterion and event statistics

As discussed in Chapter 3, NPF events can be classified as strong, moderate, weak and non-event on the basis of rate of change of number concentration in nuclei mode size ranges. Steps of procedure have been provided⁹⁶ for qualifying such events as a certain NPF event. The most important of qualifying criterion is related to the behaviour of average size of nuclei mode particles. Observance of growth in these size ranges not only qualifies such an event but also provides growth rate of observable particles. Fig. 4.21 represents a plot drawn for investigating a probable NPF peak via growth rate dynamics.

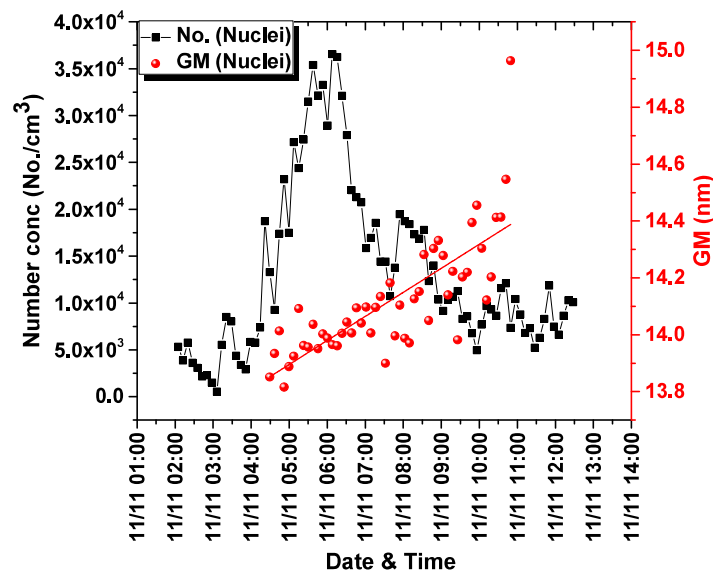


Fig. 4.21: Illustrative example for a qualified event

This peak occurred at early morning hours of 11th November when nuclei mode concentration began to increase from its background values. Superimposed graph for GM of this size range clearly shows the continuous growth of particles. Such an event amidst all

minimum detectable size of the measuring instrument, the growth of particles from nucleated clusters to the detectable size is linked to growth dynamics in apparent size ranges. For this, growth of geometric mean of nuclei mode size ranges can be used as an index. Any growth in nuclei mode particle sizes is relatable to the growth towards detectable sizes (Section 1.5). Fig. 4.20 shows the time series of total number concentration, number concentration in nuclei mode size ranges (11-20 nm) and calculated GM for this range, plotted from SMPS measured data for Diwali 2012 campaign.

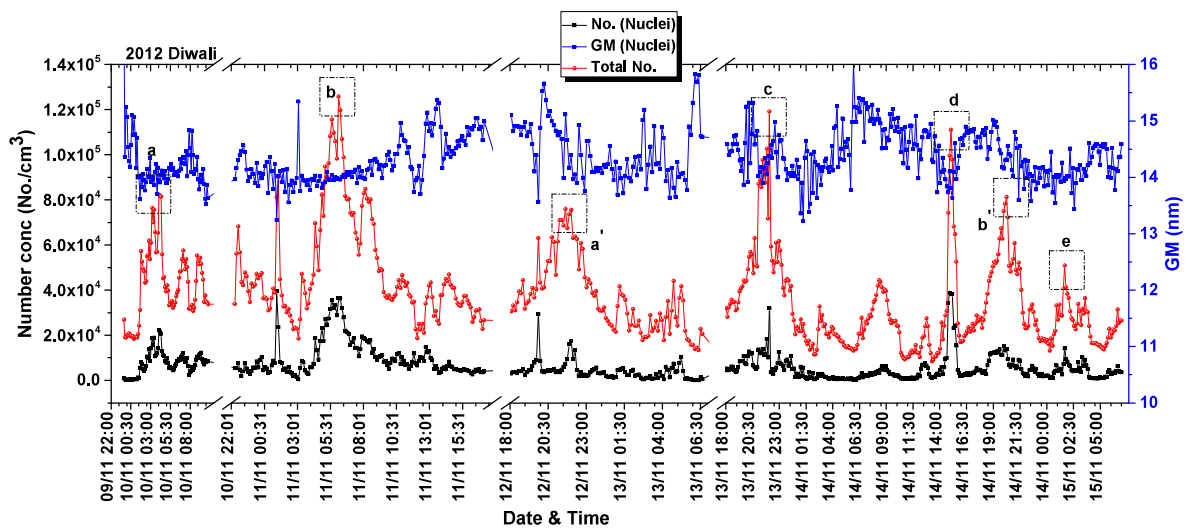


Fig. 4.20: Corroborated number concentration and geometric mean

Peaks in total as well as nuclei mode size ranges include the peaks observed at the time of fireworks. As discussed above, simultaneous increase of particles in both hints at possibility of NPF event which can be checked via tracking the growth of these particles around the peaking times. GM for nuclei mode size ranges may or may not increase following an increase in number concentration. Only those peaks for which GM shows a sign of growth were picked for second level of analysis. As marked in Fig. 4.20, some of these peaks are {a, b, c, d and e} where all three criterion i.e. increase of total number concentration, increase of concentration in nuclei mode size ranges and following increase in GM in the same range are satisfied. Other peaks such as {a', b'} are also shown where

4.4 Evolution parameters for selected nucleation events

An important conclusion deduced after studying and interpreting aerosol characteristics during and around Diwali days (2012, 2013) pertains to the behaviour of nuclei mode particles. Number concentration of aerosol particles not only increased significantly at the times of Diwali emissions, but also at some other times as well. Observance of increase of nuclei mode and Aitken mode particles is in contrast to the results obtained from similar type of study conducted in New Delhi⁶⁴.

Difference in sinks might cause such a difference for different atmospheric environments and for different events. However this provides an opportunity to identify nucleation events on the basis of dynamics of nuclei mode particles and further explore the evolution parameters for selected NPF events. As next objective of this work, extended analysis of number concentration evolutions for case study 1 was performed for estimating growth and evolution parameters of NPF events, if any. As discussed in chapter 3, such events occur in atmosphere frequently and under various background atmospheric conditions. Since mostly these are not directly measured, it becomes crucial to pick such events interpreting modifications of aerosol spectrum.

4.4.1 Picking up events

In atmosphere, aerosol number concentration evolves due to variety of reasons. For any day, total number concentration may also comprise of extremum values. In this work, it was shown that multiple peaking in time-line of number concentration is a normal feature for a mega-city. An increase in total number concentration is the first signal of abrupt change in atmospheric aerosol conditions which can further be probed for additional signs. Change in number concentration in nuclei mode size range is the next step in this direction. An increase in nuclei mode concentration resulting in increase in total number concentration hints at the possibility of occurrence of NPF events. But as the measurement is (indirect) above the

Table 4.2: Mass concentration of total suspended particles and elements

Date	Sampling time	Total mass Conc. ($\mu\text{g m}^{-3}$)	Cu	Fe	Zn	Ba	Ca	Sr	Al	Mg	Na	K
dd/mm/yy	(hh:mm)											
25/10/13	16:45-22:50	493	ND	3.94	1.37	ND	24.49	ND	2.05	44.52	73.97	34.93
27/10/13	16:05-22:05	-	ND	3.96	ND	ND	ND	ND	0.83	ND	ND	ND
28/10/13	06:05-13:45	304	ND	2.85	0.22	ND	29.76	ND	1.36	26.09	39.67	16.85
28/10/13	15:20-22:35	229	ND	2.44	0.09	ND	11.35	ND	1.15	10.92	1.72	2.87
29/10/13	15:55-00:30	281	0.07	7.65	0.97	ND	ND	ND	4.13	ND	ND	ND
30/10/13	16:00-23:00	297	0.00	6.40	0.65	ND	ND	ND	4.17	ND	ND	ND
31/10/13	05:35-12:08	201	0.03	5.86	1.94	ND	ND	ND	3.35	ND	ND	0.67
31/10/13	16:15-23:00	209	ND	4.78	0.34	ND	4.48	ND	3.09	3.40	ND	1.23
01/11/13	16:15-23:00	209	ND	5.09	0.28	0.52	ND	ND	ND	ND	ND	ND
02/11/13	15:50-23:00	279	0.09	6.25	0.47	12.41	ND	0.49	25.00	ND	ND	29.65
03/11/13	16:05-00:05	364	ND	4.56	0.29	2.89	ND	0.00	7.03	ND	ND	ND
04/11/13	08:30-14:10	161	ND	2.76	0.00	ND	ND	0.04	2.21	ND	ND	ND
04/11/13	14:50-22:50	156	ND	2.73	0.00	4.61	ND	0.08	7.55	ND	ND	ND
06/11/13	08:45-14:55	108	ND	3.55	0.17	ND	ND	ND	2.70	ND	ND	ND
06/11/13	15:20-22:50	277	ND	4.31	0.08	0.08	ND	0.03	2.78	ND	ND	ND
07/11/13	14:15-22:15	208	ND	4.82	0.34	ND	ND	0.10	2.86	ND	ND	ND
09/11/13	15:40-21:50	135	ND	4.56	0.17	ND	ND	0.03	2.36	ND	ND	ND
11/11/13	16:45-22:30	159	0.07	5.25	0.76	1.30	42.21	0.07	3.26	37.32	54.35	42.39

(Diwali days: 2-4 November)

collection. Table 4.2 shows the mass concentrations measured at different times of sampling duration including the time of Diwali emissions. As can be extracted from the table, averaged mass concentration for evening and night times on the Diwali day was measured to be $364 \mu\text{g}/\text{m}^3$. This is comparable to the values obtained by other researchers who carried out similar measurements in urban locations/mega cities. However, at many other non-Diwali days as well, mass concentration was found to be comparable. For instance, it was highest on a non-Diwali day (25th Oct, $493 \mu\text{g}/\text{m}^3$) which highlights inefficacy of this parameter for relating it with Diwali emissions without other additional information.

After gravimetric estimations, filter paper samples were extracted by due procedure by treatment with concentrate HNO_3 and concentrate HClO_4 . After treatment, samples were then analysed for mass concentration of specific elements Cu, Fe, Zn, Ba, Ca, Sr, Al, Mg, Na and K using AAS. These elements were selected on the basis of either being tracer for Diwali emissions or being ubiquitous component of atmospheric aerosol particles. On sampling during Diwali days, increase/appearance of mass concentration of Ba, Sr and Al follows conclusions as observed by other similar studies. As discussed earlier, these elements are added as colouring agents in firecrackers. High values for K concentration (tracer for biomass burning as well) is also evident but it was also high for other samples (highest on 16:45-22:30 hrs, 11th Nov). Occurrence of concentration peaks at random times in the Table indicates separate pathways for different days. Another interesting aspect is related to lesser concentration for Diwali day compared to pre-Diwali day. This may be due to the factors such as additional dilution, less feasibility for nucleation/condensation etc. Discussion of mass concentration of other atmospheric background elements is out of scope for the present work.

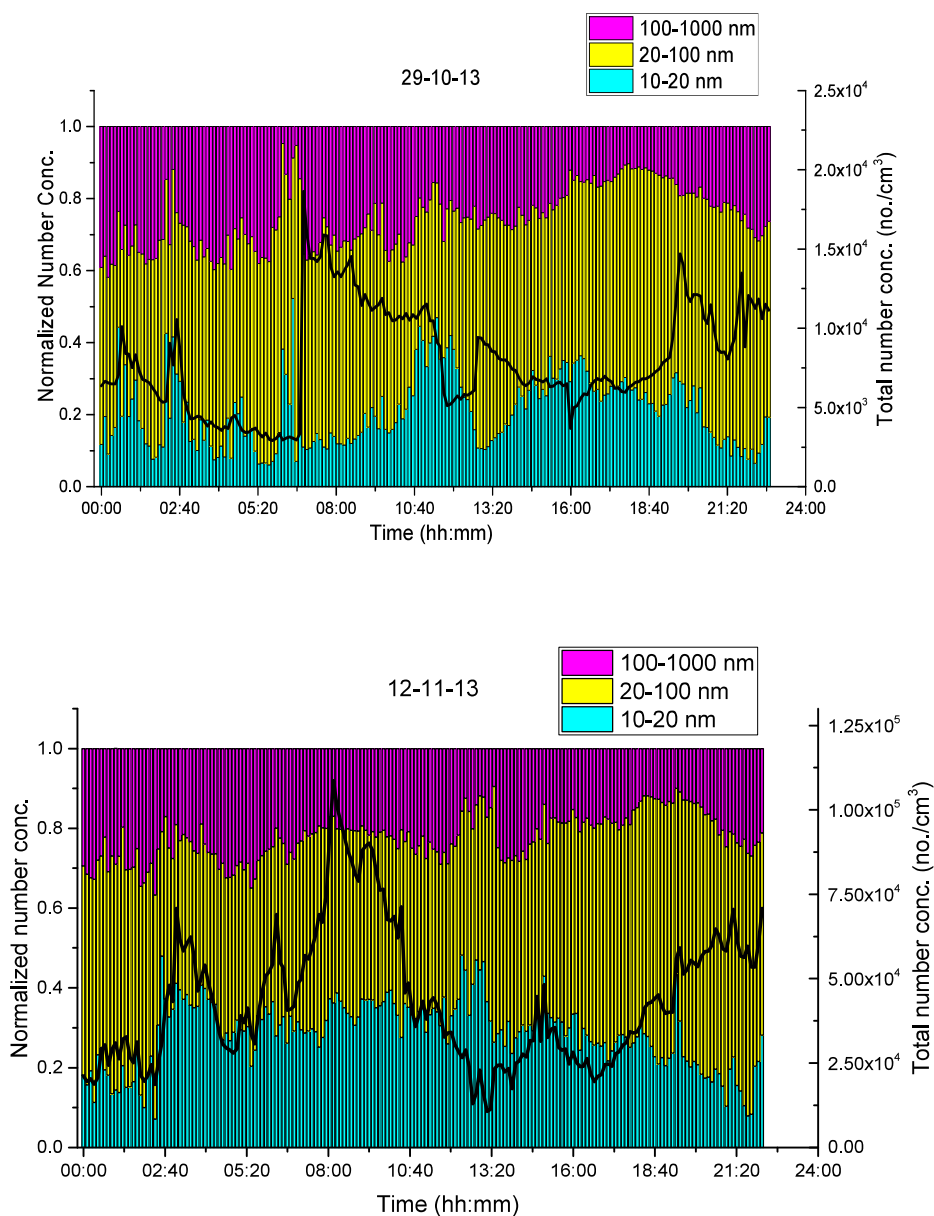


Fig. 4.19 (a-b): Diurnal variation of number concentration: Normal days

4.3.2.4 PM and chemical composition

Deductions with regards to change in mass loadings and aerosol chemical compositions are well established worldwide and in Indian studies. These parameters (Particulate mass concentration and chemical composition) were also measured during Diwali 2013. Mass concentration of aerosol particles was estimated using TSP samplers, substrates of which were then utilized for estimating elemental concentration of the trace constituents employing AAS. TSP sampler was operated at a fixed flow rate (20 Lmin^{-1}) for 4-6 hours for sample

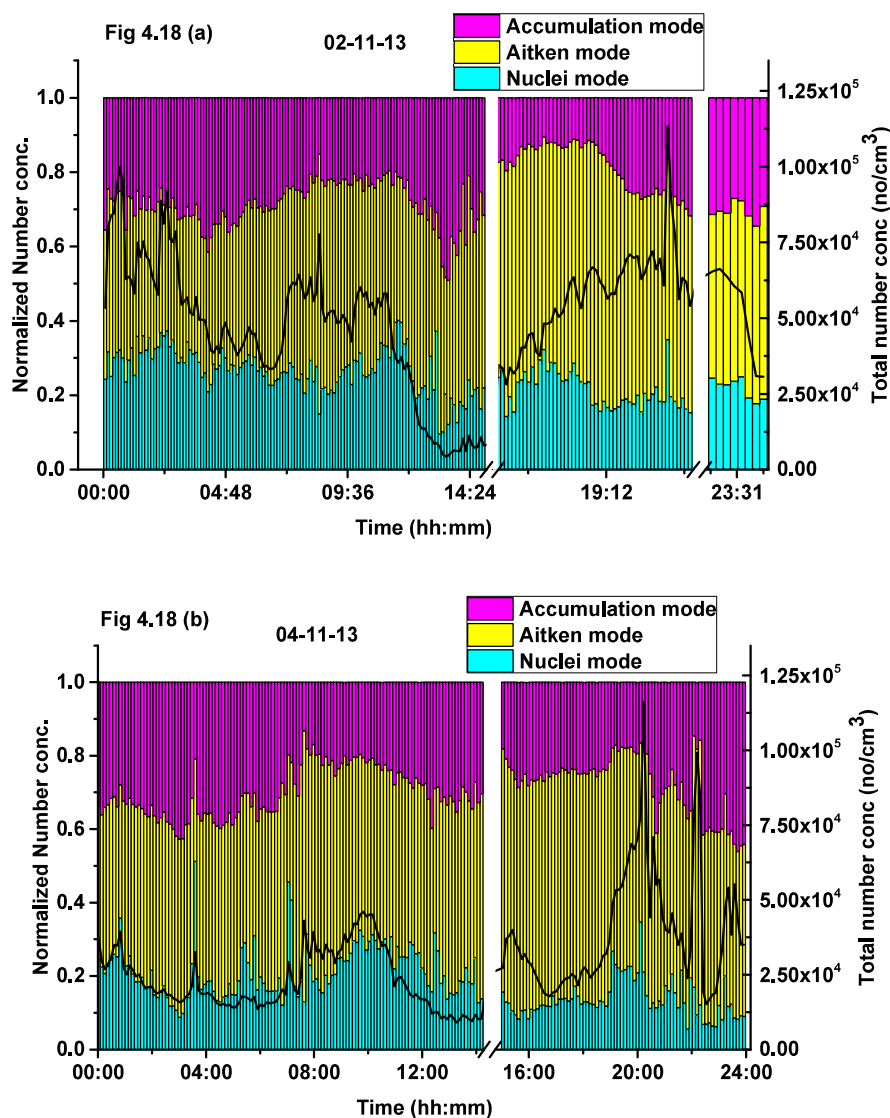


Fig. 4.18 (a-b): Diurnal variation of number concentration: Pre and Post Diwali day

Diurnal variations for two other days (October 29 and November 11) are also shown for comparisons (Fig. 4.19 (a-b)). It is difficult to link increase of total number concentration with increases in respective size ranges without additional information such as air trajectory information, source term analysis and detailed chemical composition etc. As the main purpose of this work is to study characteristics of nuclei mode particles, focus is on estimation of formation, evolution and growth parameters for selected peaks in number concentration.

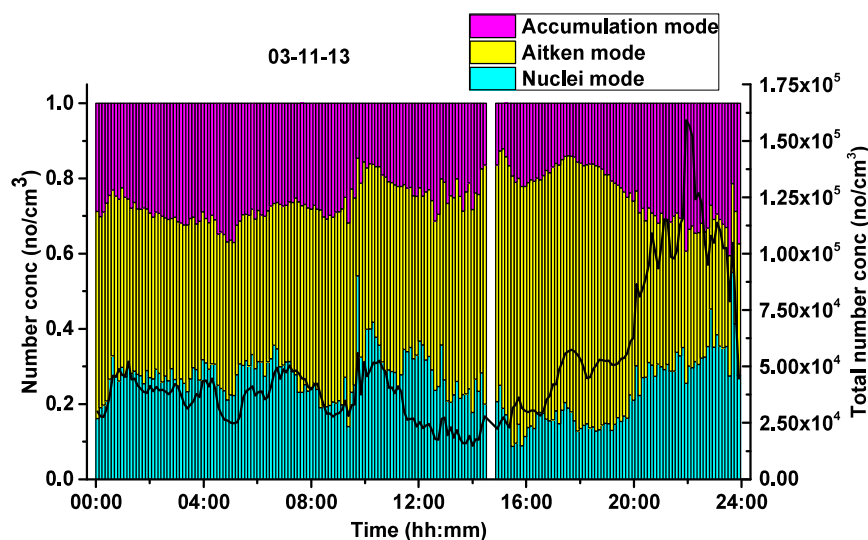


Fig. 4.17: Diurnal variation of number concentration: Diwali day

In the above figure, maxima of number concentration occurred at night times due to the emissions caused by fireworks. The rise in number concentration however can be seen starting from evening times (but mostly in accumulation mode size ranges). At the time nearly coinciding with peaking in fireworks, an increase of concentration in nuclei mode can be noted. During night times (20:00-24:00 hrs.), average number concentration comprised of 32.3, 36.6 and 31.1% particles of nuclei mode, Aitken mode and accumulation mode size ranges, respectively.

Diurnal plots for pre and post Diwali day are depicted in Fig. 4.18 (a-b). Similar conclusions as that for the above figure can be made for total number concentration, although this increase cannot be coupled to nuclei mode concentration in the straightforward way as above. At night times (20:00-24:00 hrs.); fraction of nuclei mode, Aitken mode and accumulation mode contributing to total number concentration was found to be \approx (20.3%, 52.0%, 27.7%) and (13.2%, 54.6%, 32.2%), for pre-Diwali and post-Diwali day respectively.

posed argument for the case of total number concentration. Additionally, box-whisker lengths and difference of 95th percentile and maximum value for the nuclei mode size range was seen to be closely following that for total concentration.

2) Statistical parameters deduced from Box-whisker plots were relatively consistent for Aitken mode size range. Maximum concentration reached for this size range for different days was nearly uniform (relative to other modes) for sampling days (Fig. 4.16 (b)). However in contrast, other inferential parameters as used in above discussions did not follow the trends of concentration for entire spectrum and nuclei mode size ranges.

3) Relatively smooth variation occurred for accumulation mode size ranges indicated by box-whisker lengths, mean-median ratio and maximum-95th percentile ratio for most of the days. However, distinct feature is unarguably difference of maximum to 95th percentile value for the day of Diwali. This observation along with highest mean-median ratio is consistent with the shifting of accumulation mode noticed in size distribution evolution plots (Fig. 4.12 (a-b)).

4.3.2.3 Diurnal variations

Apart from the discussion of features related to high number concentration, diurnal variations of number concentration of aerosol particles are important to study and interpret. Evolution of number concentration in a normal (non-episodic) day depends on ambient influencing factors such as the change in stagnation length during day times and anthropological influences e.g. emissions at the time of traffic etc. Interpreting variations in size segregated number concentration further improves understanding of the underlying factors. At the time of episodes, excess aerosol loading may modify the background characteristics sometimes to a significant amount. Fig. 4.17 shows diurnal variation of number concentration on the day of Diwali plotted for total as well as nuclei, Aitken and accumulation mode size ranges.

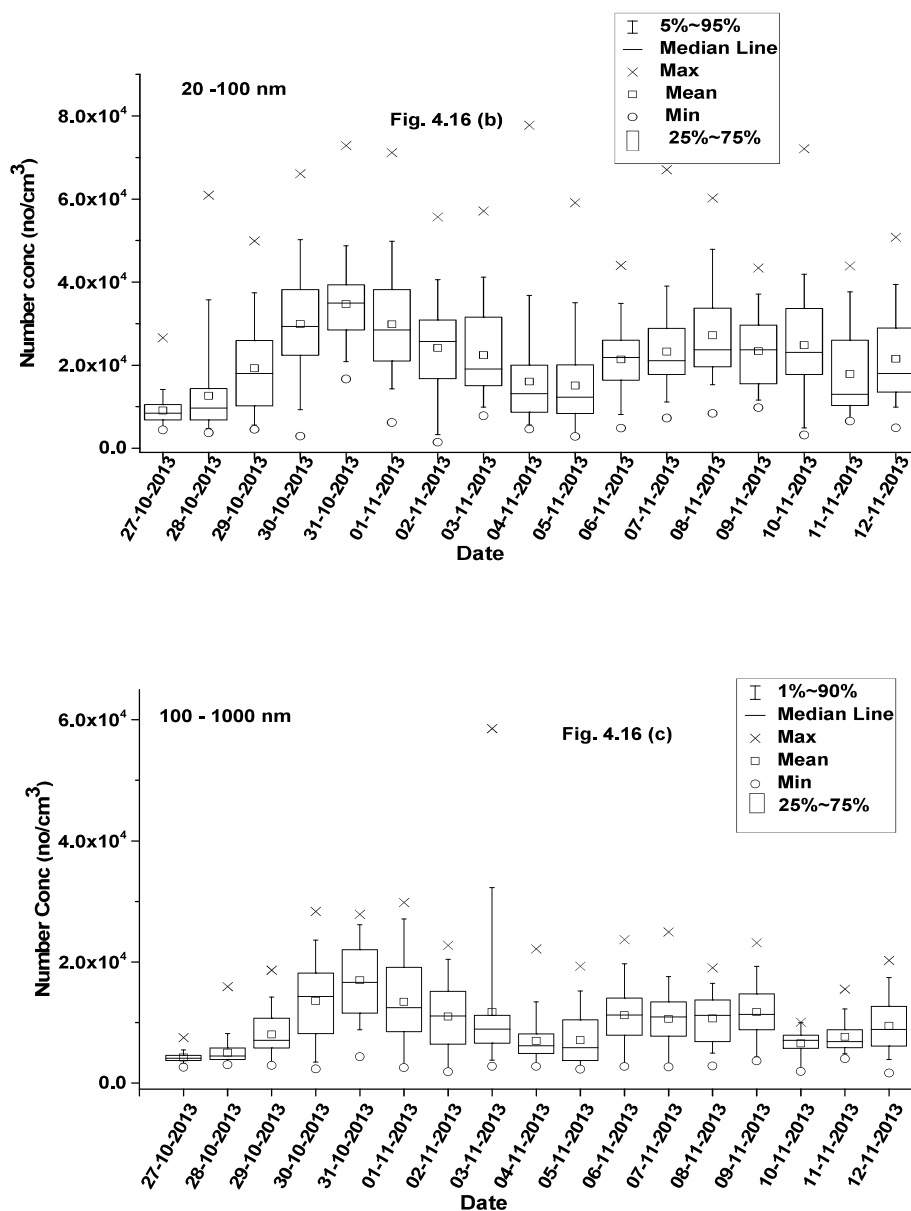


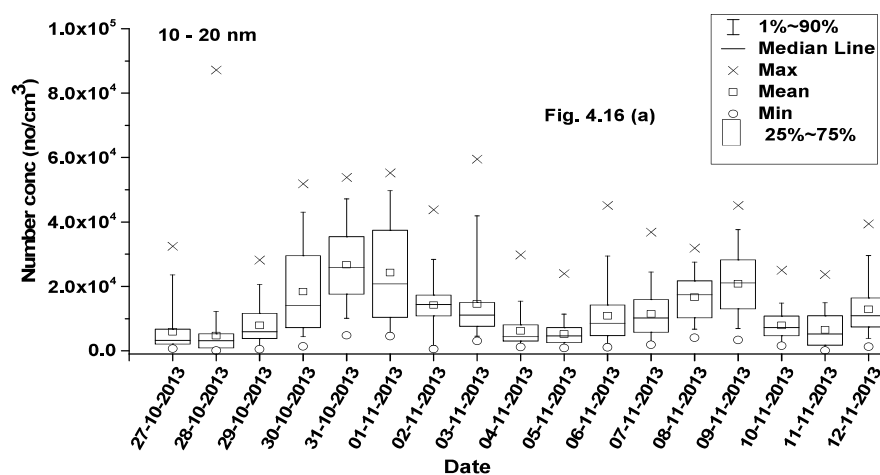
Fig. 4.16 (a-c): Box-whisker plot for all days: Concentration in different modes

These plots can be compared with day to day variations shown for total number concentration as well. Following observations were made by comparing Fig. 4.16 with Fig. 4.15:

- 1) Maximum daily concentration value for nuclei mode size range was measured on Oct 28 whereas these values for the block October 30 - November 01 and Diwali day (Nov 3) were also close. Ratio of median to mean was highest on Diwali day validating the already

3) The box length and whisker length also varied differently for different days. Highest inter-quartile range (75th percentile-25th percentile) and whisker range (95th percentile-5th percentile) was noticed during 30 Oct- 1 Nov when average parameters were also found to be maximum. This could be basically a reflection of episodic events taking place which have due capabilities to modify the background characteristics.

As a follow up step, similar analysis was performed for nuclei, Aitken and accumulation mode of number concentration of the same data. Box-whisker plots for these modes are shown in Fig. 4.16 (a-c) with similar depictions of statistical parameters as used in Fig. 4.15.



or even lesser than few other days of sampling. Both these average parameters were found to be highest on 31st Oct with closely following days 30th Oct and 1st Nov. Some other interesting deductions made on the basis of Fig. 4.15 are as follows:

1) Difference between mean and median varied for different days. This difference indicates variations in skewness of data which is expected for aerosol distributions, as they are mostly lognormal. This difference was seen to be highest on Diwali day (mean= 4.9×10^4 no/cm³, median= 4.1×10^4 no/cm³) consistent with the impact of burst production of ultrafine particles on the skewness of the data.

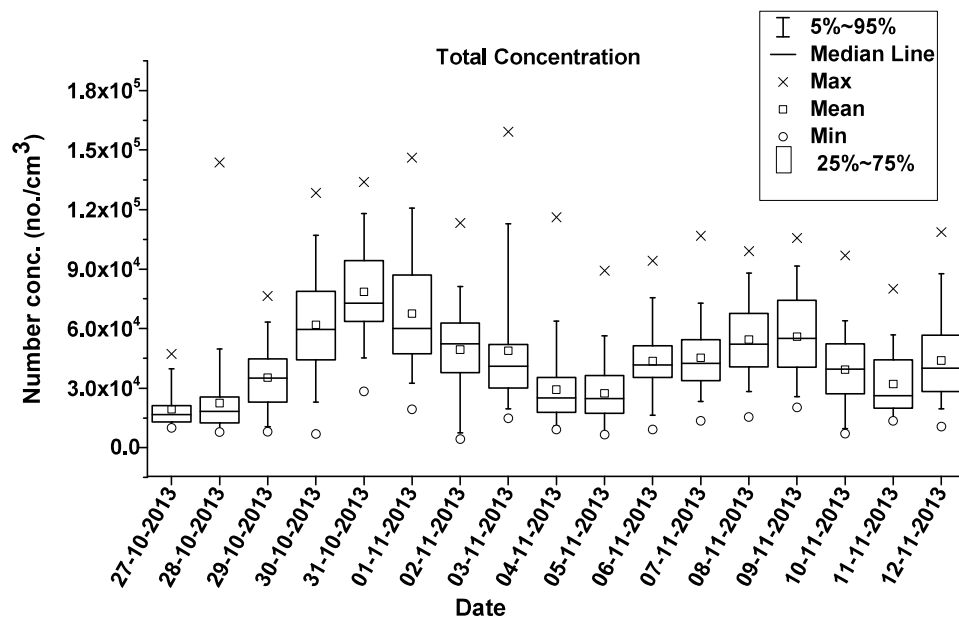


Fig. 4.15: Box-whisker plot for all days: Total concentration

2) On several days, maximum value was near to the 95th percentile (e.g. 30 Oct, 08 Nov, 11 Nov etc.). But on some days, maximum value was found to be significantly higher than the percentile value. Although this difference was highest on 28th Oct, it was significant enough for Diwali days (2 Nov-4 Nov) as well. This means that dispersion of data towards the maximum number concentration is significant. In other words, there are several instances of high concentration on that particular day.

from this figure. But most prominent feature is related to size distribution evolutions at midnight times. As evident, an increase of nuclei mode concentrations at odd times (relative to Diwali emissions) indicates possibility of aerosol formation due to background processes as well.

As presented in this section, inferences obtained from measurements conducted during 2013 campaign strengthen the conclusions drawn on the basis of Diwali 2012 campaign. The next step in this direction is related to analysing data for all days including Diwali days. This was done for two purposes; to draw statistical inferences from the measured data and to study diurnal variations of number concentration of aerosol particles.

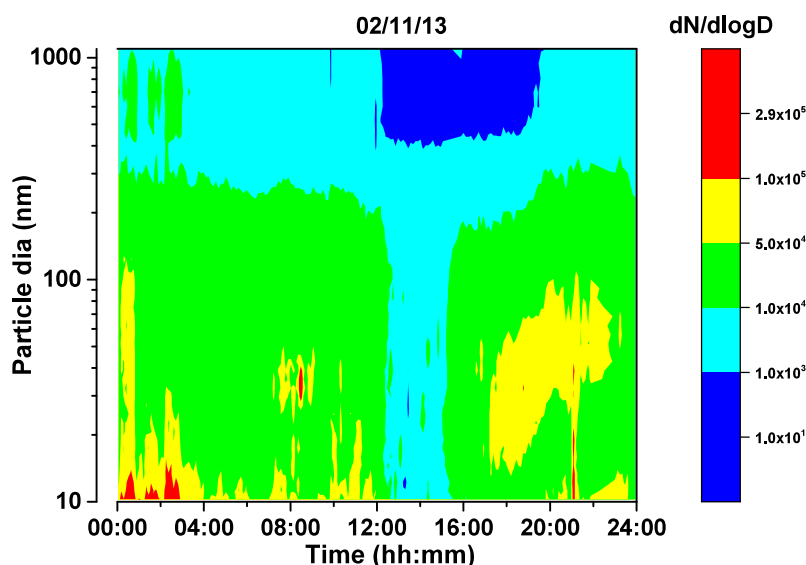


Fig. 4.14: 3D time series for size distribution for 2nd November

4.3.2.2 Statistical Analysis

Box- whisker plot for the number characteristic data for all 17 days of sampling has been shown in Fig. 4.15. Mean, median, percentiles (5th, 25th, 75th and 95th), minimum value and maximum value are used for defining this plot. As depicted, highest value of daily maximum number concentration ($\approx 1.6 \times 10^5$ no/cm³) was observed on the day of Diwali (3rd Nov). This value was however close to that measured on few other days as well (28th Oct and 1st Nov). Interestingly, average number concentration (median, mean) for Diwali day was comparable

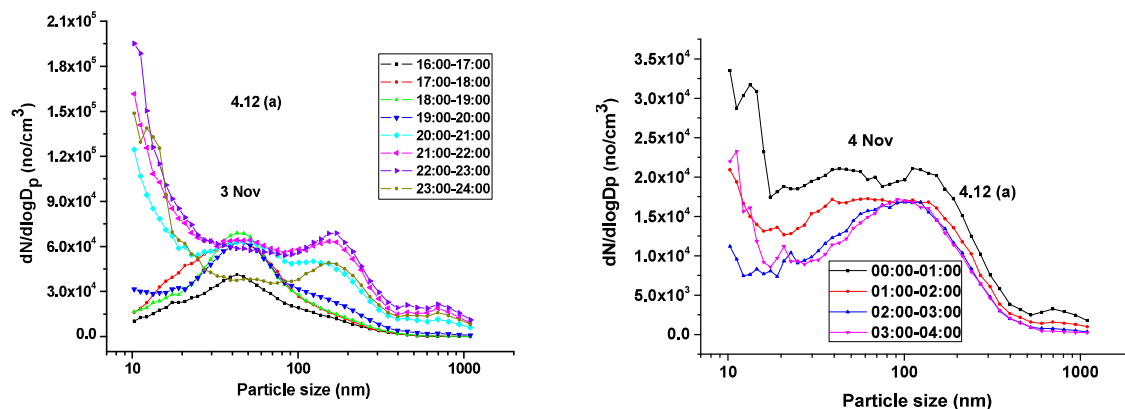


Fig. 4.12 (a-b): Hourly averaged size distribution evolution on Diwali night

For comparison, hourly averaged size distributions are also plotted for 11th November (normal day) in Fig. 4.13. None of the above discussed signature changes could be observed in size distribution evolution at different times for this case.

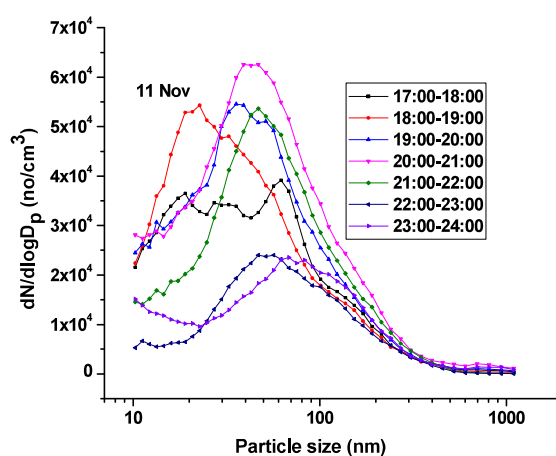


Fig 4.13: Size distribution evolution on a normal day

In order to represent typical size distribution features for the entire day, 3D size distribution evolution for pre-Diwali day (2nd November) is plotted in Fig. 4.14. This day was selected here to represent the complexity of atmospheric aerosol characteristics specifically in terms of NPF events. Signatures related to Diwali induced emissions can collectively be seen in this figure. An increase in ultrafine and accumulation mode concentration can be noticed

intensity. Apart from the distinct evolution of size spectrum near the peaks, observed increase in ultrafine concentration of particles at the time of emission requires re-validation. For this, 4 hourly averaged size distribution for different days (including 2-4 November) for evening and night time blocks are plotted in Fig. 4.11. Size distributions can be seen to be evolving in Fig. 4.11 (a) for event days. A prominent modification of size distribution (huge increase in nuclei mode concentration and shift in accumulation mode) is noticeable for the plot representing Diwali day (Fig. 4.11 (b)). Nuclei mode concentration can also be seen to be higher for pre and post Diwali days. These modifications validate findings made from measured data of 2012 campaign.

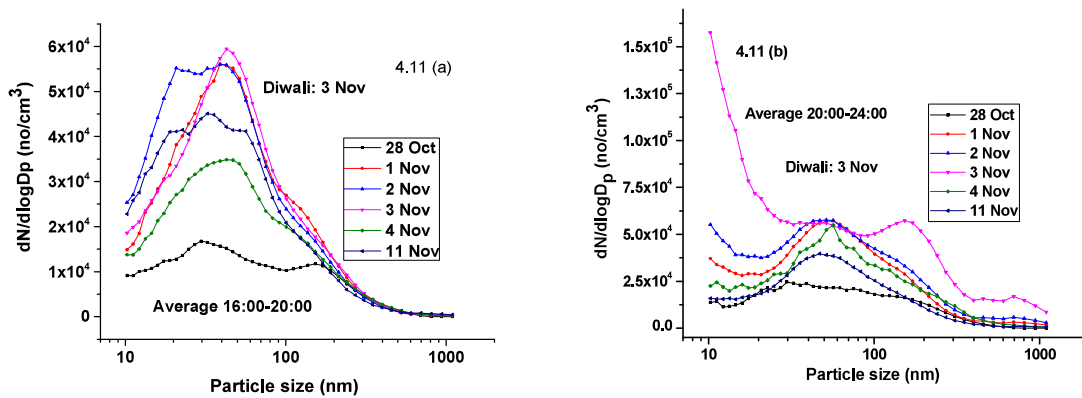


Fig. 4.11 (a-b): 4 hourly averaged size distributions for different days

Hourly averaged size distributions on the night of Diwali are also shown in Fig. 4.12 (a). It is seen that number concentration of particles < 200 nm started to increase in late evening hours (17:00-20:00 hrs.). First signal of increase of ultrafine concentration matches with the time when intensity of fireworks in surrounding region increases (20:00-21:00 hrs.). This trend as well as a shift in accumulation mode can be noticed for the following hours (21:00-00:00 hrs.) too. Following the size distributions further (fig. 4.12 (b)), these features can be seen to be diminishing with time.

series for number concentration and geometric mean for November 1-6 is separately shown in Fig. 4.10.

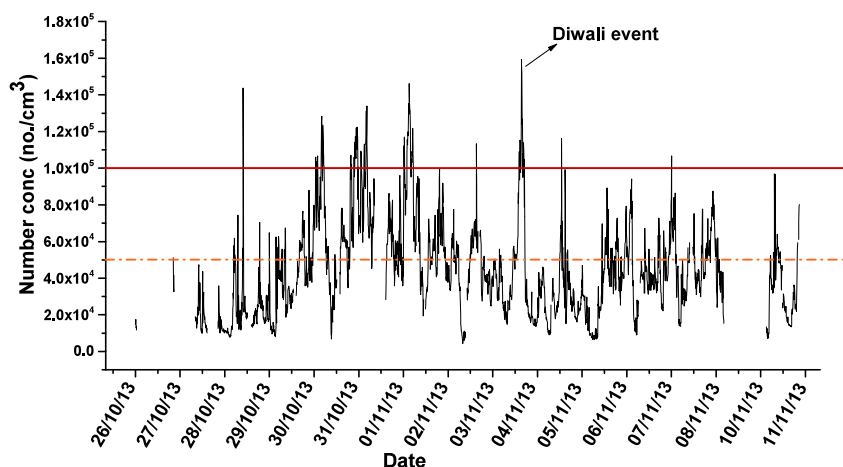


Fig. 4.9: Time series of number concentration for all days

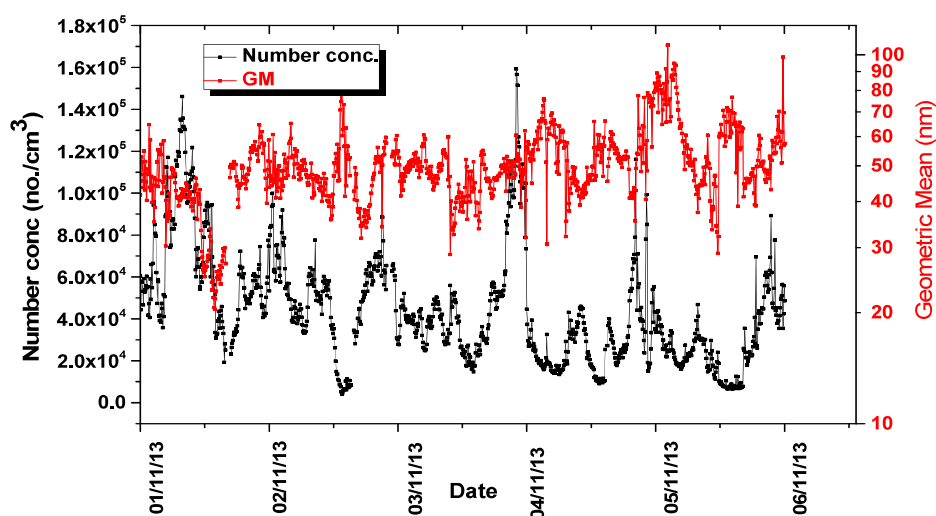


Fig. 4.10: Time series of number concentration and mean size close to event days

As evident for the case of Diwali peaks, measured GM dropped at the time of rise in number concentration (similar to the case of Diwali 2012). This observation hinting at the generation of aerosol particles in ultrafine size ranges is applicable to some non-Diwali peaks as well. Measurements made in campaign 1 of case study 1 i.e. Diwali 2012 provided number characteristic signatures distinguishing Diwali event with other background events of similar

4.3.2 Measurements during Diwali 2013

One possible drawback of the field study conducted during Diwali 2012 pertains to the relative data size for normal and episodic events. Measurements for this case were performed for 6 days including 3 days of Diwali. Apart from the observed shifting of accumulation peak, all other conclusions drawn from this study were new and sometimes contradictory to the results of previously carried out similar type of studies. Mainly, the increase in number of particles in the ultrafine size ranges and noting of intense background peaks (having number concentration similar to that reported during fireworks) was interesting but required further experimental validation. Due to the limited data size, no effort was made for interpreting ambient diurnal variations. Therefore another measurement campaign was planned during the subsequent year's Diwali period. Additional to number characteristic evolution for relatively more days (17 days), mass loading and chemical composition of particles emitted during fireworks was also assessed.

4.3.2.1 Comparison with inferences from 2012 campaign

Measurements during 2013 campaign were performed at the same location during 27 October-13 November, 2013 (Diwali days: 2-4 Nov). Similar protocols as of the previous campaign were adopted and followed. Due to the requirement of maintenance activities, sampling could not be performed continuously. Fig. 4.9 represents the time series of number concentration measured by SMPS (11-1083 nm) for entire sampling duration. Similar to inferences drawn from 2012 campaign, increase in number concentration was noticed on Diwali nights at the time of fireworks. It can again be visualized that several peaks are present at other times as well, the reasons for which are already discussed.

In Fig. 4.9, a sizeable fraction of data lies above the arbitrarily chosen dotted line (corresponding to 5×10^4 per cm^3) and solid line (corresponding to 1×10^5 per cm^3) indicating presence of several high concentration peaks which need due investigation. Time

4.3.1.4 Differential signatures of normal and episodic events

Large fluctuations in ambient aerosol parameters are expected for urban environments. For a megacity like Mumbai, the number concentrations, PM levels and chemical emissions are generally quite high. Additionally, PM levels as well as the aerosol chemical compositions vary appreciably depending on the industrial and other anthropogenic contributions. In absence of long term measurements and pre-established database of background aerosol parameters, a short term increase in characteristic parameters during an event cannot be taken as signature of that event. In megacities, presence of several contributing factors affects the levels in a complex manner and therefore, it might be misleading to relate these changes in a simple way to episodic events.

It is quite possible that aerosol parameters could be similar for the case of normal and episodic events for urban cities due to increased anthropogenic activities. Field measurements of PM levels and its variations in megacities have been performed²⁸⁹. These levels were seen to be close to or even higher than that measured at the times of and after fireworks. The perplexity increases for the case of number concentration based inferences. Even in a short span of 6 days, several peaks of number concentration were observed at random times (roughly at a frequency more than one per day). For each of the three Diwali night peaks, a closely matched number concentration peak was found. For differentiating a normal and an episodic peak, size distribution evolution analysis can be utilized. For any episodic event, primary as well as secondary size ranges of emitted particles are the function of generation processes, aerosol dynamics and controlling environment. These number characteristics for such cases are expected to be different from background aerosol phenomenon/processes. Size distribution evolution analysis exploits this key difference for differentiating an episodic event from a normal event similar on number concentration scale.

after the peak time was similar to that for the case of peak A (Fig. 4.7 a). Also, additional mode formed in ultrafine size-range was seen to be diminishing quite soon for both these cases as well.

For the case of peak E observed in day-time (November 14, 14:47 hrs.), evolution history is plotted in Fig. 4.8 (c). It is to be remembered that total number concentration corresponding to this peak was close to that of peak B and C (i.e. pre and post Diwali night peaks). But, in contrast to evolution history of these peaks, an overall increase of number concentration was observed with no noticeable mode formation. For the last peak observed in late-night i.e. peak F (November 11, 01:26), a sharp increase of number concentration was seen in nuclei-size range only (fig. 4.8 d). A spurious formation of nuclei mode particle might be the reason for such an observation.

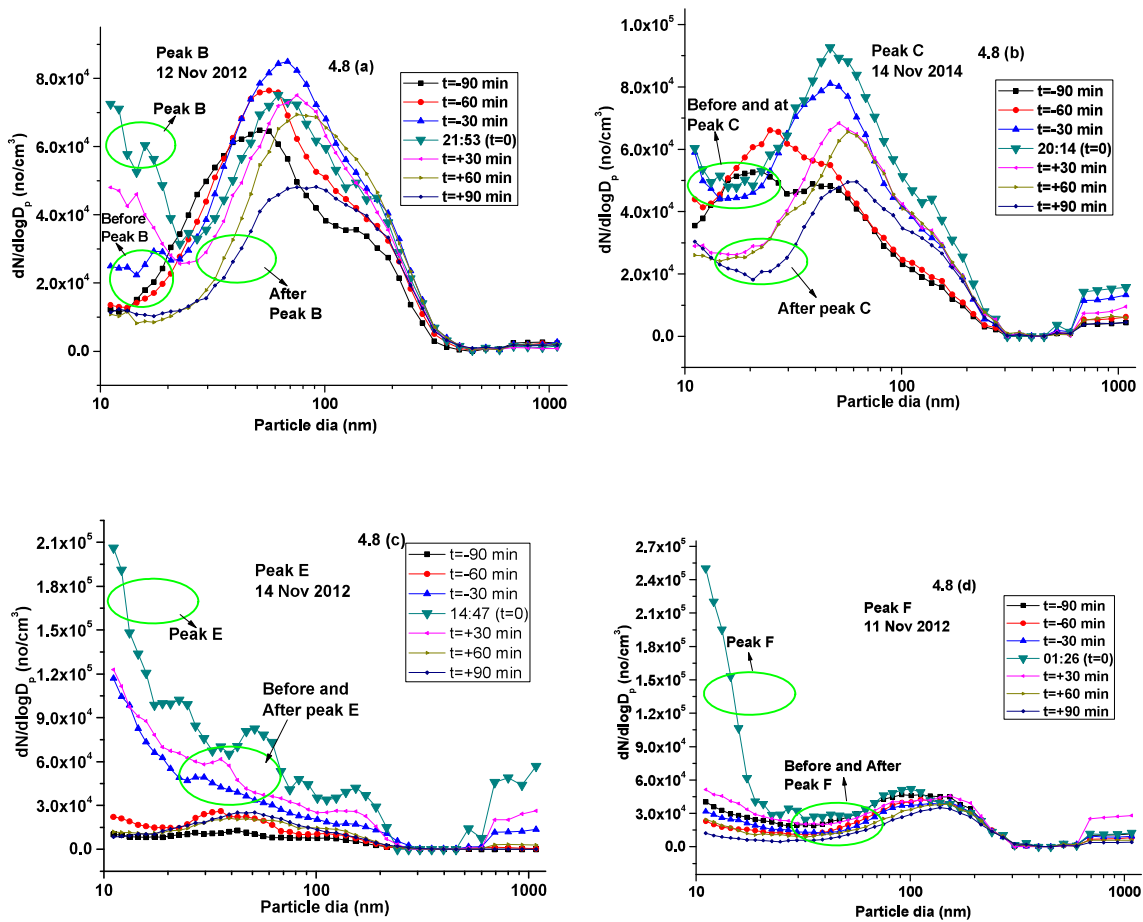
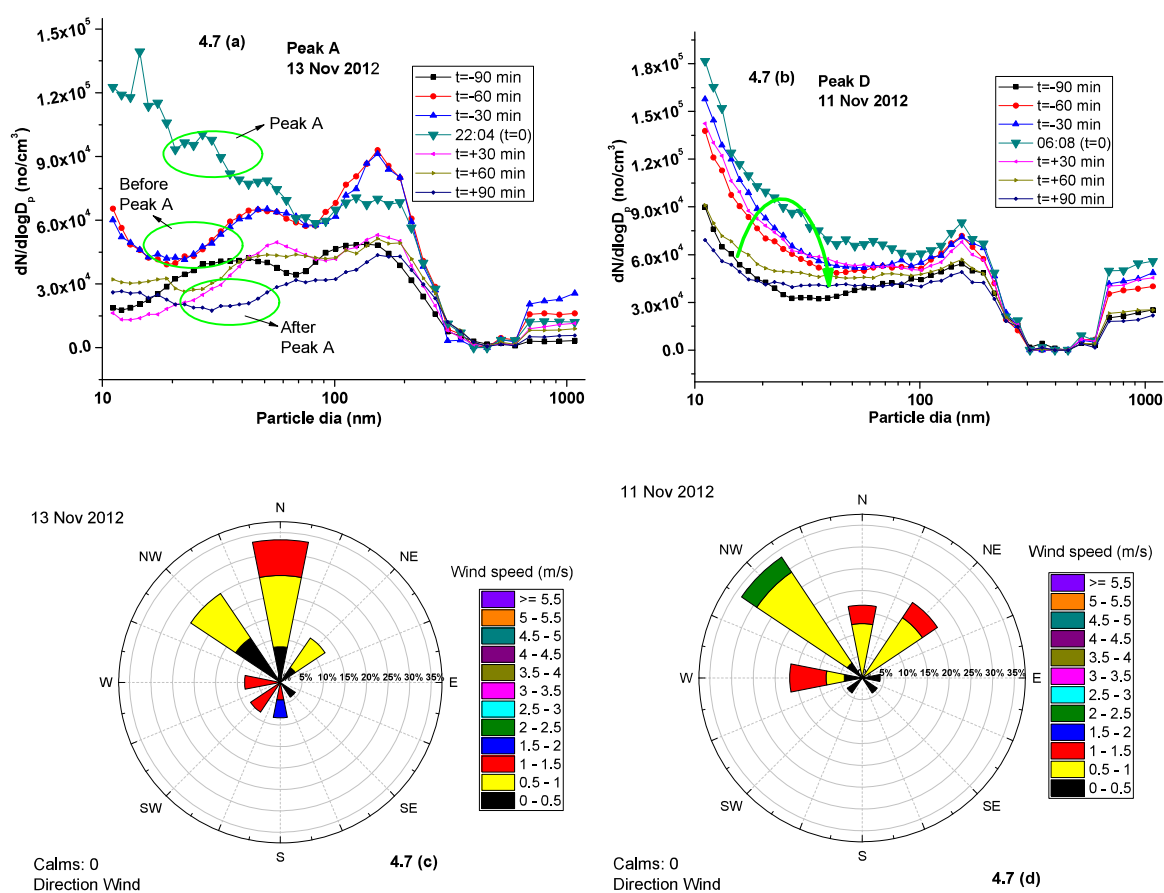


Fig. 4.8 (a-d): Evolution history of size distribution at peaks B, C, E and F of Fig. 4.1

(November 11, 06:08 hrs.). Modified size distribution also regained its pre-evolution shape in due course of time. Most importantly, no distinct mode formation or signature was observed for this case. Possibility of effect of wind flow patterns on the modifications of aerosol characteristics at these peaks was ruled out by analysing wind-rose diagram plotted for these two days. As shown in fig. 4.7 (c-d), speed of the wind (dominant direction: North-west, North and North-east) were mostly measured between 0.5-1.5 m/s.



Figs. 4.7 (a-d): Evolution history of size distribution and wind-rose diagram for the day corresponding to peaks A and D of Fig. 4.1

Similar size distribution evolution analysis was performed for remaining peaks B, C, E and F, respectively. Evolution history for these peaks is shown in Figs. 4.8 (a-d). For peak B (pre-Diwali night: November 12, 21:53) and peak C (post-Diwali night: November 14, 20:14), a characteristic evolution due to firework bursting (but of lower intensity) leading to the respective peaks was observed. Regaining of pre-evolution spectrum in a matter of time

distribution evolution of each peak. The events (i.e. peaks) were segregated into two categories: episodic events (peak A, B, C of Fig. 4.1 (a)) and normal/background events (peak D, E, F of Fig. 4.1 (a)).

Most of the studies conducted on fireworks induced emissions discuss average size distribution (more than 1 hour) and possibility of missing out a spike in nucleation mode cannot be ruled out in such a case. In this analysis, size distribution measured corresponding to the occurrence of above peaks (A-F) was compared with average size distributions of 30 minutes interval (average for 0-30, 30-60 and 60-90 minutes) before and after the peak. Following this methodology, size distribution evolution of peak A (observed on November 13, event night) and peak D (observed on November 11 morning time) was compared (Fig. 4.7 (a-b)). As can be noted from Fig. 4.1 (a), both these peaks had approximately similar gross parameters i.e. number concentration ($\approx 1.3 \times 10^5 / \text{cm}^3$) and geometric mean ($\approx 50 \text{ nm}$). Hence on a scale based on intensity of number concentration, these peaks can't be differentiated. Without additional information (chemical composition etc.), both peaks represent similar number concentration loading. Figs. 4.7 (a-b) present information on the evolution of size distribution of these 2 peaks for 3 hours around the peak time (90 minutes before the peak to 90 minutes after the peak).

It can be visualized from Fig. 4.7 (a) that size distribution corresponding to peak A began to evolve about 60 minutes before the time of the peak. Significant increase of concentration in ultrafine range and evolution of additional modes can also be noted in size distribution corresponding to peak A. However, very soon (within 30 minutes), size distribution became similar to background. Following size distributions for peak D in the similar way however, led to different conclusions. Evolution of size distribution for peak D in this case followed a different path. As can be inferred from fig. 4.7 (b), number concentration for all size-ranges increased leading to size distribution observed at the time of peak

Table 4.1: Size distribution characteristics (averaged over 4 hours)

Time-block	Date of measurement	Nucleation mode (10-20 nm)		Small Aitken mode (20-50 nm)		Large Aitken mode (50-100 nm)		Accumulation mode and higher (100- 1000 nm)	
		N _{tot} (no/cm ³)	GMD (nm)	N _{tot} (no/cm ³)	GMD (nm)	N _{tot} (no/cm ³)	GMD (nm)	N _{tot} (no/cm ³)	GMD (nm)
00:00	10 Nov	6450	14.0	6521*	31.6	9469*	71.2	19472*	182.6
-	11 Nov	6904*	13.8	5705	31.1	8183	71.8	17193	184.5
04:00	13 Nov	2432	14.1	3909	33.1	7097	70.9	13299	169.9
	14 Nov	2424	13.9	2952	33.0	4576	70.5	11916	181.9
	15 Nov	5312	14.0	5263	31.6	6897	70.3	11071	187.2
16:00	12 Nov	5577	14.4	10802	32.1	8085	67.8	9792*	166.0
-	13 Nov	5805	14.5	11582	32.0	7517	66.8	8059	168.1
20:00	14 Nov	6820*	14.6	14627*	31.8	8991*	66.2	6113	168.3
20:00	10 Nov	5130	14.2	9238	33.6	15321	69.8	16774	164.7
-	12 Nov	5398	14.5	13579	33.6	16953*	68.4	17846	160.6
24:00	13 Nov	10615*	14.2	16453*	32.2	14740	68.3	29976*	189.2**
	14 Nov	5262	14.2	10201	33.3	11561	67.9	10353	171.3

* Peak values, **Shifted accumulation mode

4.3.1.3 Size distribution evolution analysis

Hourly and 4 hourly averages were taken to interpret the distinct size distribution features of the event. As discussed above in detail, signatures of aerosol emission during fireworks (Diwali signatures) could be obtained from this analysis. Next target in this direction is related to differentiating the peaks in total number concentration with respect to their size distribution evolution around the peak. To do so, an in-depth analysis of size distribution around all higher concentration peaks of Fig. 4.1 (a) was carried out by following the size

characteristics of aerosol particles, further analysis was only done for SMPS measured distributions.

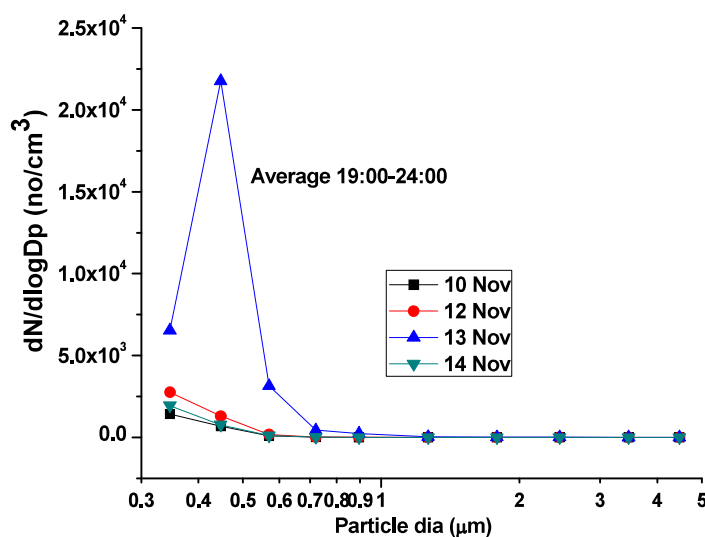


Fig. 4.6: OPC measured size distributions for time block 19:00-24:00 hrs.:

Comparison for all days

From the SMPS measured size distributions, characteristics corresponding to different modes were calculated and are shown in Table 4.1. Increase in the concentration of accumulation mode particles is consistently reported in other studies. However in contrast, particles in nucleation and small Aitken mode were seen to be highest on the night of the event. Also, a clear shifting of accumulation mode (GMD-189.2 nm) can also be seen for 20:00-24:00 hrs. time-block. Several peaks can also be noted in the duration of non-event activities as well.

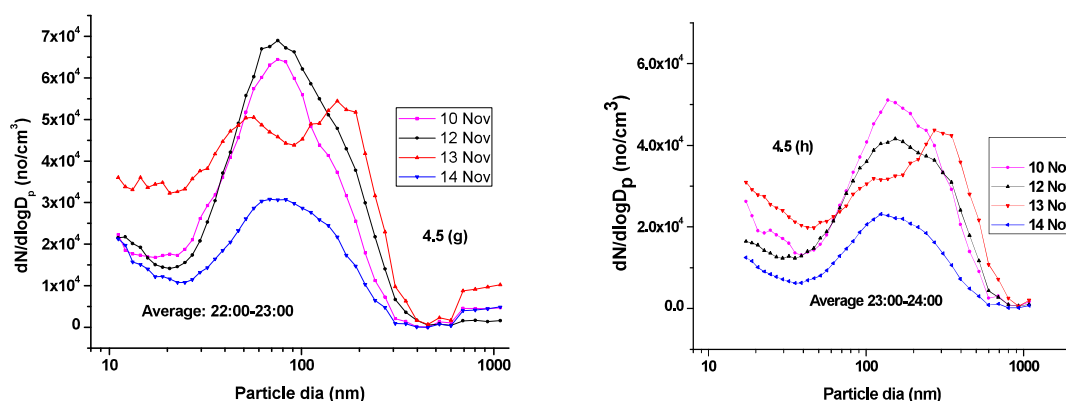
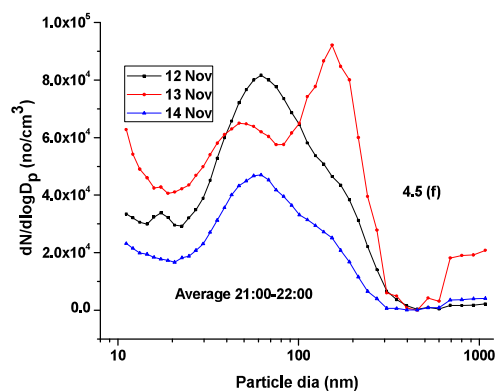
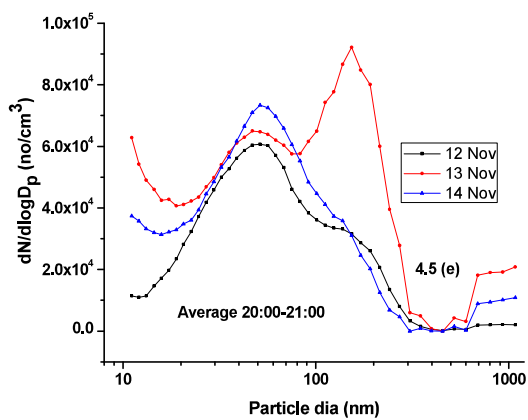
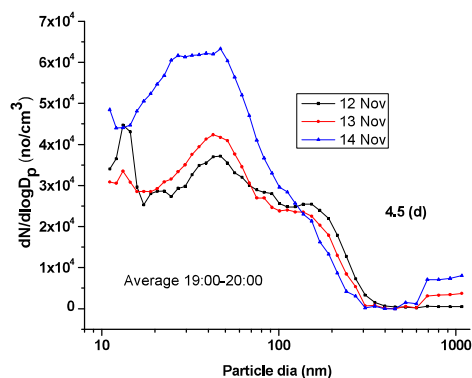
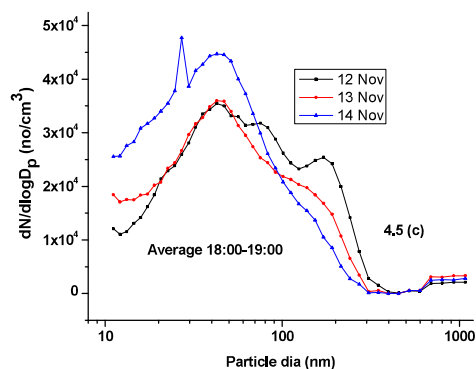
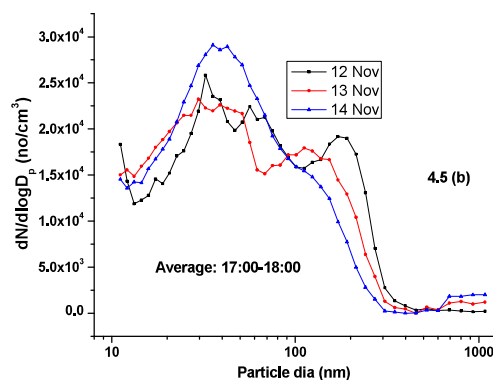
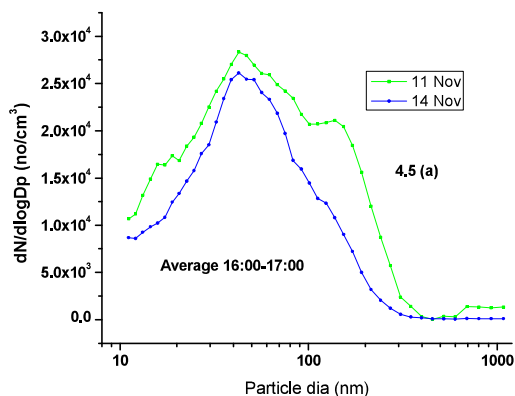


Fig. 4.5 (a-h): Hourly averaged size distribution for the time block 16:00-20:00 and 20:00-24:00 (all days)

It is apparent from Fig. 4.5 that around late evening times (time coinciding with start of intense bursting of firecrackers), background aerosol size distribution began to evolve with an increase of particles in ultrafine size-range (Fig. 4.5 (c-d)). An additional mode (around 50 nm) was also seen to emerge possibly due to presence of un-burnt combustion products of fire-cracking. Very soon, accumulation mode showed first signal towards shifting as an effect of inter and intra coagulation of generated particles (Fig. 4.5 (e-f)). The increase of number concentration in ultrafine and accumulation mode particles continued in subsequent hours. Ultimately, signatures of emission due to fireworks diminished and aerosol size distribution became similar to pre-emission distribution and also similar to that for other normal days.

The average size distribution measured by OPC for time block 19:00-24:00 hrs. has been shown in Fig. 4.6. A significant increase in size ranges (300 nm-600 nm) on the night of the event can be noted. However, no conclusive inferences could be drawn from OPC measured size distributions in regards to coarse size ranges. Changes in the number concentration of particles lesser than about 1 μm were also measured by SMPS. Most of the emissions due to firework bursting are expected to be in fine and ultrafine size ranges (for measurements made at 50 m height). As this work was focused on ultrafine and nuclei mode

(c-d)). Results for same time block for Diwali 2013 have also been shown in inset of Fig. 4.4 d (details in Section 4.5). Further probing of size distribution evolution due to Diwali induced emissions can be carried out by plotting hourly averaged (instead of 4-hourly averaged) distributions during evening and night time blocks for all days (Figs. 4.5 (a-h)).



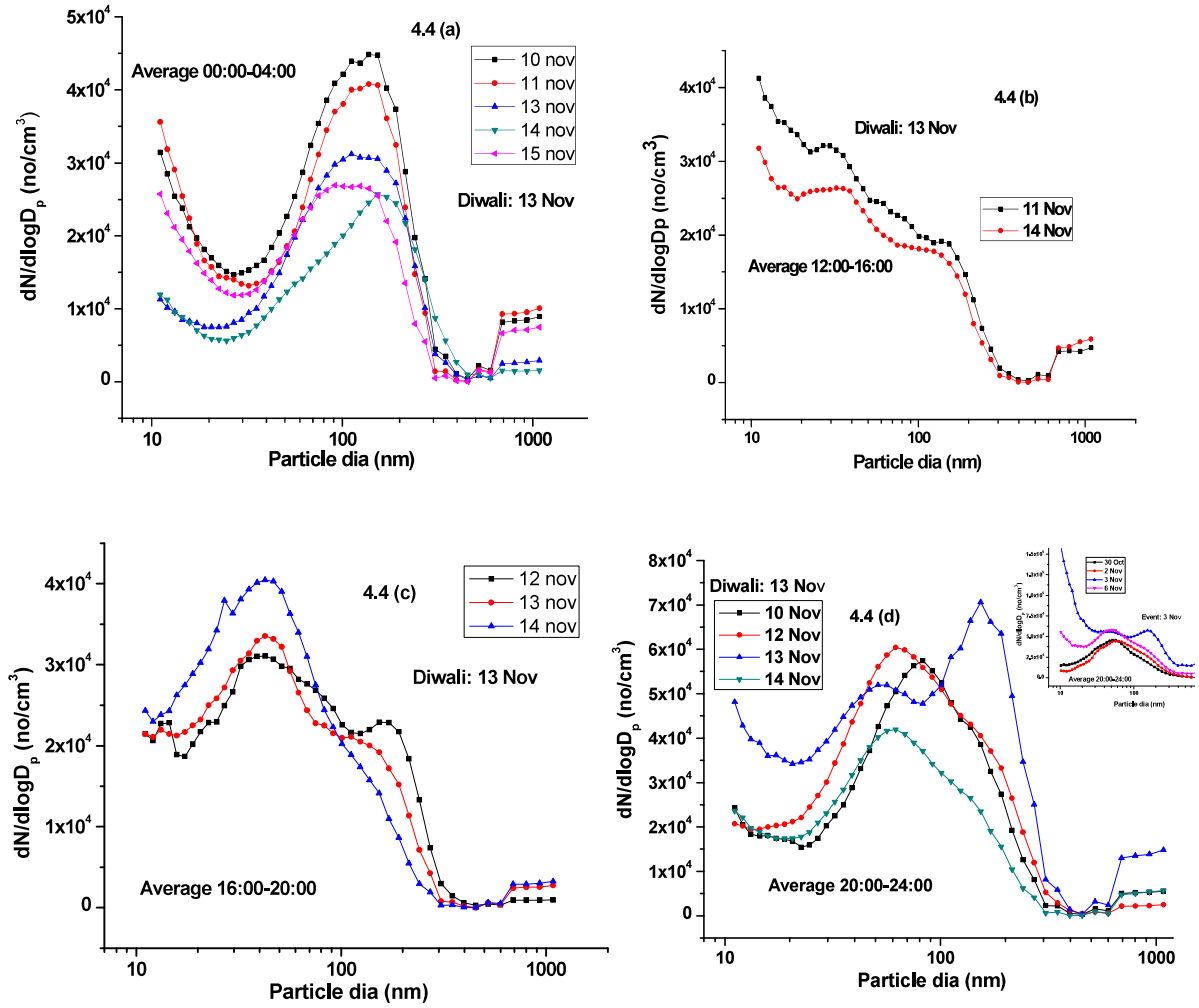


Fig 4.4 (a-d): Average number size distribution during the days of the study
(averaged over 4 hours)

It can be inferred from Fig. 4.4 (a) which was plotted for the late night time block 00:00 to 04:00 hours that an accumulation mode (100-200 nm) is always present in addition to the nucleation mode in the size spectra. Also, number concentration for the entire size-range was found to be higher for 10th and 11th November. Comparison of size spectrum at other time blocks yielded similar inferences about gross features of modes of size distributions. Mainly, it was seen that changes in number concentration in respective size ranges was similar on all sampling days. However, in the evening and then on the night of Diwali (i.e. 13th November), size distribution was seen to be distinctly evolving with formation of an additional mode in Aitken mode and a shifted accumulation mode (Fig. 4.4

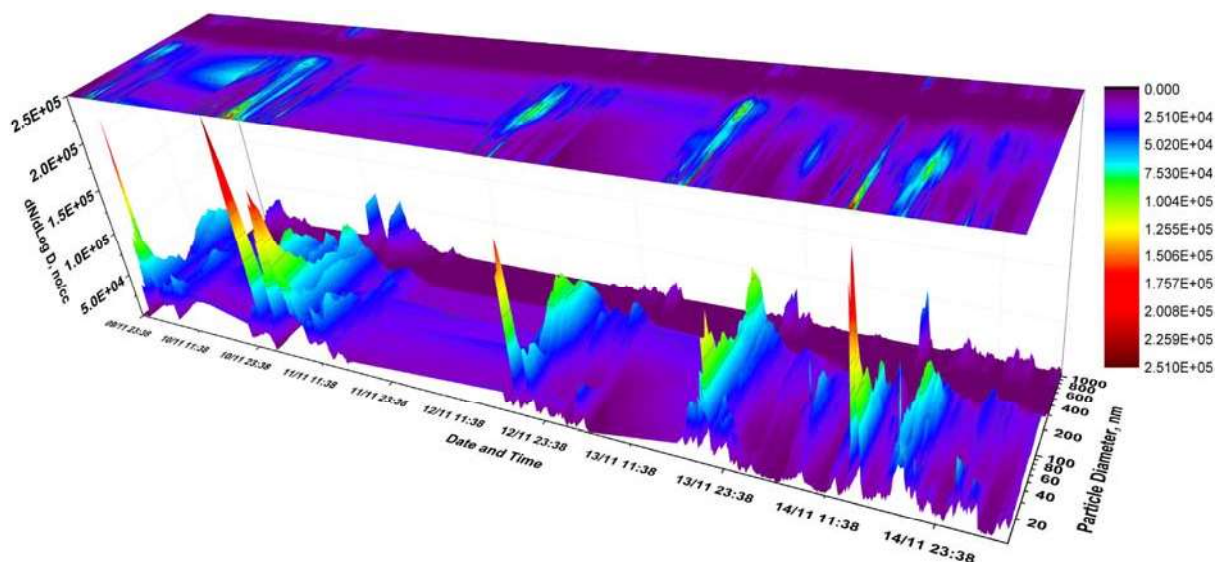


Fig. 4.3: 3D plot of aerosol size distribution (all days)

Emission in ultrafine (or nuclei mode) size ranges during non-Diwali peaks might be due to ambient changes in the atmospheric aerosol characteristics. But, the increase in ultrafine concentration at the time of fireworks is in contrast to previously published studies. This aspect can be probed in detail by studying the size distribution of aerosol particles at different times of the days. In this way, differences of emission due to firework bursting and other atmospheric processes (source term contribution) can be interpreted in terms of size distribution evolution characteristics. As a first step towards the same, 4 hourly average size distributions of all days were compared at different time-blocks (00:00-04:00, 04:00-08:00...20:00-24:00). By doing so, an attempt to segregate changes in atmospheric characteristics due to reasons such as event-induced emissions, late night behaviour, morning peak etc. was made. Fig. 4.4 shows size distribution comparison of different days at 4 selected time-blocks.

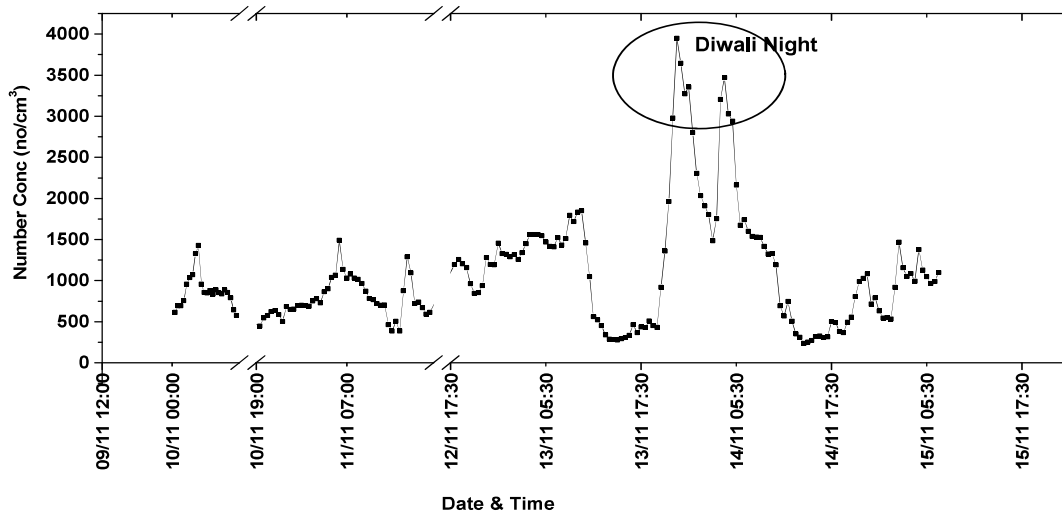


Fig. 4.2: Time series of number concentration (no/cm^3) as measured by OPC

An increase in parametric factors is generally linked to the emissions during events. It is clear from Fig. 4.1(a) that the total number concentration (similar for Diwali and non-Diwali peaks) may not be a reliable signature for differentiating the event in the absence of source characterization and background (normal days) aerosol measurements.

4.3.1.2 Size distributions

Simultaneous occurrence of maxima-minima for number concentration-geometric mean in time series for sampling duration hinted at the possibility of emissions in ultrafine regime. This observation can be probed further by plotting and analysing aerosol size distribution for the entire sampling duration. Fig. 4.3 shows a 3D plot representing time series of aerosol size distributions measured by SMPS for the entire sampling duration. Corresponding to peaks observed in Fig. 4.1 (a), sharp peak in nuclei mode size range was observed.

Peaks *B* and *C* observed at 21:53 hrs. and 20:14 hrs. observed at night times of November 12 and 14 respectively indicate aerosol emission due to limited burning of fireworks, a day prior to and post-festival. Interestingly, peaks of similar amplitude have been measured on other days/times as well. A careful examination of the time series shows that, in terms of measured number concentration ($\sim 1.1\text{--}1.3 \times 10^5 / \text{cm}^3$), peak *A* is similar/close to Peak *D* (November 11, 06:08 hrs.) and peak *E* (November 14, 14:47 hrs.). Similarly, Peak *F* observed on November 10 was comparable to pre- and post-event night peaks *B* and *C*. Apart from observing peaks due to Diwali emissions, observance of intense peaks is not surprising in a large background aerosol population⁶⁶. These peaks could be occurring due to anthropogenic activities such as industrial emissions and vehicular pollutions. No drastic change in wind flow patterns was noticed at the time of peaks. Time series of geometric mean (calculated for entire size-range) for measured size distribution has also been plotted in Fig. 4.1 (a). Interestingly, maxima in number concentration coincided with minima of geometric mean for most of the cases. It indicates that emission might be taking place in ultrafine size ranges thus shifting the geometric mean towards lower sizes.

Fig. 4.2 depicts the time series of number concentration measured by OPC for the same duration. Clearly, number concentration measured in this size range was also found to be higher as compared to background concentration. On Diwali night, the number concentration increased by a factor of about 3.5 as compared to other normal days reaching to $\approx 4000 \text{ per cm}^3$.

during the campaign. The results of the measurements and the inferences drawn are presented below.

4.3.1.1 Time series peaks

Total number concentration and geometric mean measured by SMPS has been plotted for entire sampling duration in Fig. 4.1 (a). It can be seen that multiple peaks occurred in number concentrations at different times. Such fluctuations are expected for a typical urban atmospheric environment. Except diurnal patterns, temperature and Relative humidity (RH) were found to be similar on all days of measurements (Fig. 4.1 (b)).

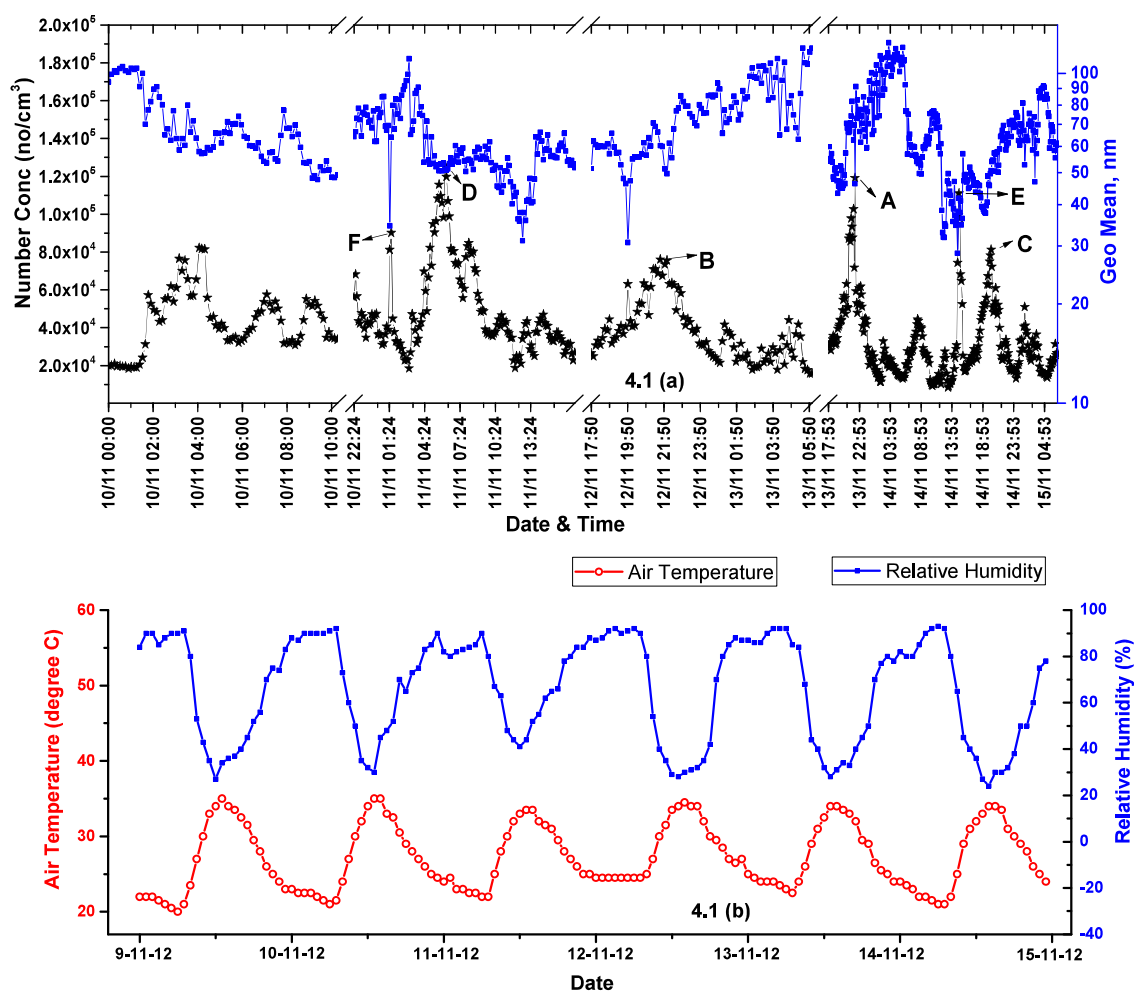


Fig. 4.1 (a-b): Time series of aerosol and meteorological parameters

A clear increase in aerosol concentration (Peak A $\sim 1.2 \times 10^5$ /cm³) at 22:10 due to intense burning of fireworks can be seen on the night of the event (November 13, 2012).

measured during this case study; focus of discussions henceforth is more towards ultrafine and nuclei mode size ranges.

4.3 Changes in atmospheric aerosol number characteristics during Diwali festival

The excursions in atmospheric aerosol characteristics (number and mass parameters, chemical composition, density etc.) sometimes may lead to evolution of parameters in such a manner that could have potential health hazards. This section discusses aerosol number characteristics before, during and after Diwali festival days in 2 consecutive years, 2012 and 2013 respectively. PM changes and chemical composition due to Diwali emissions were also measured for the year 2013.

4.3.1 Measurements during Diwali 2012

Measurements were made at approximately 50 m height in a high rise building. As opposed to ground level observations, performing measurements at sufficient height was necessary as it represents changes in regional atmospheric characteristics in a better way. Also, this sampling location was away from the main traffic-bearing roads, thereby ensuring minimum interference from sources due to vehicular emissions. This field campaign was conducted for 6 days (November 10- 15, 2012) with celebratory event on November 13, 2012. During these days, most of the fireworks bursting events were witnessed between 19:00-23:00 hrs. on November 12-14, 2012. GRIMM SMPS (5.403C:11-1083 nm) and GRIMM OPC (1.108:0.3-20 μm) were used to measure the number concentration of the aerosols at the sampling site (at intermittent times). Sampling was done through sampling pipes (length 1 m and 8 mm internal diameter) taken out from the window of the room to the open atmosphere. Aerosol losses for this sampling arrangement were calculated and found to be negligible. No drying arrangement was used for sampling atmospheric aerosols in these measurements. All protocols necessary for making accurate SMPS and OPC measurements were followed. Precautions such as periodic cleaning of SMPS inlet impactor etc. were also taken care of

studying the modifications in number characteristics of aerosol particles as an effect of fireworks during Diwali festival. Measurements were made during normal and Diwali festival days in years 2012 and 2013 in a township in Mumbai, India.

4.1 Aerosol emission due to firecrackers

Smoke containing metallic particles is generated during the burning of firecrackers. Harmful metal and metal salts (e.g. Cu, Sr, Ba, Sb_2S_3 etc.) used in firecrackers for colour and binding effects, pollute air quality by generating toxic and harmful by-products. Several consumer products varying in intensity and composition are produced in pyrotechnic industry. Huge smoke from burning of these products degrades the ambient air quality, sometimes for several hours. Mainly, these airborne pollutants are O_3 , SO_2 , NO_2 , CO and suspended particulate matter. These particulate pollutants consist of heavy metals and unburnt combustion products in the form of black powder. Due to the emission of these particles to the atmosphere, number characteristics of atmospheric aerosols get modified.

4.2 Nuclei mode particles during fireworks

Although studies have shown shifting of accumulation mode and reduction of Aitken mode particles as an effect of emissions during fireworks, doubts are prevalent for nuclei mode size ranges. Some studies have shown increase in ultrafine concentration contrasting to most of the other works. For Indian scenario, only few studies have attempted to study the effect of fireworks on the number characteristics and further on nuclei mode particles (see Section 1.6.2.2). A detailed study on this aspect can be helpful for several reasons. Changes in number characteristics of atmospheric aerosols at sufficient height can provide better insights into regional changes. Any possibility of new particle formation during Diwali can also be probed by studying the size spectrum evolution in the nuclei mode.

Although aerosol parameters like mass loading, change in chemical composition and modification in number concentration and number size distribution for entire size range were

CHAPTER 4

CHARACTERISTICS OF NUCLEI MODE ATMOSPHERIC PARTICLES: CASE STUDY 1: FIRECRACKER EVENTS

Most of the research pertaining to new particle formation has been focused towards ambient atmospheric conditions. Estimation of nuclei mode characteristics has been an important component of such studies. However, spikes in nuclei mode concentration may occur during high aerosol concentration (episodic) events as well. Such episodes e.g. dust storms, volcanic eruptions, fireworks, forest fires and biomass burning etc. modify physical, chemical and radiative characteristics of the background aerosol spectrum. These changes may induce short-term air quality degradation and long-term health complications. Such high concentration episodes have been studied mostly in terms of changes in mass loadings, optical depths and chemical compositions. However in recent times, modifications in number concentration and number size distribution have also been given due attention.

Aerosol emission during celebratory events is a major episodic activity well studied in literature (details in Section 1.6). These events are generally celebrated by burning candles and fire-crackers. Diwali festival celebrated in India is one such event in which the fireworks are used in a large scale. Several worldwide studies/campaigns have been conducted where aerosol emissions as a result of fireworks have been investigated. An equally significant amount of research has also been conducted in Indian context as well. Most of the past studies/campaigns primarily focused on measuring the changes in aerosol mass loadings or the aerosol (chemical) compositions. In events where number characteristics are measured, ambiguities exist such as the increase of ultrafine number concentration during fireworks (Section 1.6.4). As already mentioned, detailed knowledge on effect of fireworks on nuclei mode characteristics is not well documented. The possibility of formation of fresh particles (NPF events) during fireworks can't be ruled out. To address these issues, the first part of the field campaigns conducted during this research work (i.e. case study 1) is focused on

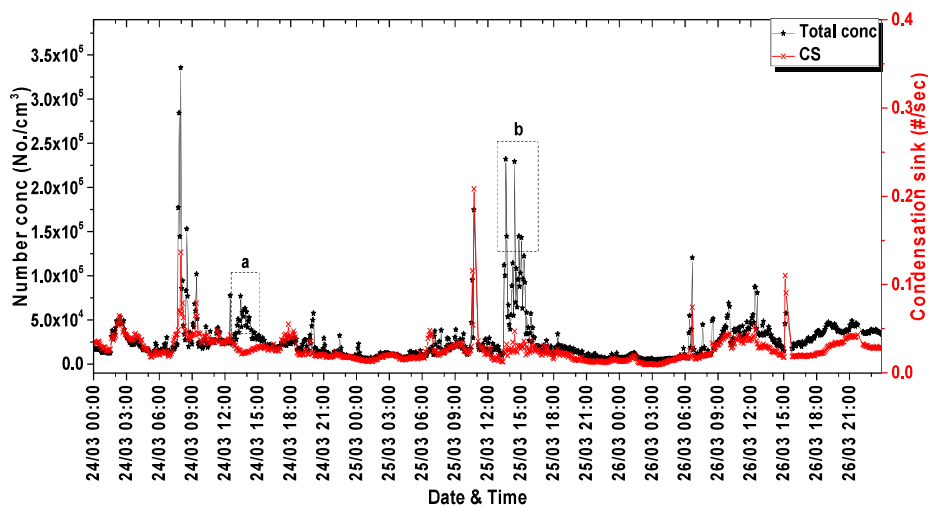


Fig. 5.16: Condensation sink and nuclei mode concentration

5.4 Summary

Number characteristic measurements of atmospheric aerosol particles during a large scale fire accident were performed as case study 2 of this work. Sampling duration was segregated into case and control days and these characteristics were compared for interpreting effect of emissions due to fire on background aerosol characteristics, if any. Similar to the conclusions inferred from case study 1 (Diwali field campaign), several peaks in integral number concentration, simultaneous dip in mean diameters around these peaks and inherent fluctuations were again noted. Size distribution evolution analysis confirmed formation of nuclei mode particles at noon times on the days of fire event. Diurnal variations of total as well as size segregated number concentration on case days were distinctly different from those expected for a background day. NPF events were picked from the measured data based on qualification criterion and rigorous analysis. For case study 2, formation rate of 5 nm particles was estimated in addition to estimations of growth rates, coagulation and condensation sinks. Formation rate of minimum detectable size and growth rate of nuclei mode particles was found to be higher for case study 2 (fire) compared to Diwali measurements (case study 1).

between 5-350 nm. Variations in number concentration values affect sink values which subsequently can be coupled to formation parameters of fresh particles. Fig. 5.12 depicts time series of coagulation sink of 5 nm particles and condensation sink (5-350 nm) for three days (when the fire was taking place) of case study 2. Fig. 5.15 represents time evolution of condensation sink and number concentration in nuclei mode size ranges simultaneously.

The sink values varied from 0.001-0.09, 0.01-0.34 (coag S₅, CS) and 0.0002-0.008, 0.01- 0.054 (coagS, CS) for case and control days, respectively. For some of the peaks (shown in fig. 5.16), drop in condensation sink could be related to the increase in total number concentration (a, b) while for others these parameters could not be related simply.

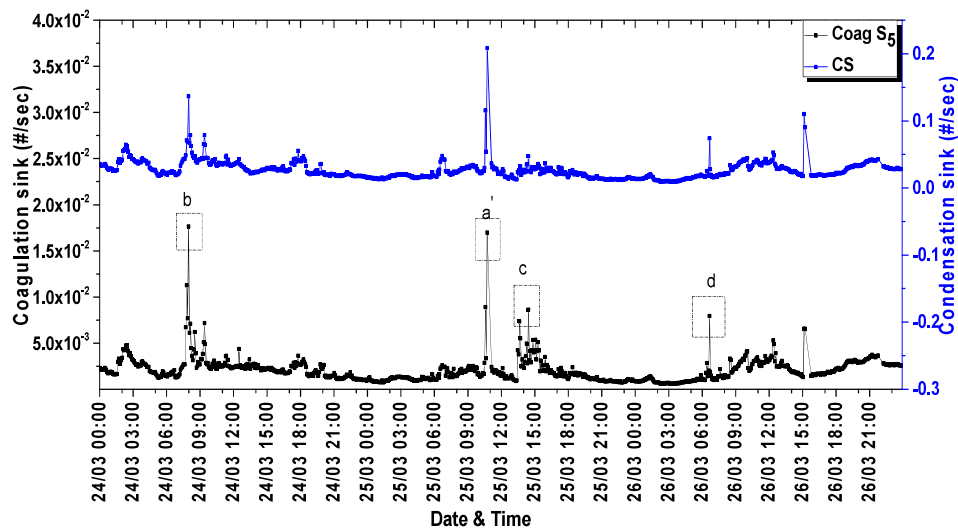


Fig. 5.15: Typical plot for coagulation and condensation sink: time-series

The values obtained under this work for background conditions are compared with those observed worldwide and are found to be as expected for polluted urban locations. In addition, the estimated values at the time of fire event add dimension to the existing database. Formation and evolution characteristics of NPF events for case study 1 (Diwali and background) and case study 2 (fire and background) are combined and compared in table 5.3.

Table 5.3: Formation and evolution characteristics of NPF events
: Comparison of case study 1 and 2

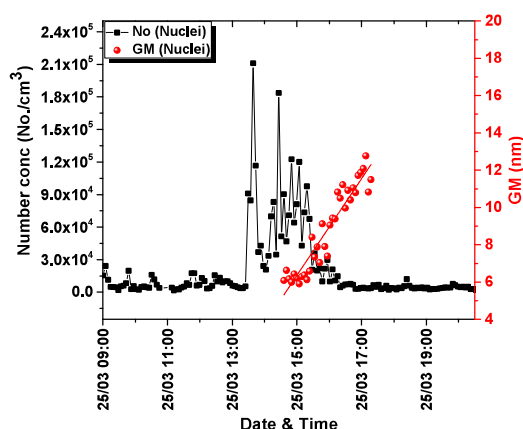
Events	Parameters		
	$dN_{11(5)-20}/dt$ (no./cm ³ /sec)	GR ₁₁₍₅₎₋₂₀ (nm/h)	J ₁₁₍₅₎ (no./cm ³ /sec)
Diwali 2012	1.35	0.17	80.55
Diwali 2013	1.54-8.67	0.28-0.73	57.31-225.44
Deonar fire	3.89-31.87	0.77-2.79	69.97-535.68
Background	1.45-15.48	0.06-1.59	15.06-241.28

In the above table, estimated rate of change of number concentration and growth rate are shown for 11-20 (Diwali) or 5-20 nm (Deonar fire) size ranges. Formation rate of minimum detected size is also different for these two cases (J₁₁ and J₅). Background refers to ambient aerosol conditions in normal (non-episodic) conditions and it includes characteristics for both 5-20 and 11-20 size ranges. As can be seen in table 5.3, rate of change of number concentration and growth rate in nuclei mode was found to be higher for fire induced emissions compared to Diwali emissions and background processes. Formation rate of minimum detectable particles was also higher for the case of fire event. Interestingly the values obtained for background aerosol formation processes at random times were observed to be on average higher than Diwali.

5.3.4: Sinks

Time evolution of coagulation and condensation sink has also been studied similar to case study 1. However coagulation sink for the present case could be estimated for particles of 5 nm or higher diameter. Also, condensation sink in this context is calculated for size spectrum

Table 5.1: Event statistics (case study 2)



Sampling days	On case days		On control days	
	3		2	
Peak classification	Instances			
	9		10	
	Events			
	Day time	Night time	Day time	Night time
Weak NPF	-	-	-	-
Moderate NPF	-	1	2	-
Strong NPF	3	1	3	-

Fig. 5.14: Parameters during a qualified event

5.3.3: Formation and evolution characteristics of events:

$\frac{dN_{5-20}}{dt}$, GR₅₋₂₀, J₅, CoagS₅ and CS represents rate of increase of nuclei mode particles (in detectable size range), growth rate of nuclei mode particles, formation rate of minimum detectable size, coagulation sink for 5 nm particles and condensation sink, respectively. Values for these parameters for field campaign of case study 2 are shown in table 5.2. Estimated values from this work shown in above table are relative to the detectable size distribution above 5 nm. Change in number concentration and growth rate in nuclei mode size ranges was found to be higher for case days during day times. Values for formation rate for 5 nm particles followed the same trend.

Table 5.2: Formation and evolution characteristics of NPF events

Events	Parameters			
	$\frac{dN_{5-20}}{dt}$ (no./cm ³ /sec)	GR ₅₋₂₀ (nm/h)	J ₅ (no./cm ³ /sec)	CoagS ₅ (#/sec)
Case days (day time)	11.04-31.87	0.77-2.82	76.39-535.68	0.0020-0.0041
Case days (night time)	3.89-19.88	1.39-2.79	69.97-131.09	0.0026-0.0039
Control days	3.28-15.48	0.65- 1.59	46.36-127.43	0.0018-0.0027

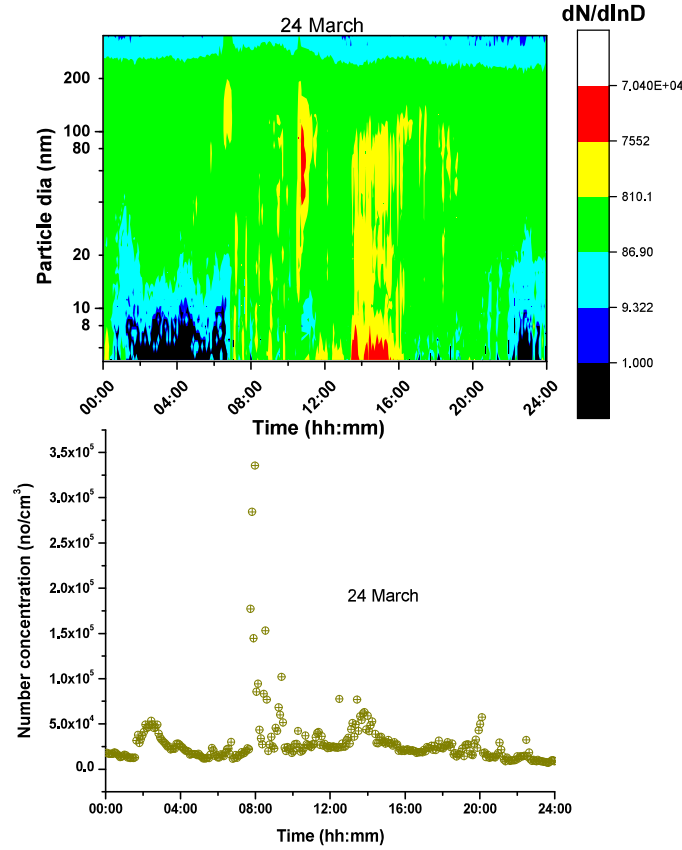


Fig. 5.13: Corroborated number concentration and size distribution for 24th March

5.3.2: Qualifying criterion and event statistics

Fig. 5.14 shows the time evolution of number concentration and mean size of nuclei mode particles around the peak observed on a case day (25th March, noon times). From this figure, dN_{5-20}/dt and GR_{5-20} can be calculated as 31.87 no/cm³/sec and 2.82 nm/h, respectively. As both of these parameters qualify the criterion discussed and interpreted in section 4.4.2, this event can be qualified as a probable NPF event. Other peaks selected from level 1 analysis were also tested in the similar way leading to selection of few certain NPF events. It can be noted that this analysis was not restricted for the days of fire only and continued for other measured data on background days. Table 5.1 presents event statistics for selected case and control days of case study 2. Out of total 9 instances of case days, only 5 could be qualified as certain NPF events. Most of these events were observed at day times. For all these events, formation and evolution were estimated subsequently.

concentration in integral/nuclei mode size ranges could not be correlated with the growth of nuclei mode particles, subsequently.

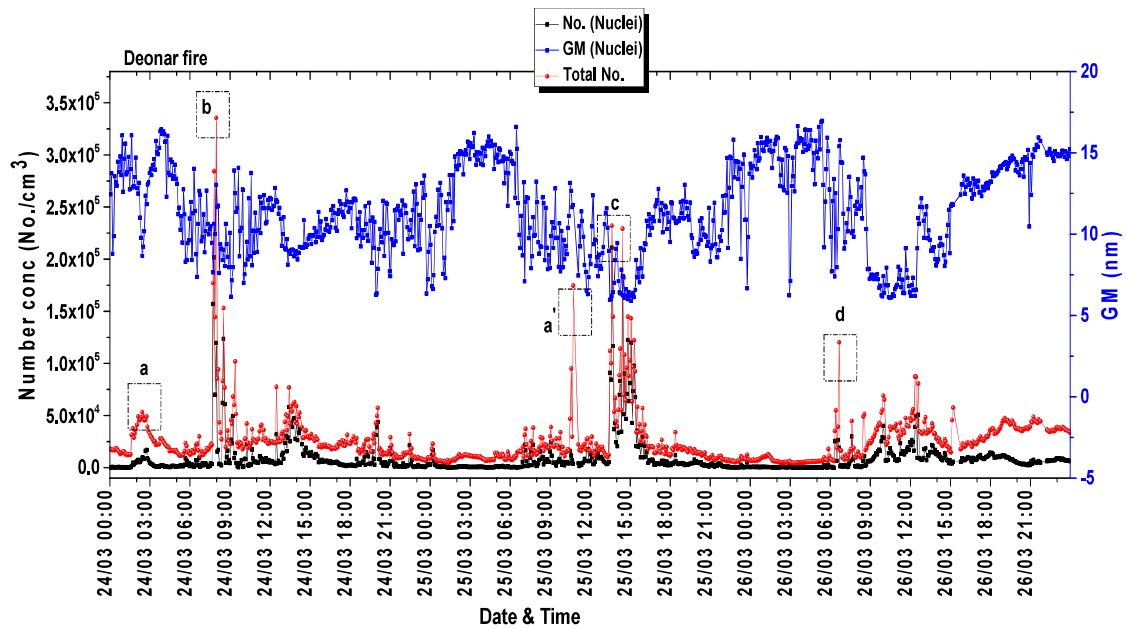


Fig. 5.12: Corroborated number concentration and geometric mean for case days

Similar approach was also used for control days as well. For the present case, NPF related parameters were also obtained and compared for day time and night time, additionally. Aerosol formation in nuclei mode size ranges can also be visualized as fig. 5. 13 representing size distribution evolution and number concentration modifications, simultaneously. Corresponding to the red spots in 3D plot, increase of integral number concentration can be noticed for 2 abruptions. One of these is due to the increase of particles in large Aitken mode for a short time while the other distinctly shows formation of particles < 8 nm diameter. The later one showing formation of particles for a considerable time can be picked for further analysis as discussed above. All peaks qualified from this analysis were re-checked studying the size distribution evolutions close to these peaks.

concentration in ultrafine size ranges increased significantly during day times on the days of fire. The role of photochemical reactions of trap gases released from dump yard resulting in generation of aerosol is crucial factor resulting in nucleation events during case days.

5.3 Evolution parameters for selected nucleation events

A clear and significant increase in nuclei mode number concentration was noted on the days of fire during noon times. The most interesting part of these observations is related to the analysis in size range 5-10 nm, the increase in which dominated the increase in nuclei mode size ranges. Similar to the analysis of microscopically probing number concentration evolution (as done for case study 1), some peaks were selected for next level qualification criterion. Further analysis was done for calculating parameters representing formation of minimum detectable size and growth of mean size of nuclei mode particles.

5.3.1 Picking up events

The first step in this direction is correlating the increase of total concentration and nuclei mode concentration at the time of peaks in number concentration. As discussed in section 4.4.1, growth of mean size of nuclei mode particles (at the time of peaking) for considerable time is the crucial link to establish these modifications as particle formation events. Fig. 5.12 shows the time series of total number concentration, number concentration in nuclei mode size ranges (5-20 nm) and calculated GM for this range, plotted from the SMPS measured data for case days (24-26 March).

Peaks for which GM showed a definite sign of growth were selected for level 2 analysis. As can be seen, there are several peaks in the time-line which were subsequently tested against the qualification criterion. Some of the peaks (e.g. a, b, c, d) for which the criterion of selection for NPF events got satisfied are shown in fig. 5.12. Additionally other peaks were also obtained (such as peak a' in above figure) for which the increase of number

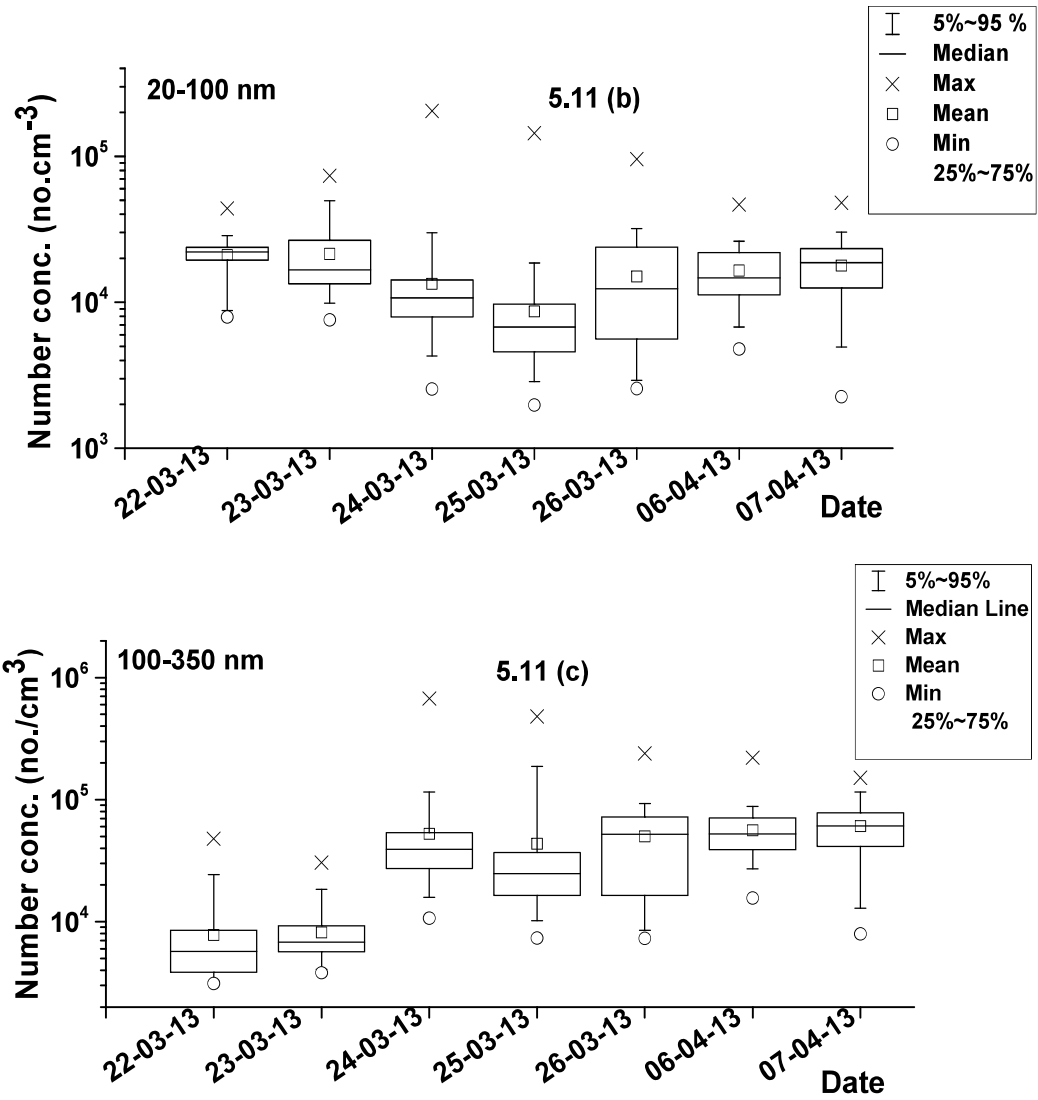
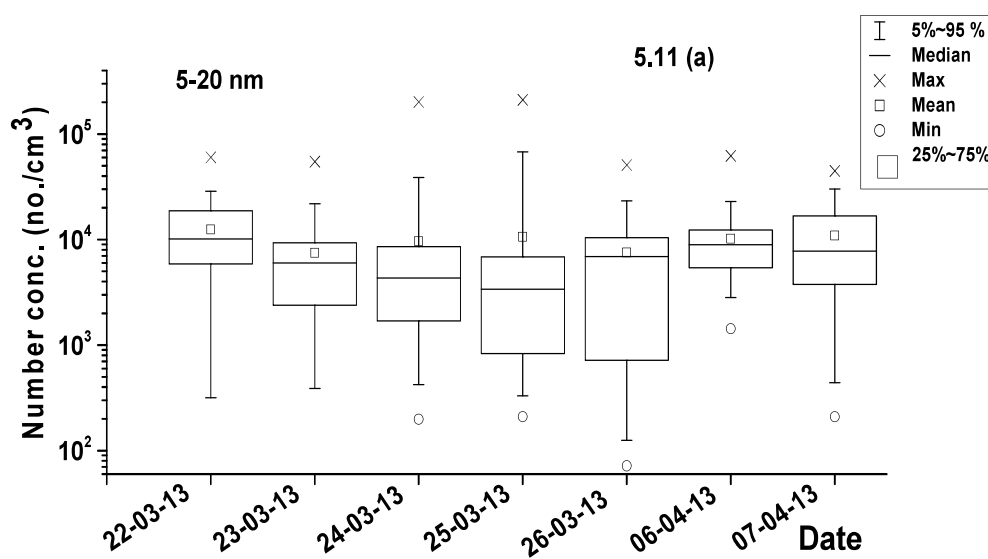


Fig. 5.11 (a-c): Box-whisker plot for number concentration in different modes: all days

5.2.4 Comparison of parameters during case and control days

As discussed above, it is difficult to distinguish case and control days on the basis of average parameters for the day. This observation applies to average number concentrations for different size ranges as well. However maximum concentrations, instances of high concentration and dispersity of data towards high concentration is relatively higher for case days in comparison to control days. This difference is mostly due to nuclei and Aitken mode size ranges only. Although on average it looked not possible to demarcate case days different from control days; size distribution evolution analysis at shorter time scale leads to conclusive insights differentiating case and control days. It was seen that number

accumulation mode and entire size range (fig. 5.10 and 5.11 (c)). Daily average concentration was seen to be varying randomly in a way not to be conclusively distinct for the case or control days. Daily maximum concentration for nuclei mode was seen to be more or less similar for all days except 24th and 25th March. Difference of mean and median concentration was quite high for these two days as well. For Aitken mode size ranges, daily maximum concentration was higher for case days (barring 22nd March). Concentration difference between 75th percentile and 95th percentile was also relatively higher for 24th and 25th March. Observed differences in concentrations (mean-median and 75th percentile-95th percentile) are similar to the case of Diwali emissions, and the possible reasons have already been discussed in chapter 4 (section 4.3.2.2).



5.2.4 Statistical Analysis:

For the days when measured data was available for entire day, box-whisker plots were drawn for discussing statistical inferences. Fig. 5.10 shows box-whisker plot for total number concentration for all days.

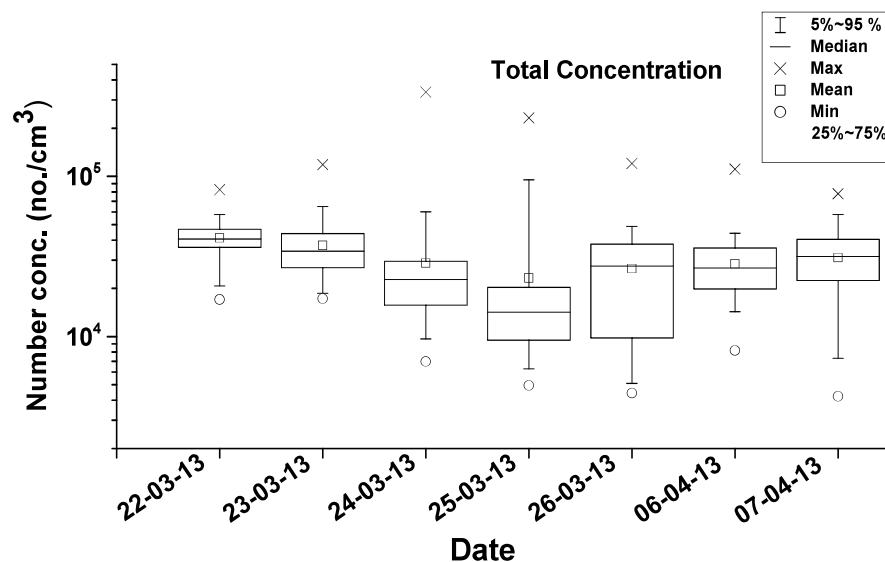


Fig. 5.10: Box-whisker plot for total number concentration: all days

Daily maximum concentration was found to be higher (range: 8×10^4 - 3.5×10^5 per cm^3) for case days (23-26 March). Maximum concentration on 6th April was also close to one of the case days. No conclusive insight was obtained while comparing mean and median concentrations for different days. However difference of mean and median concentration was seen to be distinct for 3 case days (23-25 March) in contrast to other days. This is expected when high concentration instances modify the number distribution function and similar to what was noticed for Diwali emissions as well (see fig. 4.15). Box-whisker plots for size segregated number concentration for nuclei, Aitken and accumulation mode size ranges are shown in fig. 5.11 (a-c).

As inferred from fig. 5.11, day to day variations of number concentration in nuclei mode and Aitken mode were seen to be following that of total number concentration. However, same is not true while comparing diurnal variations of number concentration in

Aitken mode number concentration. For comparison, similar diurnal variation for all modes for control days is plotted in fig. 5.9.

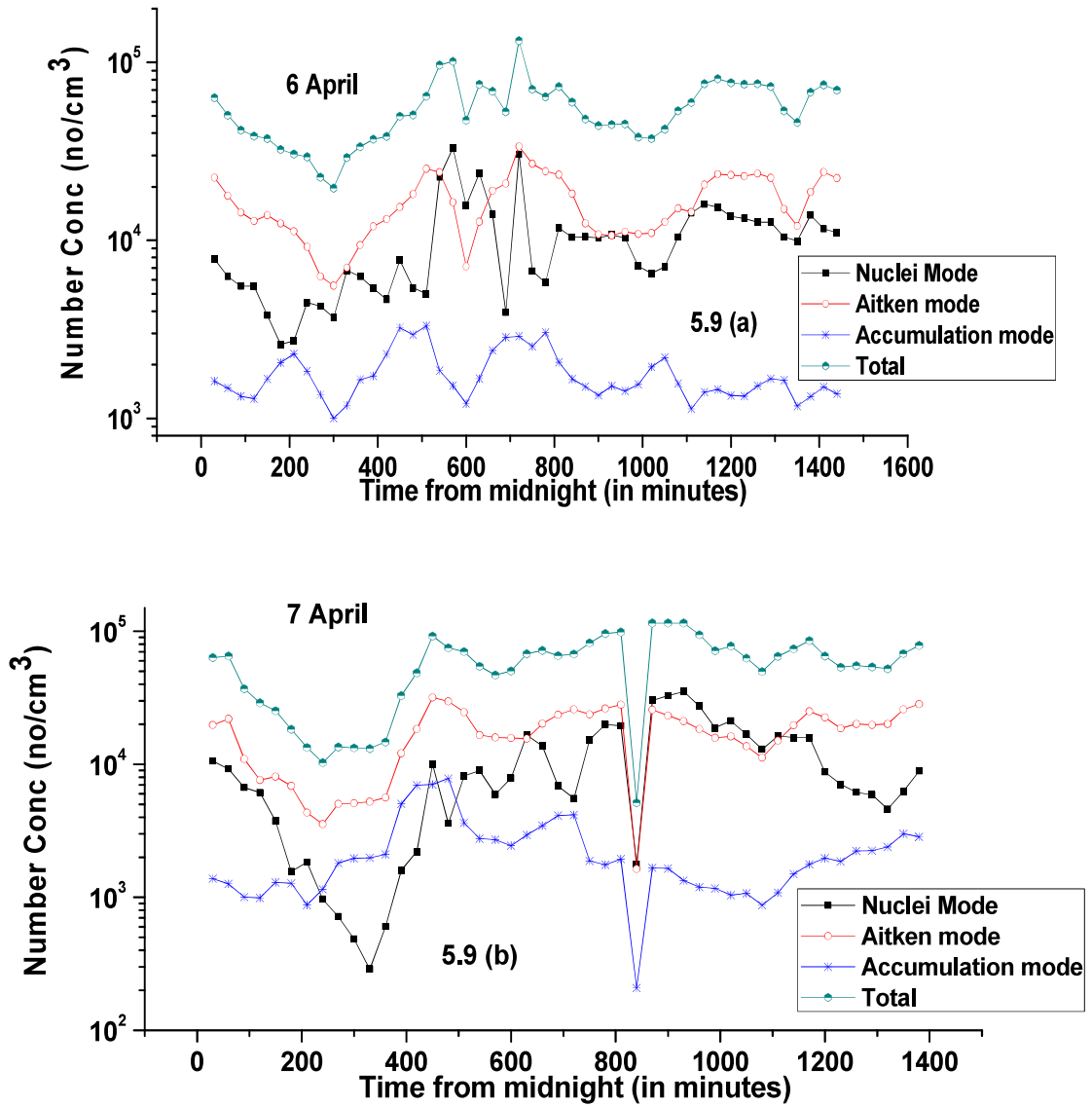


Fig. 5.9 (a-b): Diurnal variation of number concentration (total and different modes) for control days 6th and 7th April

Inferences with respect to nuclei mode particles as deduced above for the fig. 5.8 are not applicable for explaining diurnal variations shown in fig. 5.9. For this case, these variations are controlled by different size ranges at different times as usually expected for complex background atmospheric conditions.

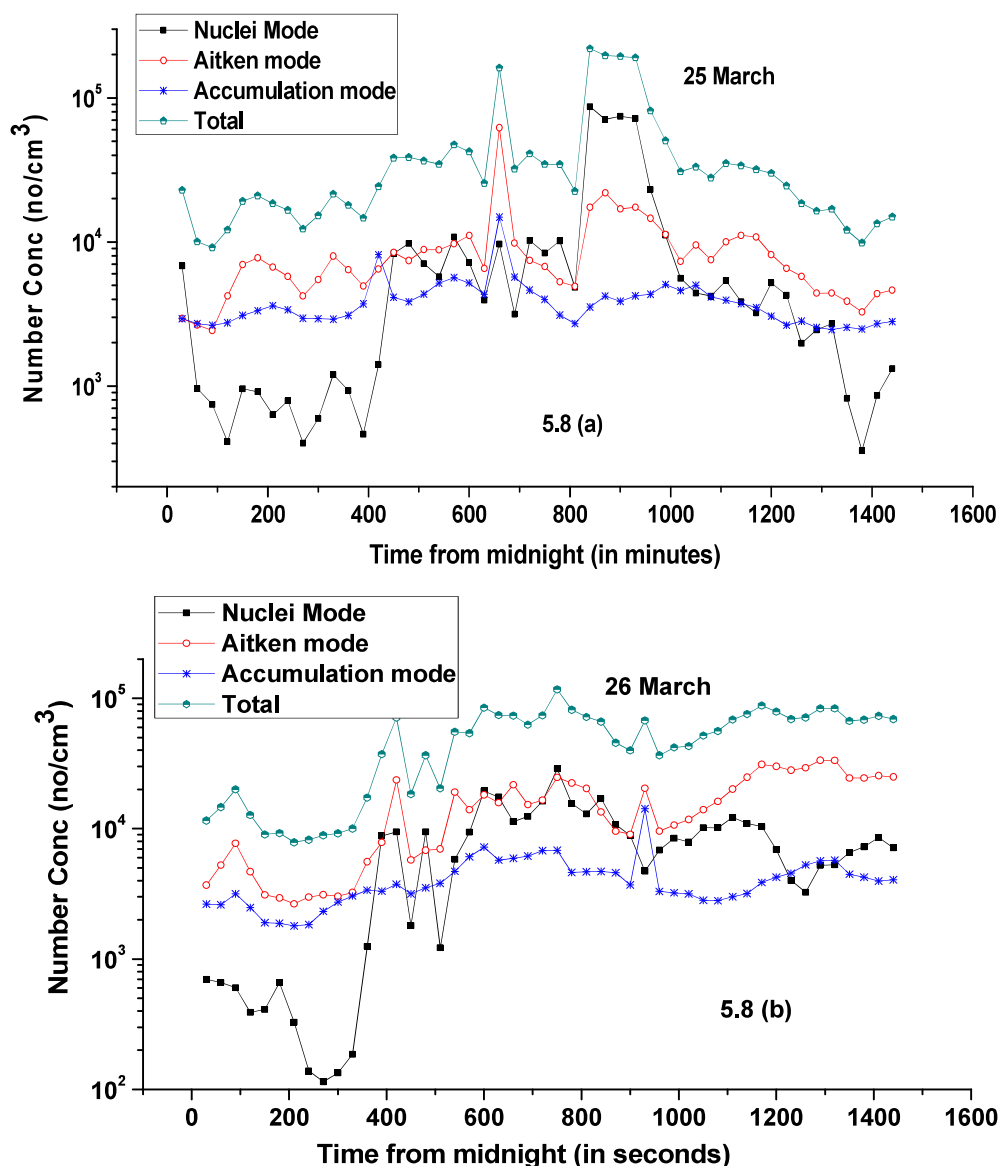


Fig. 5.8 (a-b): Diurnal variation of number concentration (total and different modes)

for case days 25th and 26th March

The contribution of nuclei mode particles towards increase of total number concentration is clearly depicted in the above figure. For both these days, increase in total number concentration was observed to be mostly dominated by increase in nuclei mode concentration (from 400-1000 minutes after midnight i.e. 07:00-17:00 hrs.). Additionally variation in total number concentration can be seen to be closely linked to the variations in

dominated by particles in the size range 5-10 nm. This effect is different from the diurnal variations of aerosol number concentration where generation of ultrafine and nuclei mode particles can be related to other factors such as traffic frequency (morning and evening times)

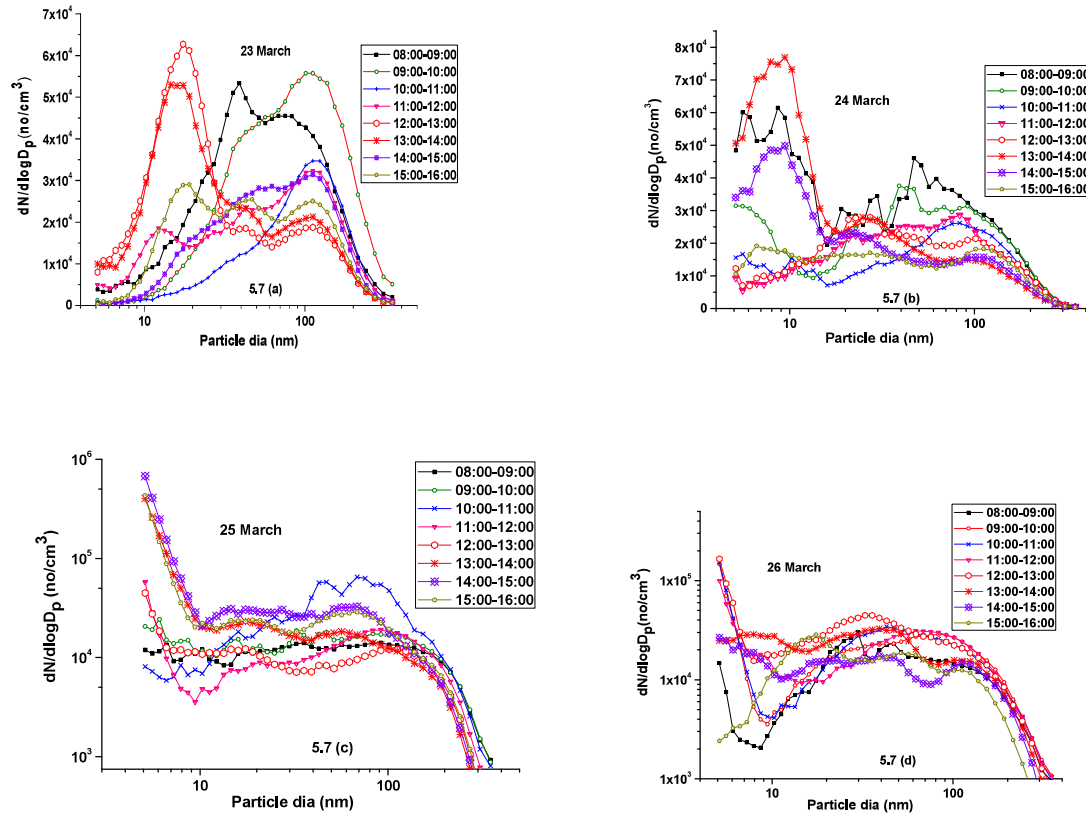


Fig. 5.7 (a-d): Modification of size characteristics during day times for case days

5.2.3 Diurnal variations

Diurnal variation for nuclei mode, Aitken mode, accumulation mode and total number concentration for 25th and 26th March (case days with highest nuclei mode particles) are shown in fig. 5.8 (a-b).

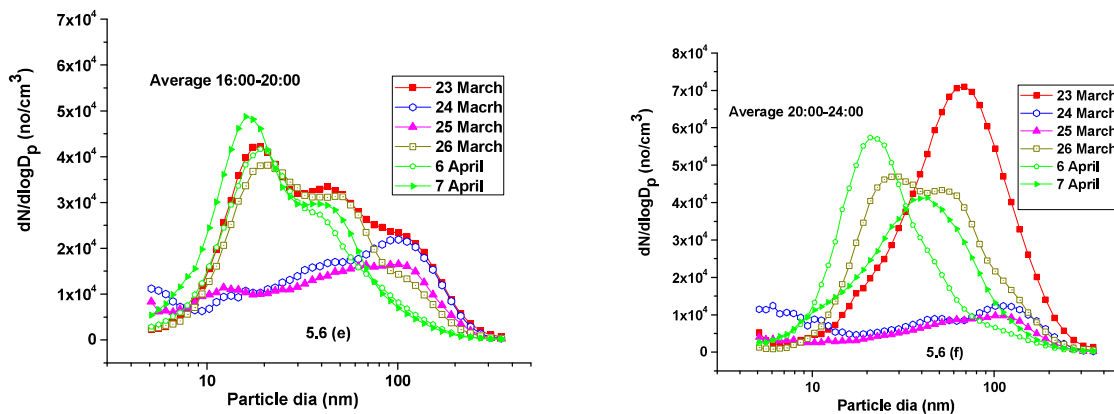
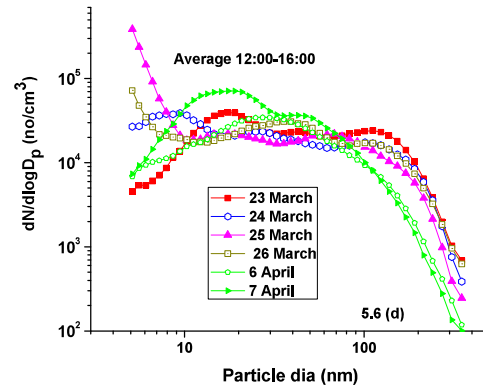
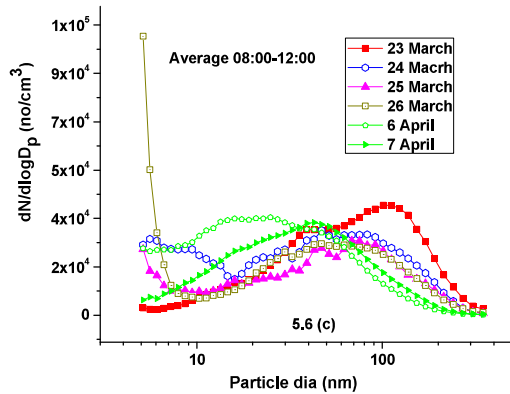
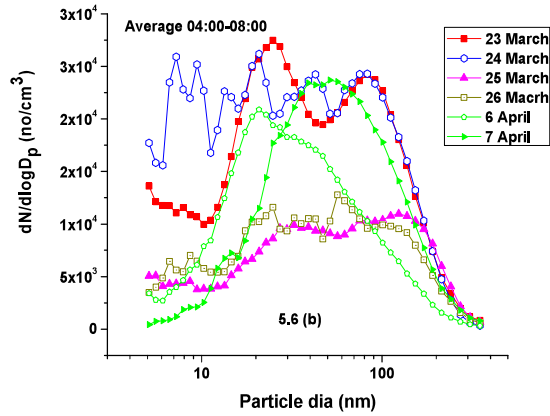
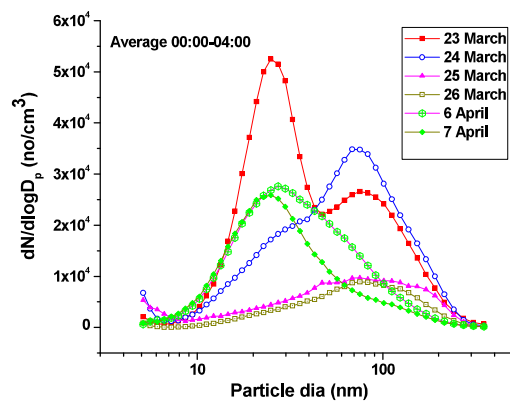


Fig. 5.6 (a-f): Size distribution evolution for case and control days: 4 hourly averages

For 08:00-12:00 hrs., a certain formation of particles in nuclei mode size ranges can be distinctly seen for 24-26 March (Fig. 5.6 (c)). Concentration in this size range was also comparable for 6th April which however got diminished with time. Highest nuclei mode concentration for the day was measured in the afternoon time block (12:00-16:00) for three (24-26 March) out of the four event days (Fig. 5.6 (d)). Ultimately size distributions for case as well as control days evolved to a typical background aerosol spectrum in evening and night time blocks (Fig. 5.6 (e-f)). Fig. 5.6 indicates that generation of nuclei mode particles is taking place during the day times. In past, frequency of NPF events has been shown to be more for sunny days, springs and/or day times. Probability of formation of particles via photochemical reactions is more at the time when sun intensity is high. For the present context, this phenomenon can be linked with particle formation by studying size distribution evolutions during day times for case days.

Fig. 5.7 represents evolution of measured size distributions as hourly averages but in day times (08:00-16:00 hrs.) for case days. A clear modification in nuclei mode size ranges indicated by a significant increase in number concentration is apparent in fig. 5.7. For all case days, this increase can be correlated with the increase in intensity of sun as the day passes. Specifically for 25th and 26th March (fig. 5.7 (c-d)), number concentration was seen to be

range. For two other case days (25, 26 March), concentration was found to be relatively lesser. Size distribution for control days (i.e. 6, 7 April) showed a distinct mode in small Aitken size ranges. Modification of size spectrum in nuclei mode size ranges is noticeable in the next time block between 04:00-08:00 hrs. for 23rd and 24th March. For both these days, size distribution approximately consisted of three separate modes in nuclei, Aitken and accumulation mode size ranges (Fig. 5.6 (b)).



5.2.2 Dynamics of size distribution

As a first level of analysis, SMPS measured size distribution were averaged for the entire day. Fig. 5.5 compares the average size distribution for 7 days (case: 23-27 March and control: 6-7 April). Size distribution for typical background conditions (size distributions for 6 and 7 April) consisted of modes in Aitken and/or accumulation mode. However on some days of event (24, 25, 26 March), a marked modification can be noted in the size spectrum specifically in nuclei mode size ranges.

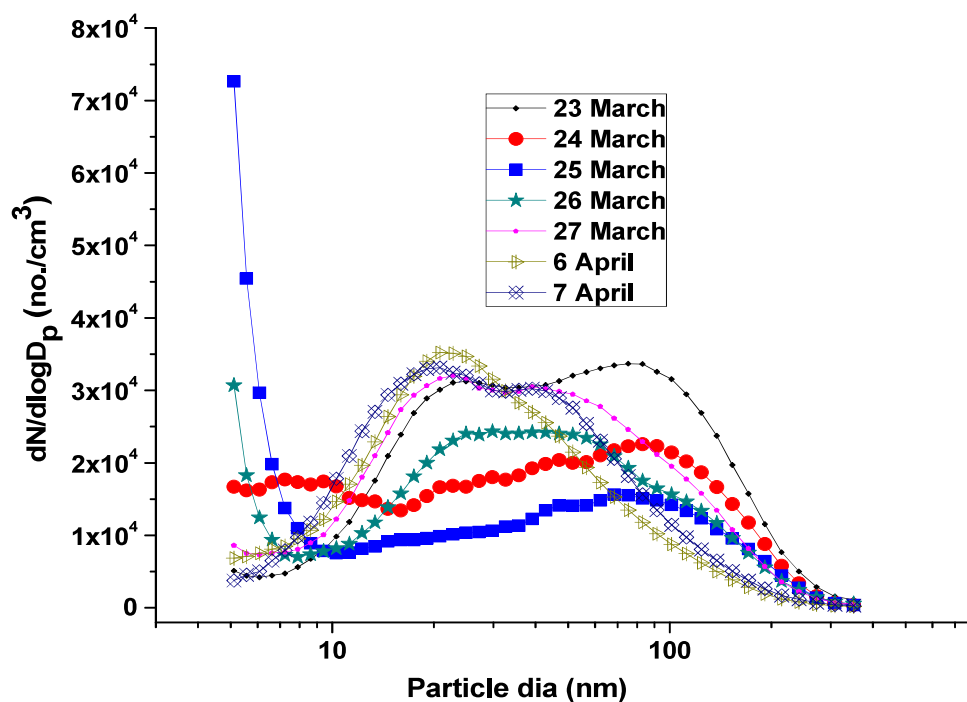


Fig. 5.5: Number size distribution for all days (averaged over 24 hours)

It can be noted that size distributions for these case days can easily be differentiated from those of control days even if averaging is done for the entire day. This hints at two possibilities: either departure from the background spectrum for nearly all times or significant deviation at few times affecting averaged inferences for the day. Subsequently to gain insight, 4 hourly averaged distributions were studied for these days and are shown in fig. 5.6. For late night time block (fig. 5.6 (a)), size distribution for 2 of case days viz. 23rd and 24th April consisted of a small Aitken mode in 20-30 nm and an accumulation mode in 100-200 nm size

patterns. Wind-rose diagram for the case days is also shown in fig. 5.4. Negligible wind was seen to be flowing from north-east-south directions at the sampling location.

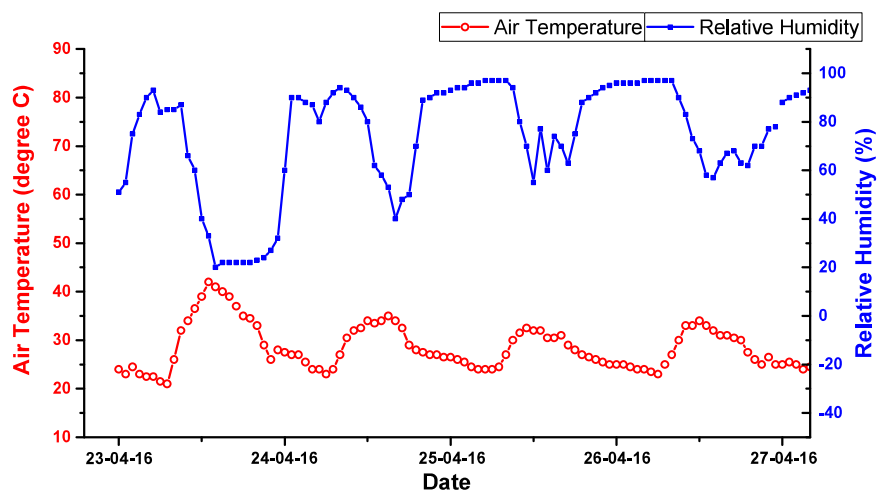


Fig. 5.3: Time-series of temperature and relative humidity for case days

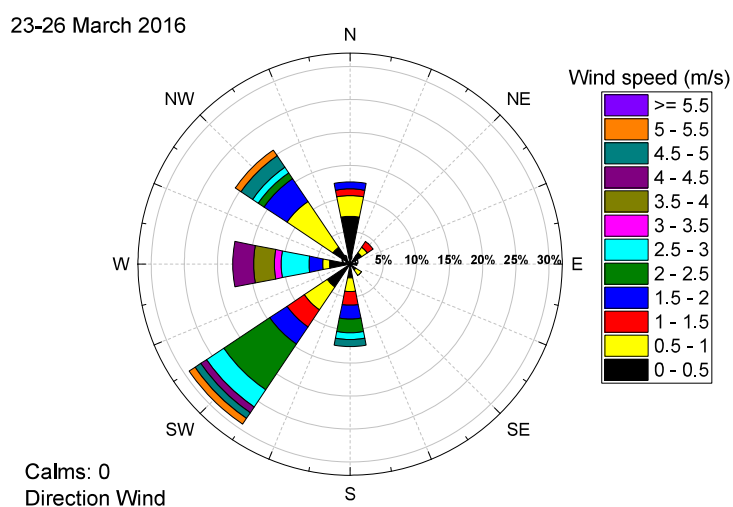


Fig. 5.4: Wind-rose diagram for case days

Another way to interpret the characteristic differences is by analysing the size distributions averaged over the entire day, time-blocks or hours. Generation of nuclei mode particles can be captured by comparing the size distributions of case and control days. Subsequently, dynamics of nuclei mode particles (5-20 nm for this case) can be studied in order to understand their evolution characteristics.

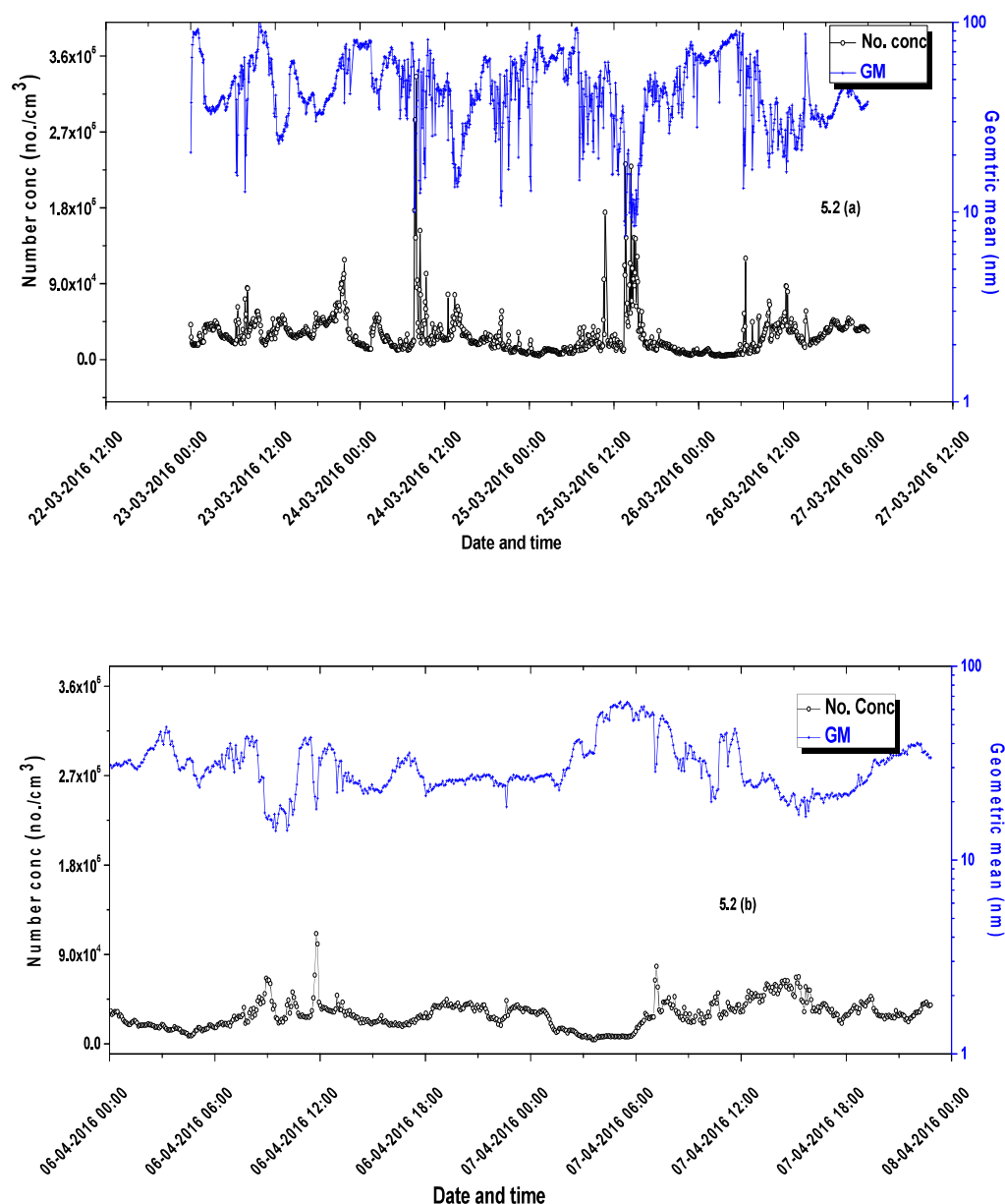


Fig. 5.2 (a-b): Case and control days: time profiles of number concentration and GMD

Air temperature and relative humidity at sampling location for case days are plotted in fig. 5.3. As can be seen, diurnal variations were found to be following similar trend and no specific abnormality/spikes could be noticed. Maximum temperature for the case days was measured at $\approx 40^{\circ}\text{C}$ (23rd April afternoon). Although relative humidity was high during night times, it was not significant enough during day times to affect particle's hygroscopic growth

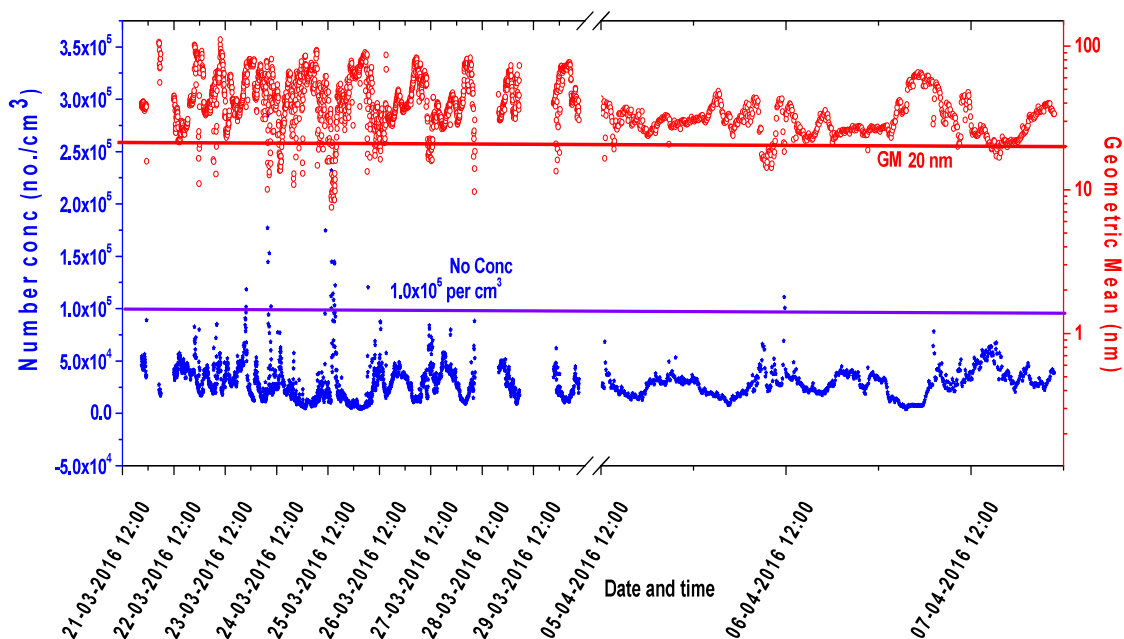


Fig. 5.1: Time series of number concentration and geometric mean (all days of case study 2)

Although these measurements were made at a sampling location slightly far from the place of fire, the above modifications can be used to quantify contribution of site generated particles to background aerosol population. Several trap gases (carbon monoxide, hydrocarbons, nitrous oxides etc.) are also expected to be released during fire in waste dump-yards^{293, 294}. Their role towards nucleation in favourable condition can't be ruled out as well.

To better compare the number concentration profile, time series of number concentration and geometric mean are also plotted separately for case and control days in fig. 5.2 (a-b). Data instances when the total number concentration was found to be more than 10^5 per cm^3 were $\approx 1.8\%$ and 0.003% (of all data points) for case and control days, respectively. Similarly $\approx 6.5\%$ and 5.3% times geometric mean decreased lesser than 20 nm for case and control days, respectively. Size distribution evolution analysis (as done for differentiating a background and an episodic event for case study 1 around the peaks can be performed for similar intensity peaks observed on case and control days. Difference in chemical composition of particles may also provide pathways to do so.

picking up nucleation events. Once such an event was qualified as a certain NPF event, formation and evolution parameters for the same were also estimated. This scenario is different from that presented while analysing measured data of case study 1 for NPF events in the last chapter. It is to be noted that although qualifying criterion established several instances during case study 1 as NPF events, analysis related to formation characteristics was limited to minimum detectable size (11 nm for this case) only. On contrary, measurements were made till 5 nm in the present case.

Total number concentration in the following discussion refers to that belonging to 5 nm to 350 nm size range of diameters. Any abrupt change in this index, coupled with change in the mean size of spectrum and/or change in the nuclei mode concentration around the same time indicates the first signal of NPF event.

5.2.1 Number concentration

Fig. 5.1 represents the time series of number concentration and geometric mean diameter for entire sampling duration. Apart from the ambient diurnal changes, effect of emission on number concentration during fire is clearly noticeable in fig. 5.1. During the days of fire, number concentration was measured at $> 10^5$ per cm^3 (arbitrarily chosen) at several occasions. For many of these peaks in number concentration profile, a concurrent dip in time series of geometric mean is similar to that obtained during Diwali measurements (See fig 4.1). Emission of un-burnt combustion products in ultrafine size range and/or generation of aerosols via gas-particle conversion might cause such a decrease in mean size parameters.

under control. During this outbreak, air quality of surrounding region and Mumbai at large remained extremely poor and became a talking point in media, public and government circles. Around this time, studies were conducted to measure aerosol mass concentration in the surrounding localities²²⁷ to investigate atmospheric mass loadings.

There are only few studies interpreting the effect of fires on the number characteristics, specifically for nuclei mode particles (section 1.6). This chapter presents and discusses results obtained from SMPS measured evolution of aerosol number characteristics due to Deonar dump yard fire event (case study 2) in a nearby location.

5.2 Measurement of aerosol number characteristics: case and control days

Case study 2 (March-April 2016) focused on estimating changes in atmospheric aerosol number characteristics (measured using SMPS) during Deonar dump yard fire. The fire started on 20th March and continued intermittently with varying intensity for about a week. Sampling was performed from an arrangement made in a high rise building situated approximately 5 km from the site of fire. These measurements were carried out from 21st March to 28th March and then from 6th April to 7th April, but intermittently. Entire data was also segregated into two domains so as to compare the number characteristics during days of fire and background days. Following this classification and also ascertaining the availability of data for almost entire day (24 hours), 23-26 March were selected as ‘case days (during fire)’ and 6-7 April as ‘control days (background)’, respectively.

Similar to the discussion of results of measurements conducted in last two campaigns (chapter 4), SMPS data was analysed mainly to interpret changes in number concentration and number size distribution. Diurnal variations of number concentration in different size ranges were interpreted. Due to the coverage till 5 nm, extended information (covering 5-11 nm particle sizes) on nuclei mode particles was available for this case. Sensitivity reduction towards lower sizes increased the accuracy of analysis of nuclei mode particles in terms of

CHAPTER 5

CHARACTERISTICS OF NUCLEI MODE ATMOSPHERIC PARTICLES: CASE STUDY 2-LARGE SCALE FIRE EVENT

Emission of trace gases and aerosol particles from large scale fires modifies atmospheric aerosol characteristics. Such fires include biomass burning, forest fires, volcanic eruptions and accidental fires etc. There are examples where such events have been seen to impact environment severely²⁹⁰. Recently air quality of Indian capital New Delhi deteriorated to alarming levels in first week of November 2016²²⁶ which was thought to be linked to unchecked burning of crop fields in the surrounding territory (<http://earthobservatory.nasa.gov/IOTD/view.php?id=89052>). Similar to the effect of emissions of episodic events presented in chapter 4, large scale fires have potential to affect aerosol properties and consequently visibility, health and climate. This chapter focuses on measuring and studying modifications in number concentration and number size distributions in the size range 5-350 nm during a large scale fire event. On the basis of these measurements, evolution of nuclei mode particles was studied. This also enabled to estimate formation rate of these particles during this event.

5.1 Deonar dump yard fire (March 2016)

Deonar dumping ground (19.0671 °N, 72.9197°E); India's largest landfill is located in Deonar locality of Mumbai. It receives huge amount of untreated waste, silt and bio-medical waste on daily basis which is stacked before disposal. Burning of dumped waste is a standard practice which reduces volume of waste and helps to recover usable or non-biodegradable material ²⁹¹, ²⁹². It is avoided in modern waste treatment plants due to the possibility of emission of trapped hazardous gases from burning of the waste. However, sometimes fire may occur inadvertently due to the triggering from uncontrollable factors. In past, several small fires broke out in Deonar dump yard in which two major ones occurred in 2016 alone. One of these massive fires broke out on March 20 and took almost 7 days to be brought completely

Inferences from experiments conducted under this study (Section 6.3.2) include experimental demonstrations/validations of aerosol oscillatory effects. Increase of number concentration in nuclei mode just near the onset of secondary peaks confirms that generation of particles is taking place via gas to particle conversion process. As the system is too complex to handle experimentally, no conclusive insight could be drawn about the amplitude and frequency of observed secondary nucleation induced oscillations. These observations however have profound significance towards understanding aerosol formation and evolution. For instance, changes in aerosol characteristics for a steady source may not be simply/always linked to controlling parameters as demonstrated by these experiments.

6.4 Summary

This chapter discussed dynamics of nuclei mode particles in closed chamber conditions. Generation of high number concentration particles in nuclei mode from HWG was utilized to study coagulation effects on their characteristics. In the first phase of experiments, coagulation peaking effects were studied. Peak characteristics depend on the source term and chamber parameters. A technique to estimate number emission rate from peak parameters was employed for HWG and incense stick. Number emission rate for incense stick (generated smoke particles) was found to be an order higher than that for HWG (metallic nanoparticles). Controlling the characteristics of nuclei mode particles is difficult but achievable. Further, coupling to/with respect to aerosol dynamical models has potential to validate and develop new technologies. Long term behaviour of vapours in closed chamber conditions was studied in the second phase. In long term size distribution evolution, sporadic peaks occurred in otherwise decaying profile of number concentration measured with CPC. In carefully controlled experiments, it was possible to relate these secondary peaks with the change in only nuclei mode particle concentrations. These experiments are step towards experimental demonstration of ‘aerosol oscillatory effects’.

As clearly seen, changes in number concentration distribution occurred in nuclei mode size ranges (< 10 nm) only thus affecting total number concentration. Similar changes in nuclei mode concentrations were observed for all such minor peaks. The modification in the size distribution indicated the role of nucleation induced generation captured by only lower size ranges. These small peaks in the decaying concentration may be attributed to the build-up of vapour pressure to cause new particle formations. It should also be noted that very soon number concentration started to decrease again due to hetero-coagulation. As the process (vapour-particle formation from HWG) was continuous, such sporadic peaks occurred at regular frequency at later times (as shown in Fig. 6.8). Changes in number concentration profile for continuous source conditions is a demonstration of phenomenon termed as ‘aerosol oscillations’.

6.3.2.2 Secondary nucleation effects: aerosol oscillations

Mathematical modelling of stirred (well mixed) systems involves taking into account nucleation, vapour condensation, coagulation, transport and removal by ventilation and wall deposition processes. Knowledge gathered from the formation and evolution of aerosols in such systems is used for designing aerosol reactors. Being non-linear, several interesting features are predicted by models used for characterizing such systems (e.g. multiple oscillations in methanol droplet formation³⁰⁷). Pratsinis et al.²⁹⁹ used method of moments to discuss oscillatory nature of the solutions including the system stability domains. However this approach considered compact particles. The solution of Pratsinis model²⁹⁹ for free molecular coagulation kernel predicts sustained oscillations in number concentration. However including Fuchs kernel in the model³⁰⁶ modifies the solution and changes the amplitude and time period of the oscillations. Oscillatory pattern seems to be suppressed due to coagulation also leading to higher steady state particle concentration due to reduction in vapour concentration loss.

Fig. 6.9 shows representative results for such analysis, where size distribution has been compared for ‘just before’ and ‘near onset’ of peak observed at 6040, 6954 and 7948 seconds (minor peaks observed in experiment 3: Fig. 6.8).

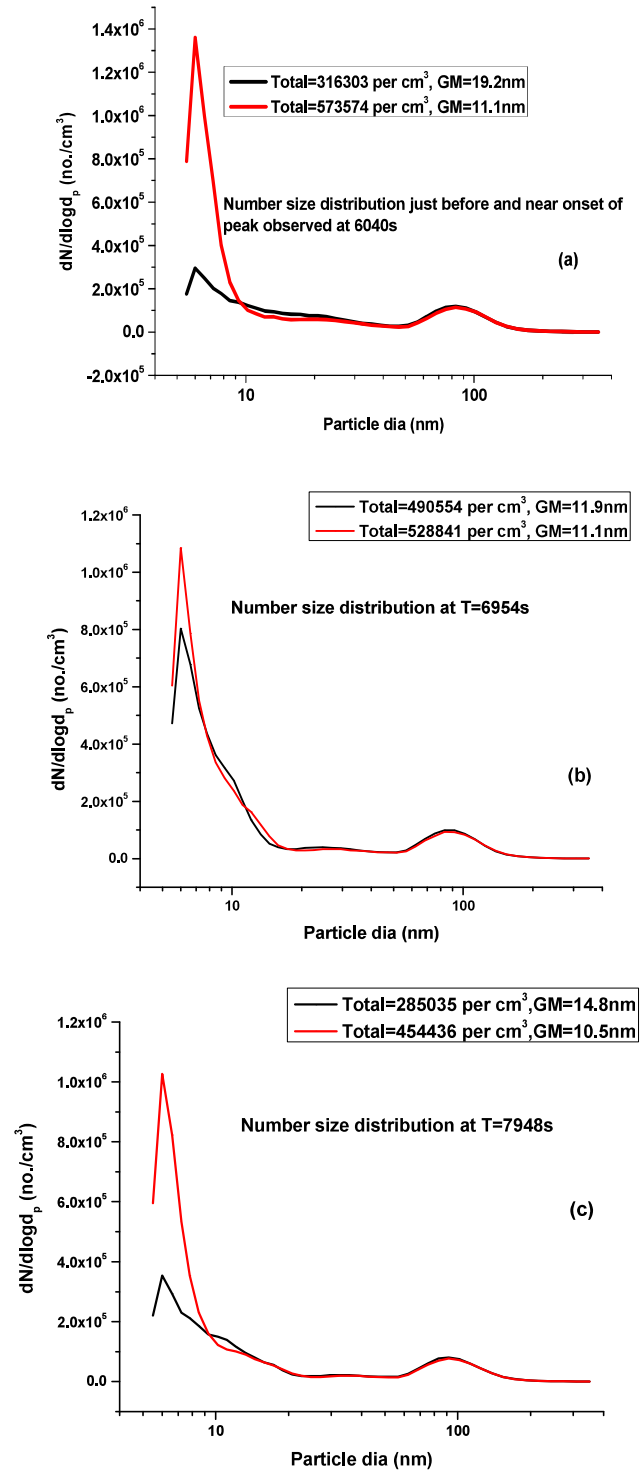


Fig. 6.9 (a-c): Abrupt change in size distribution near minor peaks of experiment 3

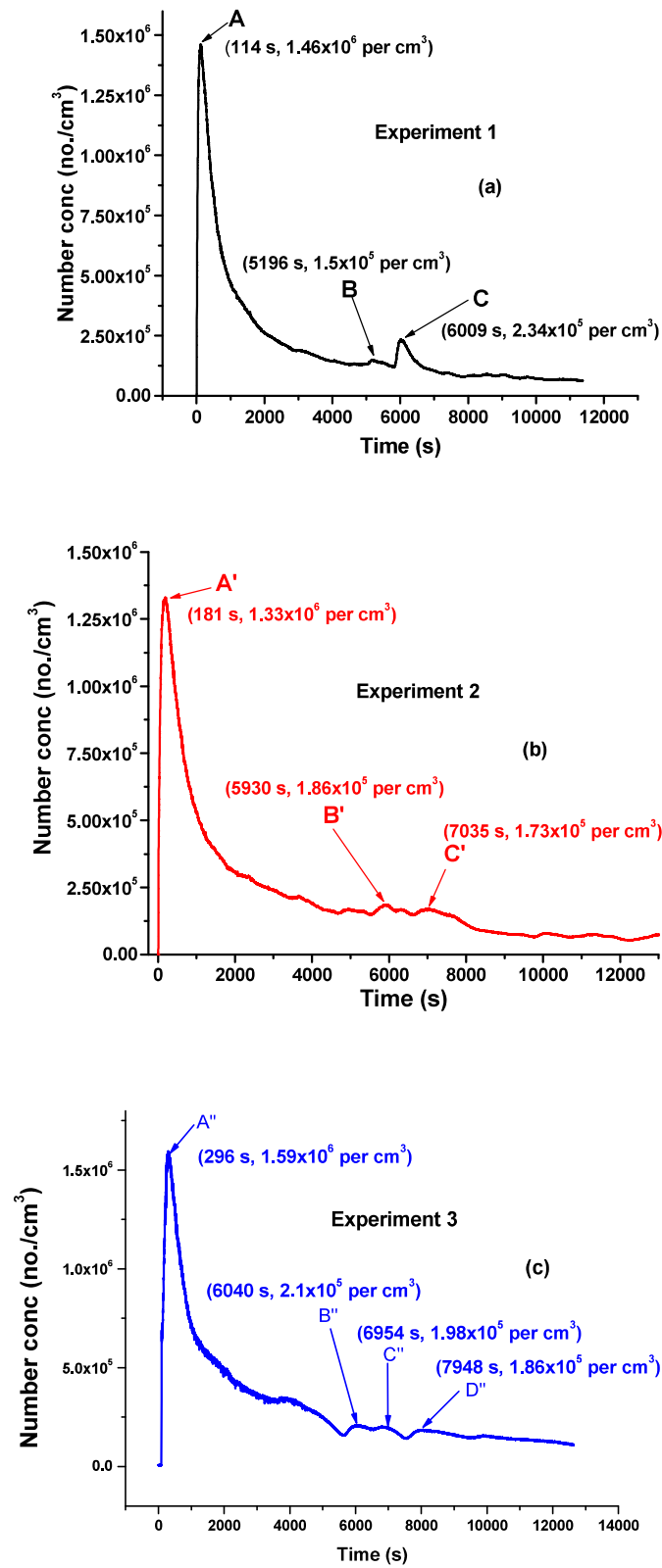


Fig. 6.8 (a-c): Selected secondary peaks in three different experiments

just near the peaks could not be quantified. Number concentration characteristics measured by CPC and SMPS were then interpreted in a series of experiments afterwards.

6.3.2.1 Experimental validations

Fig. 6.8 depicts number concentration measured by CPC in three experiments carried out in similar conditions. It can be seen that several minor peaks superimposed on decreasing profile of number concentration was common feature of these experiments. For illustrative purposes; some of these peaks (first+ 2 minor) are named as (A, B, C), (A', B', C') and (A'', B'', C'' (+D'')) for experiment 1, 2 and 3, respectively. Maximum number concentration measured in these experiments was (1.46×10^6 , 1.33×10^6 and 1.59×10^6) per cm^3 with peaking time at (114, 181 and 296) seconds, respectively. Electrical resistance of the glowing wire increases as an effect of positive temperature coefficient of resistivity of metals (usable substrates for HWG). This may result in a small decrease of operating current in the circuit which in effect may decrease the emissivity of wire. The opposite i.e. increasing emissivity at late phases thus affecting number concentration is not possible except due to the external fluctuations. As mentioned above, increasing fluctuations in applied voltage were regulated and monitored. For these peaks (Fig. 6.8), it was ascertained that such external operating factors were not influencing the formation of aerosol particles. Size distribution analysis around such peaks was then used to probe observed trend reversal (in number concentration profile) phenomenon. For this, these minor peaks were coupled to the change in size distribution around peaking time measured by SMPS.

Size distribution evolution for this experiment is also shown in Fig. 6.7. Size distribution evolution characteristics (decrease of nuclei mode particles, evolving bimodality) were similar to Fig. 6.5 as expected except a notable difference of mode occurrence below 5 nm. In this case, initial distribution consisted of modes representing primary particles (nuclei) and grown sizes (Aitken). Decrease of intensity amplitude for both these modes and a clear shifting of Aitken mode to accumulation size ranges can again be noted.

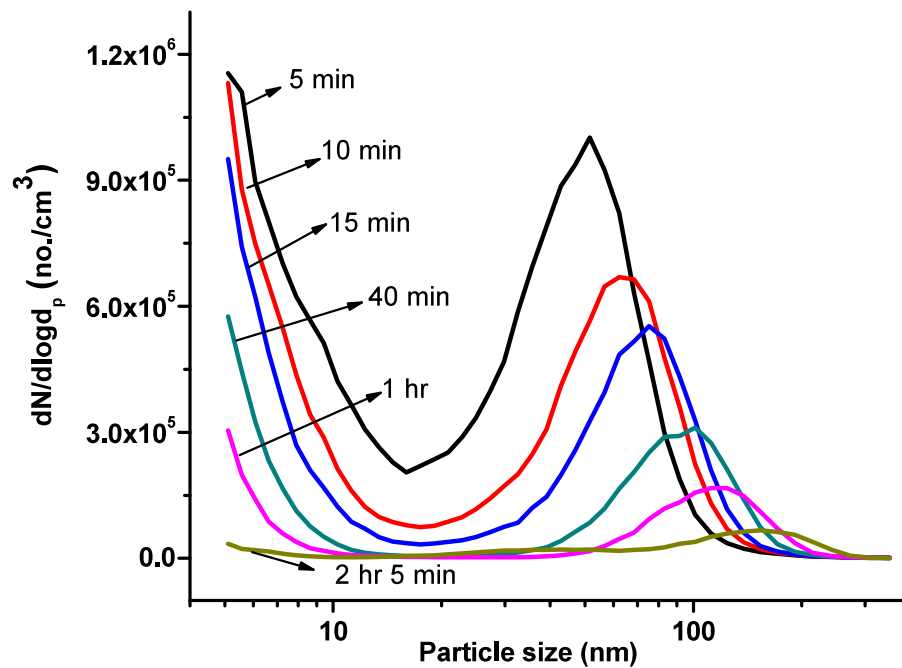


Fig. 6.7: Size distribution evolution for the case of Fig. 6.6

6.3.2 Late time peaking of number concentration in decaying profile

The sporadic peaks observed in otherwise decaying number concentration profile could be due to the slight changes in operating characteristics of the process (e.g. voltage applied to the wire in HWG) or chamber environment (e.g. mixing profile pattern). As the peak intensity is weak, even a fluctuation in such factors could be responsible for these peaks. As far as possible, all such controlling factors were monitored (particularly around each peak) during these measurements. However, changes in mixing patterns (if any) inside the chamber

6.3.1 Time series of number concentration and size distribution

For measuring the long term parameters of the aerosol size distribution (under evolution), CPC and SMPS were coupled to record number concentration and size distribution (5-350 nm) of electrical heating induced nuclei mode particles in stirred chamber conditions. As a slight departure from previous experimental arrangements, source wire was fixed inside the chamber (500 L) itself. This was done so as to reduce any sort of vapour loss expected during the transport of vapour (along with particles) from generator to chamber. Arrangement was made to connect CPC and SMPS from the same sampling port after ensuring unbiased flow biasing. This was important because SMPS characteristics were required at the time of occurrence of any significant departure of number concentration profile (measured with CPC) from its decaying profile under coagulating condition. Fig. 6.6 represents temporal response of number concentration measured by CPC for one of such experiments. As evident, few minor spikes/peaks (peak B, peak C) occurred at late times apart from the characteristic short term time (peak A). At these secondary spikes, number concentration in nuclei mode size ranges increased significantly so that these were treated as ‘peaks’ statistically in further analysis.

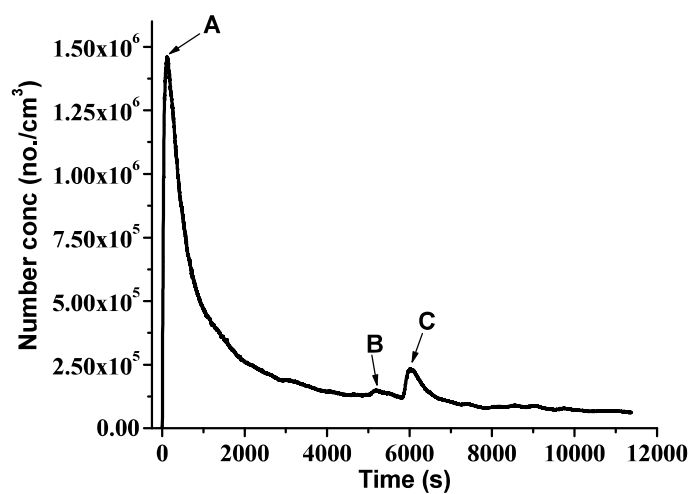


Fig. 6.6: Number concentration evolution: long term observations

Table 6.3: Size distribution parameters in different size ranges

	Nuclei mode		Aitken mode		Accumulation mode	
	N_p , #/cm ³	GM, nm	N_p , #/cm ³	GM, nm	N_p , #/cm ³	GM, nm
After 5 min	5.5×10^6	9.01	1.0×10^6	28.41	2.0×10^4	133.01
After 9 min	4.0×10^6	8.44	8.9×10^5	31.87	1.9×10^4	132.87
After 19 min	2.7×10^6	7.96	5.5×10^5	38.55	2.1×10^4	130.30
After 1 hr. 1 min	1.3×10^6	7.83	1.7×10^5	49.29	2.6×10^4	121.67
After 1 hr. 47 min	4.4×10^5	7.50	6.6×10^4	52.78	2.6×10^4	121.30

6.3 Long term behaviour of HWG aerosols in closed chamber conditions

In the second phase of experiments conducted for studying evolution of nuclei mode particles in closed chamber environment, measurements were continued for longer times (1-4 hours of operation). Ahead of short term coagulation peak, focus was shifted to late time behaviour of aerosol particles under continuous injection of vapour which nucleate to particles. An analytical study on this topic indicated the presence of sustained oscillations²⁹⁹. There are indications that inclusion of additional processes (e.g. coagulation) might introduce qualitative changes in aerosol behaviour³⁰⁶. However, not many experimental studies have been conducted to elucidate these phenomena. In the last phase of this work, such experiments were performed to investigate the occurrence or otherwise, of oscillations as indicated by models.

that distribution primarily constituted of aerosols at mode in nuclei size range and another in Aitken mode (initial distribution). While secondary peak evolved and shifted to higher sizes, intensity (number concentration) of primary peak decreased continuously, even after generation in this range.

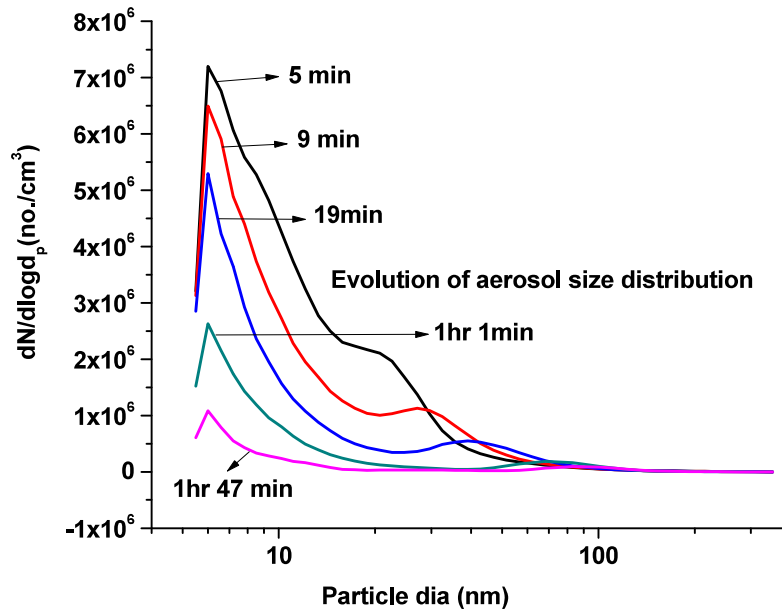


Fig 6.5: Size spectrum evolution as a result of coagulation

The number size distribution characteristics of nuclei, Aitken and accumulation mode particles for this case are also shown in Table 6.3. As discussed above, number concentration in nuclei mode size ranges decreased continuously with more or less constant mean size at late times. Increase of GM in Aitken mode is consistent with the effect of coagulation on the continuously generated nanoparticles. Shifting of number concentration to still higher accumulation size ranges is also noticeable with slowly increasing number concentration in this size range.

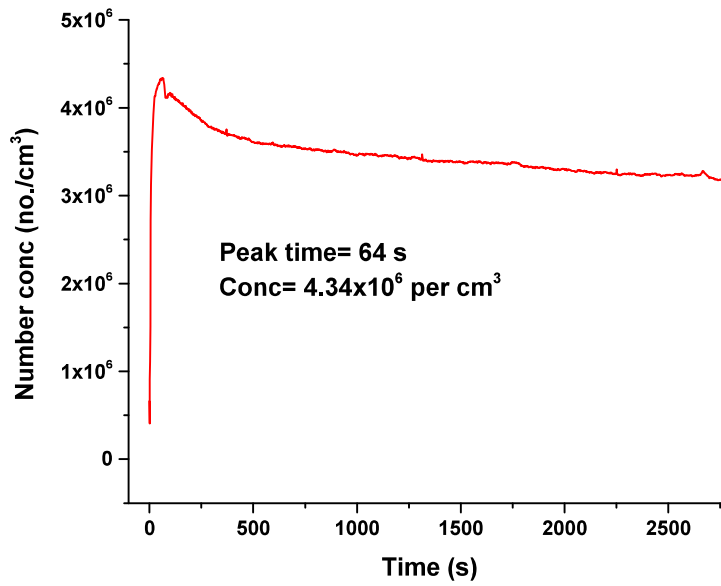


Fig. 6.4: Peaking for the case of smoke particles

Table 6.2: Comparison of emission rate for incense stick and HWG (40 L chamber)

Test source	N_p , #/cm ³	t_p , sec	Emission rate (S^*), #/sec
Incense stick	4.5×10^6	45	8.0×10^9
Incense stick	4.4×10^6	40	8.8×10^9
HWG	2.2×10^6	496	3.48×10^8

6.2.2 Size distribution evolution in different size ranges

For the case of HWG aerosol particles, nuclei mode particles which are continuously injected in closed chamber coagulate. With time, size distribution gets evolved and hetero-coagulation starts taking place between nuclei mode particles and higher size particles (in addition to self-coagulation). Fig. 6.5 shows a typical size distribution evolution measured by SMPS (5 nm-350 nm) in a closed chamber condition (500 L) for HWG aerosols. As demonstrated, aerosol size distribution of nanoparticle aerosols evolved in chamber as the time passed. It is seen

Table 6.1: Emission rate for nichrome wire used in HWG

Chamber volume (V), L	N_p , #/m ³	t_p , sec	Emission rate (S^*), #/sec
A -0.45	6.3×10^{13}	214	2.63×10^8
B - 40	2.2×10^{12}	496	3.48×10^8
C - 500	3.9×10^{11}	858	4.58×10^8

Overall uncertainty in emission rate estimates was estimated to be about 50 % where 30 % contribution comes from inherent uncertainty in locating the peak time and concentration. Smaller chambers showed lower emission rates implying the possibility of higher wall loss effects on peak values. As this process is quite fast in dynamic scale, these errors can be accepted for estimation of difficult parameter i.e. ‘number emission rate’. Subsequently experiments were also performed using incense stick generated smoke aerosols. Measurements were made till the incense sticks (2 in each experiment) burned out. Fig. 6.4 depicts the number concentration measured by CPC for one of these experiment. In contrast to the case of nichrome nanoparticle aerosols, the concentration was seen to be rising sharper and also to higher value by a factor of approximately 2. The peaks were then located for these experiments and peaking characteristics were noted. The values and estimated number emission rate for experiments conducted in 40 L chamber are shown in Table 6.2. For comparison, number emission rate estimated from HWG (nichrome) is also shown in Table 6.2. Number emission rate for incense stick (smoke aerosol particles) was found to be more than one order higher compared to HWG (metallic aerosol particles).

measured as $(6.25 \times 10^7 \text{ per cm}^3, 214 \text{ s})$, $2.16 \times 10^6 \text{ per cm}^3, 496 \text{ s})$ and $(3.93 \times 10^5 \text{ per cm}^3, 858 \text{ s})$ for chamber A, chamber B and chamber C, respectively.

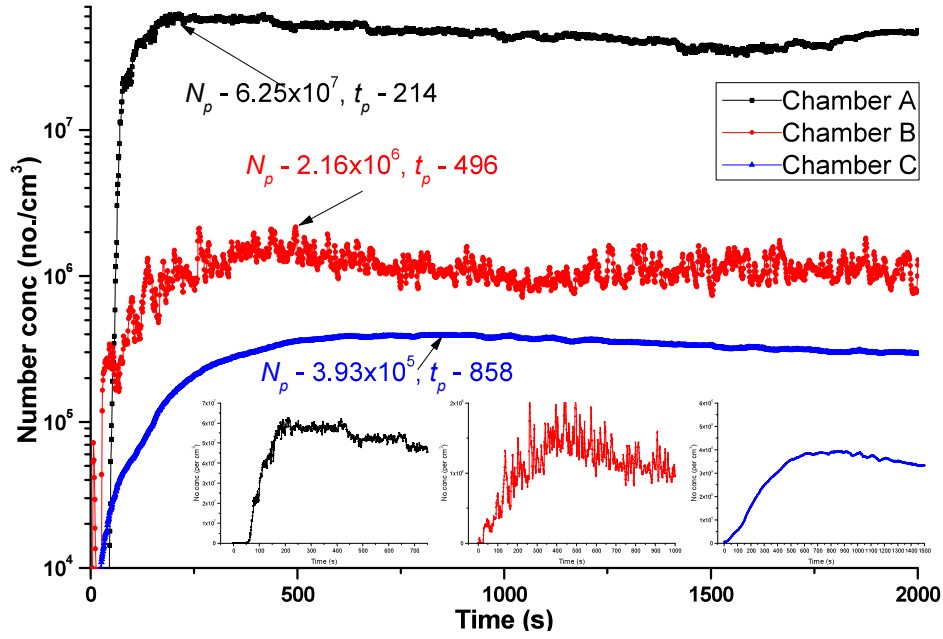


Fig. 6.3: Experimental results for number concentration evolution in all chambers

In above figure, difference in fluctuations in number concentration can also be noticed (See inset where number concentration is plotted on linear scale) apart from the peaking characteristics. Results from two smaller chambers show large fluctuations in comparison to the smooth profile obtained for 500 L chamber indicating the role of mixing in this process. Peak characteristics were picked from modal point (or its representative average) from data sheet directly avoiding role of smoothening for accuracy. Table 6.1 tabulates the results from these experiments providing number emission rate (calculated from eq. 6.3) for nichrome wire as source of metallic aerosol particles.

The rate of change of aerosol number concentration ($n(u, t)$) in the chamber due to the source injection, coagulation and removal processes is given by

$$\begin{aligned} \frac{\partial n(u, t)}{\partial t} = & \left(\frac{1}{V} \right) S^*(u, t) + \frac{1}{2} \int_0^u K(u', u - u') n(u', t) n(u - u', t) du' \\ & - n(u, t) \int_0^\infty K(u', u) n(u', t) du' - \{ \lambda_v + \lambda_d(u) \} n(u, t) \end{aligned} \quad (6.1)$$

where u - particle volume, $K(u, u')$ - coagulation kernel, λ_v - ventilation rate, $\lambda_d(u)$ - removal rate, $S^*(u, t)$ - particle number emission rate (number s^{-1}), and V -chamber volume. Number concentration and time can be scaled in terms of emission rate and particle primary coagulation coefficient³⁰⁴ using numeric and semi-analytical solutions as:

$$N^*(t^*) = N(t)/N_c, \text{ and } t^* = t/t_c \quad (6.2)$$

where $N_c = \sqrt{S^*/VK(u_0, u_0)}$ is characteristic number concentration, $t_c = 1/\sqrt{S^* K(u_0, u_0)/V}$ is characteristic time and u_0 is the volume of the emitted primary particle. In this framework, $N^*(t^*)$ always peaks at $N^* \approx 1$ for $t^* \approx 2$ regardless of the source strength. From eq. 6.2, source strength from an experimentally measured peak number concentration (N_p) at time (t_p) can be written as

$$S^* = VN_c/t_c = 2VN_p/t_p \quad (6.3)$$

By performing experiments to simulate peak characteristics, number emission rate of aerosol sources can be estimated from eq. 6.3. To demonstrate this technique, experiments were carried out using metal particles generated from HWG (nichrome wire source) injected into stirred chambers of three different volumes (Chamber A: 0.45 L, Chamber B: 40 L & Chamber C: 500 L). Fig. 6.3 represents temporal evolution of total number concentration measured by SMPS during these experiments. As discussed, peak characteristics were found to be depending on the chamber dimensions. Peak concentration and peaking time were

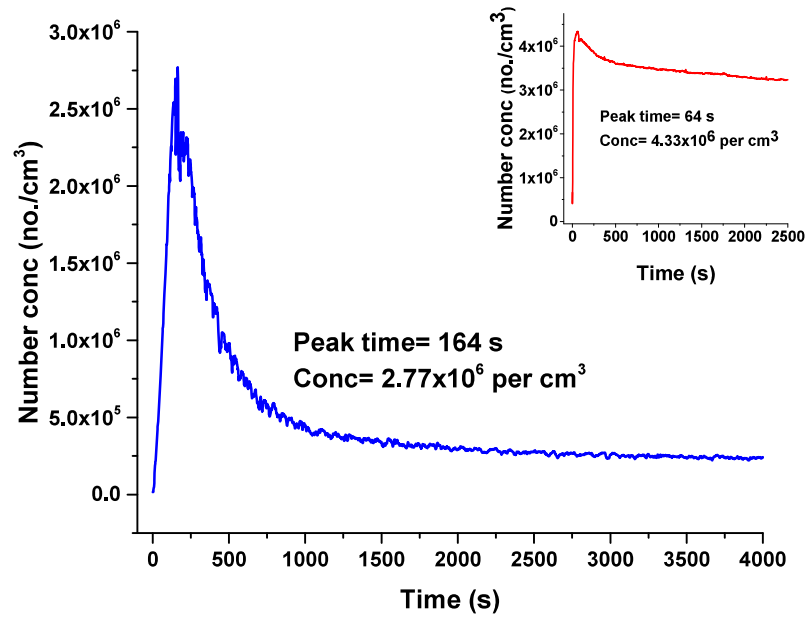


Fig. 6.2: Behaviour of continuously injected particles: coagulation peak

Inset of Fig. 6.2 represents number concentration evolution of smoke aerosol particles in similar conditions. ‘Peak concentration’ and ‘Peaking time’ are two parameters which are associated with this process. In same chamber volume and mixing patterns, their values can be different for different source terms. For the same source (such as particles generated from HWG), these values are expected to be slightly different in different chamber volumes. For the above figure, these parameters are ($\approx 2.77 \times 10^6$ per cm^3 , 164 s) for nichrome metal particles (500 L chamber) and ($\approx 4.3 \times 10^6$ per cm^3 , 64 s) for smoke particles (40 L chamber).

Characteristic coagulation peaking can also be used for estimating number emission rate of aerosol sources. Particle emission from sources can be characterised by their emission rates. Conventionally mass emission rate has been used in such applications due to the relative ease in its determination from experiments. Methods for estimating number emission rates are rare due to the difficulties associated with near source monitoring and effect of coagulation which rapidly decreases number concentration as one moves away from sources. But given its due importance for near source modelling, climatic and health implications; its estimation and development of associated methods is crucial.

respectively in these experiments. Vapour concentration was not measured during these experiments.

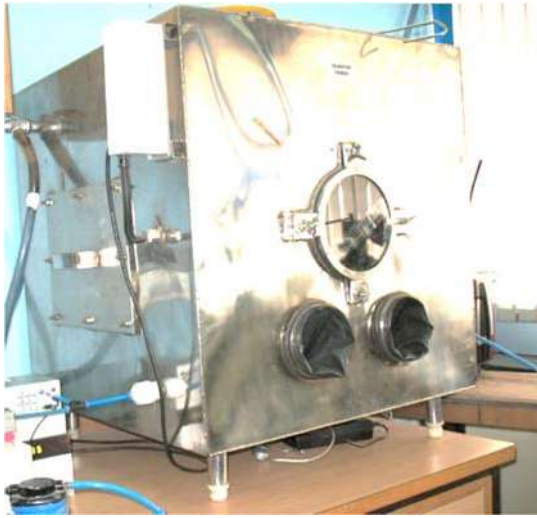


Fig. 6.1 (a): 500 L chamber used in experiments



Fig. 6.1 (b): Experimental arrangement in 40 L chamber

6.2.1 Continuous injection: Characteristic peaking effect

Particle size distribution evolves with time due to coagulation when nuclei mode particles of high number concentration are injected into a closed chamber. Under continuous source conditions, fresh nuclei mode particles coagulate with background aerosol population of evolved/evolving particle sizes. This hetero-coagulation of highly unequal size ranges results in faster depletion of number concentration. As the source is continuously on, the interplay between source rate, coagulation rate and background deposition rate decides the temporal behaviour of total number concentration representing the chamber environment. Few models³⁰⁴ have studied this phenomenon in detail and a peaking in number concentration evolution is predicted and interpreted. This kind of peak occurrence is termed as ‘coagulation peaking effect’ where the peak is the function of characteristics of aerosol particles and process parameters (e.g. chamber volume, background deposition). Fig. 6.2 shows a typical ‘coagulation characteristic peak’ observed in a continuous injection experiment performed with metallic aerosol particles of HWG in closed chamber.

6.2 Vapour to particle conversion: Role of hot wire generator

In optimized conditions, HWG can generate aerosol particles in nuclei mode and of significantly high number concentrations. The vapour (source term) gets quenched and nucleates to form particles in favourable conditions. Output from HWG can be fed to an aerosol reactor/chamber in instantaneous as well as continuous operation. As shown in Section 2.4.3, changes in operating characteristics affects vapour to particle conversion and hence HWG output can be tuned to generate different vapour-nucleated vapour combinations. For example, number concentration at HWG outlet was measured at $> 10^7$ per cm^3 for 1-1.5 Lmin^{-1} carrier flow rate which decreased (thereby increasing unutilized vapour concentration) to $< 10^5$ per cm^3 when flow rate was increased to 4 Lmin^{-1} (See Fig. 2.4 (a)). Additionally outlet number concentration (and its stability) generated by HWG (Section 2.4.4) is appropriate to design experiments for studying coagulation effects at smaller time scales. In this work, HWG experiments were performed in two levels. In the first one, coagulation features and behaviour of nuclei mode particles was studied and long term effects under vapour-particle interactions were targeted in the second level.

6.2 Experiments with high concentration nanoparticle aerosols

These experiments were performed in a closed chamber under continuous source term conditions. Three chambers (generator cell itself, Perspex chamber and aluminium chamber) of volumes 0.45, 40 and 500 litres respectively, were used for this purpose. Two of the larger ones are shown in Fig. 6.1 along with schematic experimental arrangement followed during the experiments. Except the measurements taken directly from the generator; generator was connected to the chamber under flow conditions for online sampling. As shown in Fig. 6.1, fans were used in the chamber for providing uniform mixing conditions to the generated aerosol particles (except for generator itself where measurements were taken as such). CPC and SMPS were used for measurement of number concentration and number size distribution

particular assumption on size distribution function, computational time becomes a limiting factor for complex aerosol systems. Method of moments relying on statistical variables calculated from the moment equations of distribution function is an alternate solution method for GDE^{297, 298}. These methods take relatively lesser solution time but have been shown to be limited for some cases. Pratsinis²⁹⁹ developed the moment method to include contribution of aerosol coagulation to particle growth. Holding distribution function as lognormal, all growth processes can be handled in this method. McGraw³⁰⁰ proposed quadrature method of moments to describe the aerosol dynamics. All of the above mentioned methods have been successfully implemented in various contexts in the past^{296, 301} and efforts are being continued for precise simulation of complex aerosol systems. Anand and Mayya³⁰² discussed a diffusion-coagulation model targeting the quantification of effective contribution of emission sources to background aerosols. Same authors also developed a set of equations for describing the intra puff/plume coagulation effects in the presence of atmospheric dispersion³⁰³. Using their approach, number survival fractions can be obtained employing atmospheric and aerosol parameters. This working group also modelled aerosol coagulation process for a constant source of nanoparticles³⁰⁴.

Several measurements and controlled experiments³⁰⁵ have been performed in order to test the prediction capability of aerosol behavioural models. There are interesting features predicted by these models requiring due experimental validations and similarly experimental findings for which modelling is needed. Particularly, behaviour of nuclei mode particles continuously injected in a closed chamber undergoing coagulation offer one such domain where coupling of controlled experimental measurements and models is needed. This study explored this important aspect linking the objectives of present work with the recent developments in this field.

CHAPTER 6
CHARACTERISTICS OF NUCLEI MODE
PARTICLES IN CONFINED ENVIRONMENTS:
CASE STUDY 3- HOT WIRE GENERATED NANOPARTICLE AEROSOLS

In the next phase of experiments, evolution characteristics of nanoparticle aerosols were studied in stirred closed chamber conditions. HWG was employed as the source while CPC and SMPS were coupled to provide the features of number concentration and size distribution evolution, respectively. In contrast to atmospheric conditions where an aerosol sink is always present for nuclei mode particles, background aerosol concentration could be controlled for this case. Under continuous source term conditions, freshly formed particles interact with dynamically evolving Aitken and accumulation mode particles. These kinds of experiments serve as a way to probe the growth characteristics of nuclei mode particles. Additionally they can validate GDE based models specifically focused on predicting effects at extremum size ranges, high concentrations and/or multiple processes.

6.1 Role of experimental studies: validation of general dynamic equation

Vapour to particle conversion (nucleation) is significant source term towards global emissions of atmospheric aerosols (natural and anthropogenic) and an important part of aerosol evolution models. General dynamic equation presents a mathematical framework to study aerosol dynamics including interaction processes. Be it external depositional effects e.g. settling, phoresis, dilution etc. or internal modulating factors such as coagulation, condensation etc.; changes in distribution functions are predicted by solving GDEs. Models for these internal/external modulations together with nucleation are necessary to describe coupled vapour-particle dynamics. Discrete type methods such as sectional methods²⁹⁵ and nodal methods²⁹⁶ are adopted to describe the evolution of particle size distribution function. In general, these methods divide the particle volume space into discrete sections/nodes spaced in a logarithmic/geometric size scale. Number concentration of aerosol particles are measured at each section/node during the size spectrum evolution. Although involving no

more field campaigns to deduce precise conclusions which can be utilized for broader applications. Characteristics of observed new particle formation events at both background and episodic times need to be validated in a long term campaign. These should be focused on measurements near 1 nm particle size and of other gases (sulphuric acid, ammonia) in the atmosphere. Formation and evolution parameters for freshly generated as well as detectable particles need to be coupled to aerosol module of atmospheric circulation models. New extended modelling approaches can also be developed for estimating these characteristics.

size distribution evolution. It was seen that exactly at the times of these secondary peaks, number concentration in nuclei mode increased possibly due to condensational effects. These experiments are experimental demonstration of ‘aerosol oscillatory effects’.

8. Different mechanisms operate for new particle formation in the atmospheric and controlled chamber conditions. While background sinks are always present in the atmosphere, their characteristics can be controlled in chamber experiments. In that way, dynamical evolutions of nuclei mode particles can be tuned in chamber conditions. Since nucleation rate in atmosphere is an important parameter, its determination and simulation is crucial. Atmospheric measurements provide the real time features of the formation processes. However complex models intended for such conditions can be validated/evolved on the basis of chamber experiments.

8.1 Future scope for this work

Hot wire generator developed under this work can be used as an aerosol nanoparticle generator of controlled and tunable characteristics. Temperature of the wire surface and of nearby environment is directly linked with thermal quenching affecting aerosol formation. The temperature profile gets modified with changes in the flow rate of carrier gas. A CFD study can be undertaken to study these effects, the conclusions of which can be used for modelling nucleation phenomenon at the source. Estimate of number emission rate can be extended to wider and important aerosol sources such as fuels, fires etc. Exciting aerosol oscillatory evidences extracted from this work need to be studied in detail by conducting more experiments and performing simulations.

Increase of ultrafine and nuclei mode concentration at the times of Diwali and fire events are required to be coupled to depositional and other aerosol dynamical models. The understanding based on worldwide studies for such cases needs to be widen with

distribution evolutions. Their values were found to be higher than those measured for urban atmospheric conditions. For case study 2, formation rate of 5 nm particles was estimated for the case as well as control days. Values/ranges of parameters obtained during Diwali, fire and background were also compared. In general, formation rate of minimum detectable particles and growth rate of nuclei mode particles were found to be higher for fire event. Source term to the environment was seen to be modified during fire event.

7. In the last phase of experiments (case study 3), evolution characteristics of nanoparticle aerosols generated from HWG were studied in mixed closed chamber conditions. CPC and SMPS were coupled to provide number concentration and size distribution features. In the first part of these experiments, coagulation features and behaviour of nuclei mode particles were studied. Long term effect of vapour-particle interactions for high concentration continuous source term conditions was then studied in the second part. Under continuous source term condition, interplay between source rate, coagulation rate and background deposition rate decides the temporal behaviour of total number concentration. A peaking in number concentration is predicted in such conditions termed as coagulation peaking effect where the peak is a function of characteristics of aerosol particles and process parameters. Number emission rate of aerosol sources can be estimated using characteristic coagulation peaking. In scaled terms, number concentration peaks at the same time regardless of the source strength providing a way to calculate number emission rate. On the basis of results from series of experiments, number emission rate for incense stick (generated smoke particles) was found to be an order higher than that for HWG (metallic nanoparticles). Sporadic peaks in otherwise decaying profile of number concentration were observed while conducting experiments with HWG and measuring long term

the time of maxima in number concentration were noted similar to case study 1. A marked modification of size distribution specifically in nuclei mode size ranges was observed when size distributions averaged for the entire day were compared. An analysis on the basis of 4 hourly and hourly averaged size distributions lead to the evidence of aerosol formation in nuclei mode size ranges at day times coinciding with higher solar intensity. Diurnal variations of total number concentration were seen to be followed closely by concentrations in nuclei and Aitken size ranges. Daily maximum for number concentration was found to be higher for case days. Difference of mean and median concentration was also seen to be distinctly higher for 3 case days (March 23-25) in contrast to other days. This indicates effect of high concentration instances on the modification of number distribution function.

6. An added dimension to the results obtained from measurement campaigns conducted under case study 1 and case study 2 is related to the linking of NPF with the dynamics of measurable nuclei mode particles. Any simultaneous increase in total number concentration and nuclei mode concentration indicates the possibility of aerosol formation via gas to particle conversion. Such instances can be tested by adopting qualifying criterion to pick nucleation/NPF events. Qualifying criterion based on the rate of increase of nuclei mode number concentration and growth rate of mean size in nuclei mode was adopted for checking entire data (episodic as well as background peaks). For case study 1, such events were then studied for their evolution characteristics on Diwali and non-Diwali times. Formation rate of 11 nm diameter particles and their growth rate were estimated from a simplistic approximate model taken from literature. These values were found to be 57-225 no./cm³/sec and 15-240 no./cm³/sec for Diwali and background peaks, respectively. Coagulation sink for 11 nm particles and condensation sink was also calculated on the basis of measured size

of particles affecting the skewness of the data. Box-whisker plots were also drawn for different size ranges and the variations with respect to days in these plots were correlated with the variations seen for the total number concentration. A distinct marked shift of parametric values was noticed for accumulation mode in these plots. Next, diurnal variations of number concentration (total and different modes) were interpreted for different days. On the night of Diwali, average number concentration comprised of 32.3, 36.6 and 31.1 % of nuclei mode, Aitken mode and accumulation mode size ranges, respectively. Average mass concentration for evening and night times on the Diwali day was measured at $364 \mu\text{g}/\text{m}^3$. At other times also, mass concentration was found to be comparable. Filter paper samples were treated for estimating elemental mass concentration of Cu, Fe, Zn, Ba, Ca, Sr, Al, Mg, Na and K using AAS. Ba, Sr and Al concentration were found to be increasing at the time of Diwali emissions consistent with the findings of other similar studies. K was also found to be increasing at the time of emission, but it was found to be high for other days as well.

5. The effect of emissions of trap gases and particles from a large scale fire on aerosol number characteristics was studied as case study 2 of this work. A massive fire broke out in Deonar dump yard (Mumbai) on March 20, 2016 and took nearly 7 days to be brought completely under control. M-DMA was used for SMPS measurements covering size ranges 5-350 nm during this campaign and measuring evolution of number concentration and number size distribution. These measurements were performed intermittently from March 21 to March 28 and then from April 6 to April 8 during which period March 23-26 were selected as ‘case days’ and April 6-7 as ‘control days’, respectively. Number concentration was observed to be higher than $> 10^5$ per cm^3 at several instances during the days of fire. Minima in geometric mean at

number concentration varies significantly in megacities and also can be similar or even higher than that expected at the times of Diwali emissions. Hence it is imperative to perform a long term field campaign and background measurements before linking these emissions to events.

4. In second field campaign focused on studying the effect of aerosol emissions during celebratory fireworks on background aerosol characteristics, SMPS measurements were performed at the same location during October 27-November 13, 2013 (Diwali days: November 2-4). Apart from re-validating the conclusions drawn from 2012 campaign, additional inferences (mass loading, change in aerosol chemical composition, diurnal variations and statistical interpretations) were targeted. Several number concentration peaks coinciding with drop in geometric mean at Diwali and non-Diwali times were observed. Analysis of size distribution evolution of Diwali peaks confirmed the signature conclusions drawn from the previous campaign. Increase of particles in ultrafine (and nuclei) mode size ranges, formation of mode around 50 nm and shifting of accumulation mode was again observed. Increase of nuclei mode concentration was also noted for odd non-Diwali times as well indicating the role of background aerosol formation processes for the same. Box-whisker plots for number size distribution data for all sampling days were drawn. Highest value of daily maximum number concentration ($\approx 1.6 \times 10^5 \text{ no/cm}^3$) was observed on the day of Diwali (Nov 3) but this value was not far from that measured on few other days as well. Average number concentration (both mean and median) for Diwali day was found to be comparable or even lesser than other days. These values were seen to be higher during Oct 30- Nov 1 than all other sampling days. Difference of mean and median values also varied, observed to be maximum on the day of Diwali (mean= $4.9 \times 10^4 \text{ no/cm}^3$, median= $4.1 \times 10^4 \text{ no/cm}^3$). This indicates the impact of burst production

relate measurement results in a better connected way with regional atmospheric characteristics (in comparison to local ground level effects). Although the combination of SMPS and OPC provided size distribution from ≈ 10 nm to $20\text{ }\mu\text{m}$, focus was made limited to SMPS results specifically in ultrafine domain. Several peaks in number concentration profile were observed in temporal evolution recorded by SMPS during these study days. On Diwali night (November 13, 2012), maximum recorded number concentration was noted to be at 1.2×10^5 no/cm³. Peaks were observed for pre-Diwali and post-Diwali night times as well. Interestingly, few other peaks of similar number concentration intensity were also recorded at random non-Diwali times as well. For most of these peaks, maxima in number concentration coincided with minima of geometric mean indicating emission in the ultrafine size ranges. From SMPS measured size distributions, size distribution evolution characteristics were studied. Concentration of accumulation mode particles was observed to be increasing at the times of emissions consistent with other similar kind of studies. However in contrast, significant increase of particles in ultrafine (and nuclei) mode size ranges was also noted. Such spikes in ultrafine concentrations can be harmful to health due to their larger probability to reach deeper lung regions. In order to distinguish a normal peak and an episodic peak of approximately same total number concentration, size distribution evolution analysis around each observed peak was performed. It was seen that for the case of Diwali peaks, size distribution evolved with signatures in the form of formation of nuclei and Aitken mode (≈ 50 nm) and shifting of accumulation mode of the spectrum. These signatures diminished soon but elating the background aerosol levels higher after emissions. For other peaks, no particular signature was noted and mostly modifications in size spectrum occurred for entire size range. PM concentration, trace elemental chemical concentration and

concentrations and harmonisation plots were drawn. Concentration ratio was found to be increasing with aerosol number concentration. The conclusions and protocols derived from this part were used in a case study to quantify radiative impacts of light absorbing black carbon.

2. Three case studies were performed under this work mainly focusing on number characteristics of nuclei mode particles. The first case study pertains to the measurements made around and during Diwali festival days. Effects of firework's emissions on background aerosol characteristics have been interpreted by measuring number concentration and number size distribution using SMPS. Two campaigns were conducted for case study 1 at the time of Diwali festival in 2012 and 2013. Sampling was performed for 6 days (including 3 Diwali days) in 2012 and for 17 days (3 Diwali days) in 2013, respectively. Effect of emissions of trap gases and aerosol particles on background aerosol characteristics due to a large scale fire was studied as case study 2 of this work. A large scale fire broke out in March 2016 in a dump yard facility and took many days to be brought under complete control. During the period of the fire and after it was controlled, SMPS measurements were carried out at a location approximately 5 km from the place of fire. The third and last case study i.e. case study 3 discusses results of the controlled experiments performed in closed mixed chamber conditions with HWG generated high concentration nanoparticle aerosols. These experiments were focused on providing experimental validations to theoretically predicted features at high particle and/or vapour concentration conditions.
3. Measurements during Diwali 2012 were made for 6 days from November 10 to November 15, 2012. Sampling location for this campaign was selected at 50 m height in a building of a residential colony in Mumbai. This was done mainly in order to

Hot wire generator was developed under this work in order to be employed as an aerosol generator in case study 3. This case study was designed to interpret the characteristics of nanoparticles/nuclei mode particles in controlled laboratory conditions. A metallic wire of defined electrical resistivity can be used as a substrate in this generator (mostly nichrome was used as substrate in this work). Based on the optimization experiments; operating parameters viz. applied voltage 6-9 Volts, equivalent power 30-50 Watts, carrier gas flow rate: 1-1.5 Lmin⁻¹ were fixed for the experiments. This generator was able to generate particles of high number concentration ($> 10^7$ per cm³) with geometric mean size varying from 15-20 nm (calculated from measured sizes). Mean size was seen to be preserved for considerable long times as well. Primary particles generated from this generator were seen to be as low as 3 nm in a separate TEM analysis. A detailed inter-comparison study with GRIMM-SMPS (model no 5.403C) and TSI-SMPS (classifier 3080 with CPC 3775) was undertaken as a part of this work to strengthen the protocols related to ultrafine measurements with SMPS. CPCs of these devices were challenged with ambient and laboratory generated conditions before testing SMPS units. For ambient conditions, number concentration measured by CPCs were found to be matching closely while a difference of about 20% was observed for SMPS. Only a small part of this difference could be linked to the CPC differences ($\approx 5\%$). For elevated concentration laboratory experiments, CPC as well as SMPS differences increased. GRIMM SMPS was found to be measuring higher concentration by a factor of about 1.881(± 0.078) with respect to TSI SMPS in experiments with atomised NaCl aerosols (similar large factor for the case of (NH₄)₂SO₄ aerosol particles as well). Relative concentration factors were found to be size dependent reaching as high as 4 for nuclei mode size ranges. The observed differences were scaled in terms of measured

CHAPTER 7

SUMMARY AND CONCLUSIONS

This work focuses on studying the number characteristics of nuclei mode particles in high concentration ambient and laboratory conditions. The work started with developing nanoparticle aerosol generator intended for controlled chamber experiments. A study to harmonise ultrafine concentration measurements with multiple CPCs and SMPSs was also undertaken as a pre-step to refine measurement protocols. Three case studies (2 in atmospheric and 1 in laboratory conditions) were undertaken for this work. Evolution of measured total number concentration, number concentration in different size ranges and number size distribution (entire range) was studied and interpreted. Nuclei mode characteristics of particles were studied comprehensively for these case studies. New particle formation events were selected from the measurement data. Formation and growth characteristics of nuclei mode particles for these events were estimated, afterwards. Following are the summary and conclusions drawn from this work:

1. A multitude of techniques and instrumentation are employed for the measurement of aerosol characteristics. It is now possible to make measurements at good sensitivities and finer resolutions. Due to the necessity of usage of several types of instruments in field campaigns; issues such as calibration, inversions, coupling of different equivalent diameters, inter-instrumental differences etc. should be taken care. In this work, TSP sampler was used for measuring mass concentration of aerosols during one of the field campaigns. Sampled filter papers were also chemically treated for estimation of elemental mass concentration using AAS. SMPS (5-350 nm; 11-1083 nm) and OPC (0.3-20 μm) were used for size distribution measurements during field campaigns while an additionally coupled standalone CPC was employed for measurement of number concentration evolution in the case of chamber experiments.